Biomaterials 305 (2024) 122428

Contents lists available at ScienceDirect

Biomaterials

journal homepage: www.elsevier.com/locate/biomaterials

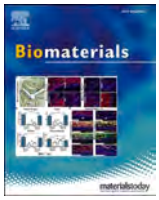

Engineered 3D *ex vivo* models to recapitulate the complex stromal and immune interactions within the tumor microenvironment

Kalpana Ravi [a,1], Twinkle Jina Minette Manoharan [a,1], Kuei-Chun Wang [a], Barbara Pockaj [c], Mehdi Nikkhah [a,b,*]

[a] School of Biological and Health Systems Engineering (SBHSE), Arizona State University, Tempe, AZ, 85287, USA
[b] Biodesign Virginia G. Piper Center for Personalized Diagnostics, Arizona State University, Tempe, AZ, 85287, USA
[c] Department of Surgery, Mayo Clinic, Phoenix, AZ, USA

ARTICLE INFO

Keywords:
3D-engineered models
Microfluidics
Tumor microenvironment (TME)
Tumor immune microenvironment (TIME)
3D printed
Immune crosstalk
Tumor-on-chip

ABSTRACT

Cancer thrives in a complex environment where interactions between cellular and acellular components, surrounding the tumor, play a crucial role in disease development and progression. Despite significant progress in cancer research, the mechanism driving tumor growth and therapeutic outcomes remains elusive. Two-dimensional (2D) cell culture assays and *in vivo* animal models are commonly used in cancer research and therapeutic testing. However, these models suffer from numerous shortcomings including lack of key features of the tumor microenvironment (TME) & cellular composition, cost, and ethical clearance. To that end, there is an increased interest in incorporating and elucidating the influence of TME on cancer progression. Advancements in 3D-engineered *ex vivo* models, leveraging biomaterials and microengineering technologies, have provided an unprecedented ability to reconstruct native-like bioengineered cancer models to study the heterotypic interactions of TME with a spatiotemporal organization. These bioengineered cancer models have shown excellent capabilities to bridge the gap between oversimplified 2D systems and animal models. In this review article, we primarily provide an overview of the immune and stromal cellular components of the TME and then discuss the latest state-of-the-art 3D-engineered *ex vivo* platforms aiming to recapitulate the complex TME features. The engineered TME model, discussed herein, are categorized into three main sections according to the cellular interactions within TME: (i) Tumor-Stromal interactions, (ii) Tumor-Immune interactions, and (iii) Complex TME interactions. Finally, we will conclude the article with a perspective on how these models can be instrumental for cancer translational studies and therapeutic testing.

1. Introduction

The 'tumor microenvironment' (TME) is a dynamic ecosystem encompassing cellular and acellular components [1,2]. Cellular components of TME are a heterogeneous population of cancerous and non-cancerous cells. Non-cancerous cells are an umbrella term utilized for the immune (i.e., macrophages, T cells, B cells, dendritic cells) and stromal cells (i.e., cancer-associated fibroblasts (CAFs), endothelial cells, adipocytes) [3]. The acellular compartment of the TME comprises an extracellular matrix (ECM), growth factor, and cytokines [4]. Multifaceted interactions between cancer, immune, and stromal cells alongside the tissue ECM and cytokines have been shown to be a strong determinant of tumorigenesis [5]. Evolving knowledge about the intricate TME has revolutionized how cancer treatments are centered. Consequently, in the past few years there have been an increased emphasis on incorporation of TME components in a holistic view to better comprehend their impact on cancer biology and response to therapy [6] (see Table 1).

To date, various models have been proposed to better understand the cellular and molecular processes that drive tumor development, progression, and therapeutic outcomes. A wealth of information has been obtained from *in vivo* animal models and standard two-dimensional (2D) cell culture assays [7,8]. While animal models are considered gold standard for oncological studies, their TME composition markedly vary from that of humans [9]. Moreover, animal models are both time-consuming and require financial investments, not to mention the ethical concerns [10]. Conversely, traditional 2D cell culture assays

* Corresponding author. School of Biological and Health Systems Engineering (SBHSE), Arizona State University, Tempe, AZ, 85287, USA.
E-mail address: mnikkhah@asu.edu (M. Nikkhah).
[1] These co-authors contributed equally to this work.

https://doi.org/10.1016/j.biomaterials.2023.122428
Received 14 August 2023; Received in revised form 4 December 2023; Accepted 8 December 2023
Available online 19 December 2023

Abbreviations

TME	Tumor Microenvironment
CAF	Cancer-Associated Fibroblasts
ECM	Extra Cellular Matrix
2D	Two-Dimensional
3D	Three-Dimensional
DC	Dendritic Cells
TAM	Tumor-Associated Macrophages
APC	Antigen Presenting Cells
PD1	Programmed Death 1
CTLA4	Cytotoxic T Lymphocyte Antigen 4
CCL	C–C motif Chemokine Ligand
NK cells	Natural Killer Cells
α-SMA	Alpha-Smooth Muscle Actin
EC	Endothelial Cell
bASCS	Breast Adipose-Derived Mesenchymal Stromal/Stem Cells
MCTS	Multi Cellular Tumor Spheroids
PDO	Patient-Derived Organoids
HUVECs	Human Umbilical Vein Endothelial Cells
GBM	Glioblastoma Multiforme
GSC	Glioma Stem Cells
CAR-T	Chimeric Antigen Receptor T Cells

have been unable to replicate the critical aspects of the TME, including interactions between tumors and the ECM, as well as the 3D complex tissue organization [11]. Intriguingly, the decline in clinical effectiveness of oncological drugs can be attributed to the lack of pre-clinical tools, representing a critical bottleneck in accurately assessing the efficacy of drugs [12,13]. Recognizing these profound limitations, the holy grail in accurate modeling of the TME is establishing platforms that can faithfully recapitulate the critical features of the TME *ex vivo*. Such platforms would better mimic TME features, facilitating the direct translation of discoveries into therapeutic strategies for human applications.

In line with this momentum, engineered 3D *ex vivo* tissue models, developed in the past few years, have generated a notable thrust for accurate human disease modeling, such as cancer [14–17]. Significant progress in tissue engineering, microfabrication techniques, and cellular biology has led to the development of organotypic TME models with a higher degree of complexity for mechanistic biological studies and therapeutic testing [18–21]. Advanced model systems have also made it possible to recreate essential cellular components aspects of TME *in vivo*, along with native-like mechanical cues (i.e., matrix stiffness, shear stress), to maintain the cells and the engineered tissue in a physiologically relevant microenvironment [22–26]. Additionally, 3D-engineered models that incorporate TME features can advance effective therapeutic outcomes more accurately [27].

A Plethora of 3D models have been thus far developed to mimic and parse out the influence of TME. One such model is the 3D tumor spheroids, which are microsized cell aggregates that exhibit tumor-like properties such as oxygen gradient, quiescent intermediate region, and limited molecular transport. Given their *in vivo* tumor features, spheroids are routinely used for drug screening studies [28]. To understand the inherent tumor heterogeneity and pathophysiology, organoid models are the most suitable platform. Scaffold-based tumor models have been also developed to achieve more biomimetic properties of native tissues. These scaffolds, made from synthetic and/or natural biomaterials, provide the cultured cells with a physiologically relevant environment. Furthermore, scaffolds are often integrated with other models such as spheroids and organoids to create complex models with physico-chemical properties similar to those of the native ECM [29]. Microfluidics and 3D printing models are compelling platforms for investigating cellular crosstalk, due to their ability to control spatial confinement and replicate organ-level functions. These engineered platforms are advanced systems for modeling tumors *in vitro*.

This review article provides a comprehensive overview of the latest advancements in the development of 3D *ex vivo* models for cancer research and the utilization of these model systems for foundational biological studies and therapeutic testing. We will delve into the crucial role of the heterogeneous TME cellular compartment in cancer progression and provide a detailed account of the 3D models that have significantly expedited cancer studies. Recognizing the importance of comprehending the interaction between cancer cells and their surrounding environment, we will review the inclusion of various stromal cells, immune cells, and a combination of both cell types (complex) in engineered tumor models. We will focus specifically on four engineered models: spheroids, organoids, microfluidics, and 3D printing models, to cover a wide range of *in vitro* models, including more sophisticated model systems. Finally, we discuss some strategies for further development and translation of these platforms from the bench side to clinical testing.

2. Cellular composition of TME

There has been a long-standing history linking the association between cancer and the cellular composition of the TME [30,31]. TME harbors diverse cells that exert both tumor-promoting and tumor-suppressing effects on cancer progression (Fig. 1). The dual nature of TME, with respect to its cell composition, has significantly changed the paradigm in cancer research [32,33]. Thus, there is an ever-growing focus on understanding the composition and function of TME in cancer biology and progression. This ensuing section will summarize critical stromal and immune cell functions and their role in tumorigenesis.

2.1. Immune constituents of TME

The immune system is generally classified into innate and adaptive immunity. Innate immunity, also referred to as 'non-specific immunity' constitutes an antigen-independent defense mechanism. Its main purpose is the immediate prevention of the spread of foreign pathogens when encountered. This is achieved by the rapid recruitment of immune cells to the site of inflammation through chemokine and cytokine secretion. Key cellular players in innate immunity include macrophages, dendritic cells, and neutrophils [28]. When innate immunity is not effective in eliminating the pathogens, its actions aid in the development of a long-lasting adaptive immune response after sustained exposure to antigens. The adaptive immune cells – T cells and B cells get activated into matured effector T cells and antibody-producing B cells and can develop a memory of past infections to enhance the immune response.

A common paradox in cancer biology is that despite the presence of numerous cancer antigens, the body fails to create immune-mediated destruction. This failure in immune system functionality has led to more in-depth studies into TME to gain insights into the mechanism of tumor resistance [34]. The following section discusses the immune components of TME and provides a few brief examples of cancer-immune cell crosstalk.

2.1.1. Macrophages

Macrophages are mononuclear phagocytic cells that are considered the primary immune infiltrate of the TME. Macrophages in the TME are termed 'tumor-associated macrophages' (TAMs) and account for up to 50 % of most solid tumors. TAMs are highly plastic cells and respond to

Table 1
Summary of list of 3D microengineered models that recapitulated the heterogenous TME features.

Study	Model	Fabrication Technique	Cancer type	Media Composition	Assays and readouts	Key outcome	Reference
Tumor-Stromal Interactions	Spheroid	384-well round bottom plates. 200–300 μm spheroids.	Breast Cancer	Spheroid Medium: Phenol red free Dulbecco's modified Eagle's Medium + 1 % Fetal Bovine Serum + 0.1 nM estrogen + Penicillin-Streptomycin + pyruvate	Tumor spheroid invasion in a complex hydrogel. - Porosity of hydrogel - Influence of CAFs on breast cancer invasion - CXCL12-CXCR4 mediated migration	**Influence of stromal and ECM composition on tumor invasion.** Matrix embedded spheroid model showed fibroblast-led invasion of cancer cells within a 3D matrix. Involvement of CXCL12-CXCR4 signaling on cancer progression	[108]
	Organoid	Hanging drop method.	Lung Cancer	StemPro human embryonic stem cell serum-free medium	Influence of CAFs on tumor formation - Patient derived organoid - Growth rate of tumor cells in the presence of CAFs	**Assessment of lung organoid proliferation in the presence of podoplanin CAFs.** Growth promoting effect was pronounced in co-culture organoids.	[150]
	Microfluidics	Rod-based PDMS model	Breast Cancer	Not available	*In vitro* 3D TME migration model. - ECM influence on MMP production - Migration potential of cancer cells in the presence of CAFs and fibroblast.	**Role of CAFs and ECM components**. Fibronectin rich matrix showed increased migration of cancer cells in the presence of normal fibroblast with higher MMP secretion.	[200]
	Microfluidics	Organotypic vascularized tumor-on chip model (PDMS)	Breast Cancer	70:30 ratio of Endothelial Growth Medium -2 bullet kit +50 ng/mL VEGF and cancer cell media (DMEM+Fetal Bovine Serum+ L-glutamine+Penicillin Streptomycin)	3D intravasation model - Intravasation of cancer cells through vasculature - Cytokines signals involved in tumor-stromal crosstalk	**Tumor-Vascular crosstalk in metastatic cascade**. Presence of vasculature increased the invading potential of cancer cells. In turn disrupted the vascular network leading to formation of thinner and more permeable vessels.	[195]
	3D Printing	Extrusion based 3D printer	Breast Cancer	Dulbecco's modified Eagle's medium Complete Media+10 % Fetal Bovine Serum and 1 % Penicillin-Streptomycin)	Breast TME model - Low-cost setup for printing. - Basic viability screening.	**Tumor-Adipocyte interaction in breast cancer.** Proof of concept to demonstrate the use of custom-built printers for mimicking breast TME.	[245]
	3D Printing	Acoustic based 3D printer	Colorectal Cancer	Not available	Cancer invasion dynamics - Time lapse imaging based migratory studies. - Drug screening model.	**Invasion model for colorectal microtissue- CAF interaction.** Observed outward migratory potential of tumor cells towards CAFs.	[247]
Tumor-Immune Interactions	Spheroid	Embedded spheroid model	Breast Cancer and Pediatric Osteosarcoma	Rosewell Park Memorial Institute /Dulbecco's modified Eagle's Medium +10 % Fetal Calf Serum+1 % Penicillin-Strepotomycin	Macrophage polarization model - Protein secretion quantification. - Drug response screening.	**Phenotype of macrophages in spheroid co-culture.** Hydrogel embedded spheroid influenced the polarization of macrophages confirming the synergistic combination between tumor and ECM cues.	[118]
	Organoid	Matrix embedded method	CRC, Non-small-cell lung cancer	Dulbecco's modified Eagle's Medium /F12+2 mM ultra glutamine I+10 mM HEPES + Penicillin-Streptomycin+10 % Noggin conditioned medium+1x B27 without vitamin A+50 ng/mL human EGF	*In vitro* T cell sensitivity assessment - Inducing T cell reactivity. - Specificity and killing ability of T cells.	**Tumor reactive T-cell response to cancer organoids.** Delineating interaction and mechanism of T cells in epithelial organoids.	[156]
	Microfluidics	Parallel channel PDMS model	Pancreatic Cancer	Iscove's modified Dulbecco's Media supplemented with 5 % human serum and 1 % Penicillin-Streptomycin	3D macrophage migration system - Macrophage sensitivity - Cytokine expression	**Evaluating Physical and Chemical cues in the TME.** Macrophage migration remained elevated when exposed to a saturating concentration of recombinant IL-8 or CCL2.	[206]
	Microfluidics	Parallel channel PDMS model	Hepatocellular carcinoma	R10 medium supplemented with DRAQ7 containing AIM-V 2 % human AB serum plus rIL-2 with/without addition of IFN-γ and TNF-α	3D T cell preclinical model - T cells chemotaxis migration. - Antitumor response of T cells	**Testing the functionality of engineered T cell.** 3D model shows the effect of oxygen level and environmental factor on T-cell function	[212]

(*continued on next page*)

Table 1 (*continued*)

Study	Model	Fabrication Technique	Cancer type	Media Composition	Assays and readouts	Key outcome	Reference
	3D Printing	Extrusion based 3D printer	Glioblastoma	1:1 of Roswell Paark Memorial Institute +Dulbeccos Modified Eagle Medium+10%Fetal Bovine Serum+1% Penicillin-Streptomycin	3D brain model for tumor biology studies - Paracrine and juxtracrine signaling assays. - Transcriptomic profiling	**Mini Brain to study glioblastoma- macrophage interaction** Co-culturing of macrophages with glioma cells increases the invasive potential of glioma cells.	[249]
Complex TME Interactions	Spheroid	Parallel channel PDMS model	Hepatocellular carcinoma	Endothelial Growth Medium-2 +1 % antibiotic-antimycotic	Perfusion model for drug delivery - Secretome analysis. - Drug uptake through vascular dynamic evaluation.	**Vascularized tumor spheroid model for enhanced drug delivery.** Tri-culture of multicellular spheroid with perfusable vasculature showed increased uptake of drug.	[130]
	Spheroid	Droplet based microfluidic spheroid formation	Breast Cancer	Iscoves Modified Dulbeccos Medium+10 % Fetal Bovine Serum+1 % antibiotic-antimycotic+10 μg/mL human recombinant insulin, 0.5 mM 2-mercaptoethanol+0.1 mM hypoxanthine+0.016 mM thymidine	Dynamic tumor-stromal interaction - Bioinspired ECM scaffold. - Immunomodulation of macrophages - Oxidative stress and apoptosis	**High throughput breast TME model.** Upregulation of protein involved in cellular interaction and immunomodulation.	[127]
	Organoid	Air-liquid and Matrigel® on top method	Melanoma	40 % Advanced Dulbecco's modified Eagle's Medium/F12 medium+ 50 % Wnt3a + RSPO1+ Noggin-conditioned media+ 10 % inactivated fetal calf serum+ 1 mM HEPES+1 × Glutamax +10 mM Nicotinamide + 1 mM N-Acetylcysteine + 1 × B27 without vitamin A +0.5 μM A83-01 + 1 × Penicillin-Streptomycin + Glutamine + 10 nM Gastrin +10 μM SB-202190 + 50 ng/mL EGF+ 50 ng/mL FGF-1	Organoids for immunotherapy screening - Verification of parental tumor feature - Immunotherapeutic screening. - Cytotoxicity assessment.	**Patient derived organoid model for lymphocyte cytotoxicity.** Patient derived organoid preserved intra-and inter-tumor heterogeneity. $CD8^+$ T cells exposed to *anti*-PD1 exhibited more cytotoxicity.	[161]
	Microfluidics	Additive photopatterning	Breast Cancer	50 % endothelial media and 50 % monocyte media	Immune cell infiltration study - T cell infiltration into hydrogel. - Phenotypic changes of immune cells	**Evaluating the role of hypoxia as well as cellular interactions in immune cell recruitment.** Spheroid models had more recruitment of T cells with increased expression of CCL4, CCL5, and CCL11	[218]
	Microfluidics	Parallel channel PDMS model	Pancreatic Cancer	Endothelial Growth Medium-2	Immune cell migration dynamics - Migratory behavior of T cells in the presence of various cells of TME. - Cytokine expression of activation state of T cells	**Infiltration of T cells.** Quantitative assessment of T cell infiltration in the presence of other TME cellular component showed T cell trafficking by ECs.	[222]
	3D Printing	3D Bioplotter system	Glioblastoma	Mixed medium (1:1 ratio) of Dulbecco's modified Eagle's Medium and astrocytes medium.	Heterogenic glioma TME - Biomechanical evaluation of bioink - Transcriptomic comparison between 2D and 3D model.	**Sophisticated Glioblastoma Model** Proof of concept assessess the printing method to incorporate penta–culture of different cell types.	[254]

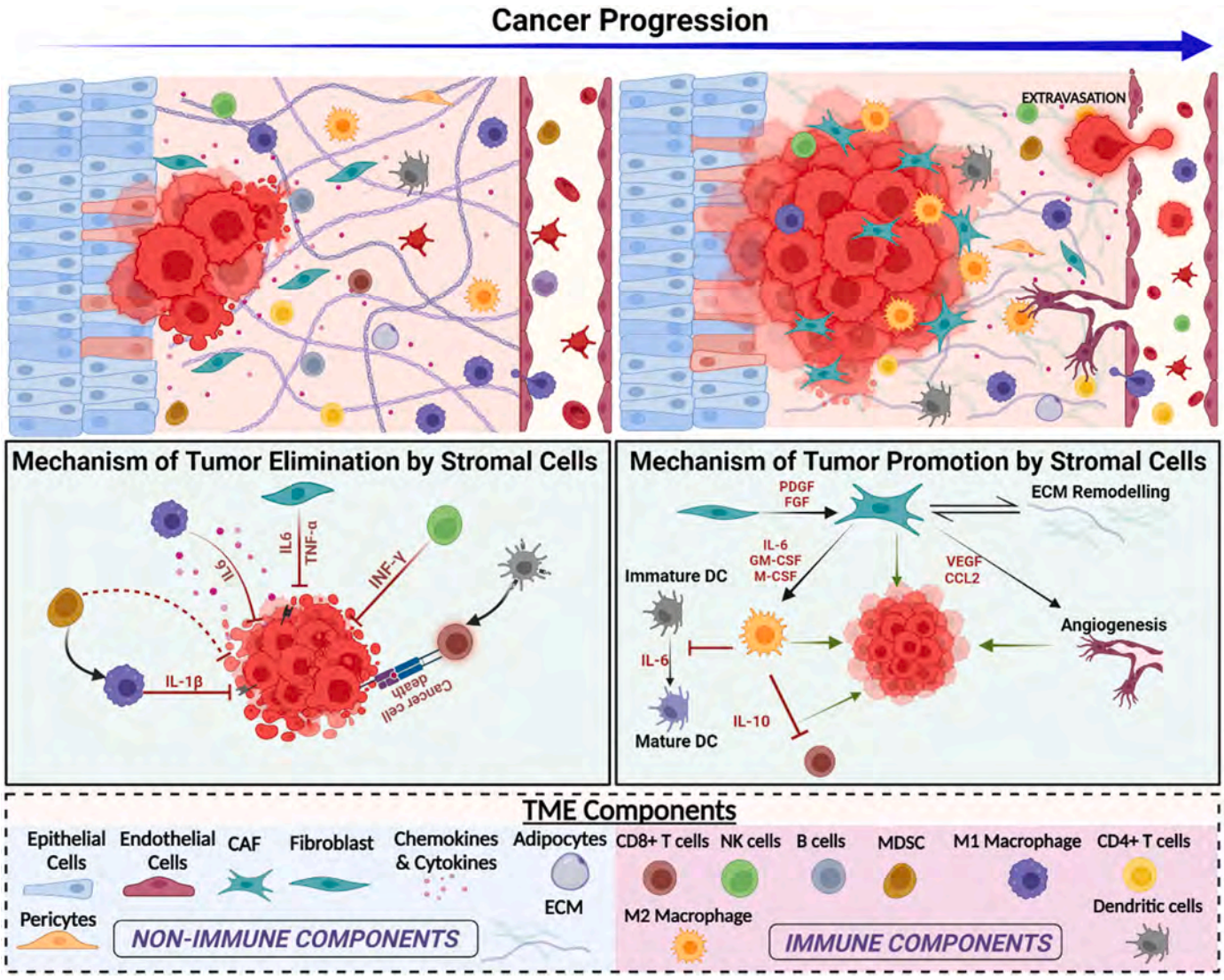

Fig. 1. Schematic representation of TME components and their role in cancer progression. Dynamic TME constantly evolves as the malignant cells undergo successive cellular events. During the initial stages of cancer development cellular components of TME such as fibroblasts, M1 macrophages, NK cells and DCs aims at eliminating the neoplastic cells through various mechanism. As cancer progress, tumor cells hijack the microenvironmental components to favor its growth. During this phase of cancer progression, there is a multifaceted crosstalk between tumor-stromal-immune components as well as between stromal-immune components. Fibroblasts within the TME are actively involved in ECM remodeling as well as produces cytokines such as IL-6 and CSF to macrophages to differentiate them into TAMs (M2 macrophage). Though initially TME components looked like just a bystander, they play a pivotal role in cancer progression starting from development, all the way through metastasis to a distant site. Thus, it is a natural interest to mechanistically delineate the complex cellular interactions of TME. Created with BioRender.com.

microenvironmental cues such as cytokine factors and nutrient constraints. Based on their activated phenotype, TAMs are classified as (i) M1-classically activated macrophages and (ii) M2-alternatively activated macrophages [35]. M1 macrophages release proinflammatory cytokines such as IL-6, IL-12, and TNF-**α** and play a vital role in anti-tumor functionality. On the other hand, M2 phenotypes are pro-tumorigenic and are characterized by anti-inflammatory cytokines such as IL-10 and TGF-β [36]. Alongside these factors, the other key regulator of TAMs fate is dictated by its distribution within the TME. Specifically, macrophages located in the tumor core that are hypoxic in nature are highly immunosuppressive (i.e., M2) and are known to produce angiogenic factors. TAMs are known to be involved in cancer progression, exhibiting an M1 phenotype during the initial stages and an M2 phenotype during the later stages of cancer [37]. Furthermore, various studies have highlighted the tumor-promoting effects of chemokines and cytokines derived from TAMs. For instance, prolonged exposure to TNF-**α** a well-known pro-inflammatory cytokine is shown to increase cancer stem cells in the oral squamous cell carcinoma [38]. Likewise, TAM-derived IL-6 is involved in cancer cell proliferation and plays a key role in inhibiting apoptosis through the activation of the JAK/STAT pathway [39]. Thus, unresolved chronic inflammation leads to an imbalance in pro-inflammatory cytokines and favors the development of tumors. Furthermore, TAM-related cytokines such as transforming growth factor-beta (TGF-β) and IL-10 can alter the recognition of antigen-presenting cells (APCs), thereby facilitating immune evasion and fostering a metastatic milieu [40].

2.1.2. Dendritic cells

Dendritic cells (DCs) are one of the major APCs that are actively involved in the immunosurveillance [41]. Like other immune cell types, DCs are further divided into conventional DCs (cDCs), plasmacytoid DCs (pDCs), and monocyte-derived DCs (moDCs) [42]. cDCs play a critical role in tumor elimination by cross-presenting tumor antigens and through elevated cytokine production [43]. Growing bodies of research

have highlighted the significance of DCs cytokines such as IL-12 and INF-ɣ in priming T cell-mediated anti-tumor effects [44,45]. Though DCs are known to inherently possess anti-tumor properties, cancer cells within TME can create an environment supportive of its growth. DCs are no exception to this, and mounting evidence has confirmed the impaired functional state of DCs within the TME. For instance, expression of chemokines such as C–C motif chemokine ligand (CCL) – CCL19 and CCL21 impairs the migration and excludes DCs from the tumor [46]. Additionally, environmental factors like hypoxia and nitric oxide production are crucial factors underlying the deficiencies of DCs in TME [47].

2.1.3. T cells

T-lymphocytes (T cells) belonging to adaptive immunity are potent anti-cancer effector cells. T cells within the tissue microenvironment are classified as naïve, memory ($CD8^+$), helper ($CD4^+$), and regulatory (T_{reg}) lymphocytes [48]. Effective priming of T cells regulated by the APCs is crucial for the cytotoxic trafficking of the tumor [49]. Programmed Death-1 (PD-1) and Cytotoxic T-Lymphocyte Antigen-4 are the two well-known T cell checkpoint receptors that regulate and fine-tune their immune response [50]. $CD4^+$ T cells orchestrate anti-tumor response by producing cytokines and chemokines with pro-inflammatory properties, whilst $CD8^+$ cells exert a cytotoxic reaction that directly kills neoplastic cells [51]. Though lymphocytes keep cancer under check, evolving tumors subvert the anti-tumor immunity, facilitating immune evasion and destruction. For instance, tumor cells actively evade immune destruction by upregulating T cell checkpoint molecules, thus limiting the T cell's anti-tumor response [52]. At the same time, T lymphocytes are rendered impotent by the TME through prolonged weak antigen stimulation, thus enabling immune escape [53]. Tregs, on the other hand, exhibit a distinct cytokine profile from that of $CD4^+$ and $CD8^+$ T cells with immunosuppressive function [54]. Their notable mechanism of action involves the secretion of inhibitory cytokines, including IL-10 and TGF-β [55]. They impede effective T cell priming and inhibit the activity of cytotoxic T cells, thus fostering an environment conducive to immune evasion and tumor progression.

2.1.4. B cells

B cells, the second population of adaptive immune components within the TME, have recently been appreciated for their role in anti-tumor immunity. Principally, B cells serve as APCs that promotes T-cell mediated anti-tumor response [56]. In the tumor milieu, B cells perform a plethora of roles mediating both pro- and anti-tumor effects [57]. B cells within specialized structures called tertiary-lymphoid structures **[**Glossary**]** are known to orchestrate $CD8^+$ cytotoxicity through the secretion of IL-12 and INF-ɣ [58]. A subtype of B cells called regulatory B cells (B_{regs}), primarily contributes to the pro-tumorigenic effects. In specific, B_{regs} downregulate T-cell-specific immune responses through the secretion of IL-10 and TGF-β [59,60]. Moreover, they create an immunosuppressive environment through the PD-1/PDL-1 axis [61].

2.1.5. Natural Killer cells

Natural Killer (NK) cells are innate lymphoid cells that actively eliminate tumor cells. These cells function by activating signals originating from NK-inhibitory receptors and NK-activating receptors [62]. NK cells maintain equilibrium within the TME by eliminating tumor cells through direct contact or through cytokine secretion [63]. NK cells are classified as INF-ɣ [$CD56^{high}CD16^{low}$] and cytotoxic NK [$CD56^{low}CD16^{high}$] cells based on surface marker expression of CD56 and CD16. However, environmental factors such as TGF-β produced by tumor cells and cellular metabolism within the TME can impair NK cell functions [64,65].

2.2. Stromal constituents of TME

Besides immune cells, stroma comprises other support cells such as fibroblasts, adipocytes, and endothelial cells that assist in tumor progression. It has been well established and accepted that cancer cells exist and co-evolve with the surrounding stromal components, creating an environment permissive to their growth and survival [5]. This section highlights some of the standard stromal cells (non-immune) within the TME and their role in tumor immunity.

2.2.1. Cancer-associated fibroblasts

Fibroblasts in the tumor milieu are termed CAFs. CAFs are the key stromal component which have been shown in numerous studies to play a pivotal role in tumor growth, progression, and immune evasion [66]. CAFs are a highly heterogeneous population suggesting their functional diversity. Recent research identified three subtypes of CAFs, namely myofibroblast CAFs, inflammatory CAFs, and antigen-presenting CAFs [67]. Though most of the CAFs have tumor-promoting effects, some populations of CAFs, namely restraining CAFs (rCAFs), exhibit a tumor-restraining effect [68]. However, an increasing number of research reported the role of CAFs in sculpting an immunosuppressive microenvironment favorable for tumor growth [69]. For example, CAFs expressing CXCL12 cytokine inhibit the migration of $CD8^+$ T cells in the pancreatic ductal adenocarcinoma [70].

2.2.2. Adipocytes

Cancer-Associated Adipocytes are vital TME contributors in angiogenesis, apoptotic resistance, and metastasis [71]. Cancer-Associated Adipocytes are regarded as lipid-enriched cells that act as a source of energy to cancer cells, thereby promoting cancer growth. These cells in TME, through direct cell-to-cell contact or by releasing signaling molecules such as adipokines and hormones, promote cancer invasion and immune resistance within the TME [71]. Adipocytes are recruited to the microenvironment via chemotactic factors such as TNF-α and IL-6 that are commonly secreted by the tumor cells. Additionally, other stromal cells within TME like CAFs also recruit adipocytes through the secretion of FGG-2 and TGF-β.

2.2.3. Endothelial cells and pericytes

Endothelial cells (ECs) within tumor microvasculature are phenotypically, genetically, and functionally distinct EC populations [72]. Growing bodies of experimental studies through single-cell RNA sequencing (sc-RNAseq) have identified dynamic gene landscape specific to tumor ECs [73,74]. Cancer cells express various soluble and angiogenic chemokines such as vascular endothelial growth factor, basic fibroblast growth factor, and angiopoietin to initiate angiogenesis. The overall process results in immature and aberrant vessel formation with abnormal pericyte coverage [75]. Pericytes are mural-supportive cells that play a crucial role in blood vessel stabilization and maturation [76]. Preceding findings have suggested the dysregulated role of tumor EC-pericyte communication on disorganized blood vessel formation [77]. These processes eventually lead to the inhibition of chemoattractant expression by ECs and prepare the environment favorable for cancer metastasis. Intriguingly, additional roles of pericytes associated with modulating an immunosuppressive TME are reported [78,79]. For instance, blunt-ended vessels provide an inconsistent blood flow to the tumor cells and limit the supply of nutrients to the cells since the functional vessel is far off from the cells in demand. These processes lead to hypoxic and acidic TME that mediates immunosuppressive immune cell infiltration and favors creating an immunosuppressive TME. For example, hypoxic-induced factors recruit TAMs and stimulate them into M2 phenotype [80]. Additionally, during tumor angiogenesis, impaired interactions between ECs and pericytes leads to dysfunctional tumor vasculature and eventually leads to evasion of the immune surveillance [77].

As discussed above, cancer development involves complex

interactions between various cell types, organs, and organ systems. Therefore, it is essential to incorporate different cell types into *in vitro* models to gain a better understanding of the mechanism that governs cancer progression. By increasing the cellular complexity of such models, we can develop more physiologically accurate representations of cancer. As we further our understanding of the intricate cellular interactions within the TME, we will be able to identify new strategies for targeting cancer cells, which are constantly evolving and multiplying.

3. Engineered models of complex stromal-immune interactions within the TME

As of 2023, only 3.5 % of oncology drug candidates have progressed to clinical trials, creating a bottleneck in precision medicine development [81]. To develop more reliable therapeutic regimens, comprehensive testing platforms must incorporate TME elements such as cellular heterogeneity, cell-cell, cell-ECM interactions, and spatial architecture. Dichotomy cellular interactions within TME can exert pro-tumoral/anti-tumoral environment for tumor growth [82]. Therefore, it is crucial to mimic this crosstalk in *in vitro* models to better comprehend cancer mechanisms right from tumor initiation, proliferation, and metastasis to better understand the tumor biology and aid in development of effective drug candidates that can prevent the relapse of cancer [83]. In that line, 3D-engineered *ex vivo* models are an ever-growing field for both mechanistic studies as well as for predicting patient response [84,85]. As outlined in Fig. 2, technological advancements have led to the development of various sophisticated 3D cancer models with increasing biological complexity. However, the complexity of *in vivo* models as whole cannot be recapitulated but the existing 3D-engineered models, such as multicellular spheroids, tumor organoids, 3D scaffold-based models, and microfluidics aim to mimic a 'minimally functional unit' while capturing the essential components for studying various aspects of tumor progression [86,87]. In the ensuing section, we discuss in detail four engineered models (spheroids, organoids, microfluidics, and 3D printed models) owing to their ability to represent *in vivo* TME.

3.1. Spheroid models

Remarkable advancement in 3D culture techniques has led to the development of models that faithfully recapitulate various processes of tumor growth. In that line, spheroid models have been one of the most versatile and commonly used 3D models for oncological studies. Spheroids are 3D cellular aggregates that capture several key features of a solid tumor, such as the gradient of nutrient diffusion, oxygenation, necrotic core, and cell-cell communications [88,89]. These inherent features of spheroids make them appropriate models for drug screening studies [90,91]. Based on the engineering techniques used for the fabrication of spheroids, they are classified into scaffold-based and scaffold-free models [Box 1]. The most common scaffold-free fabrication

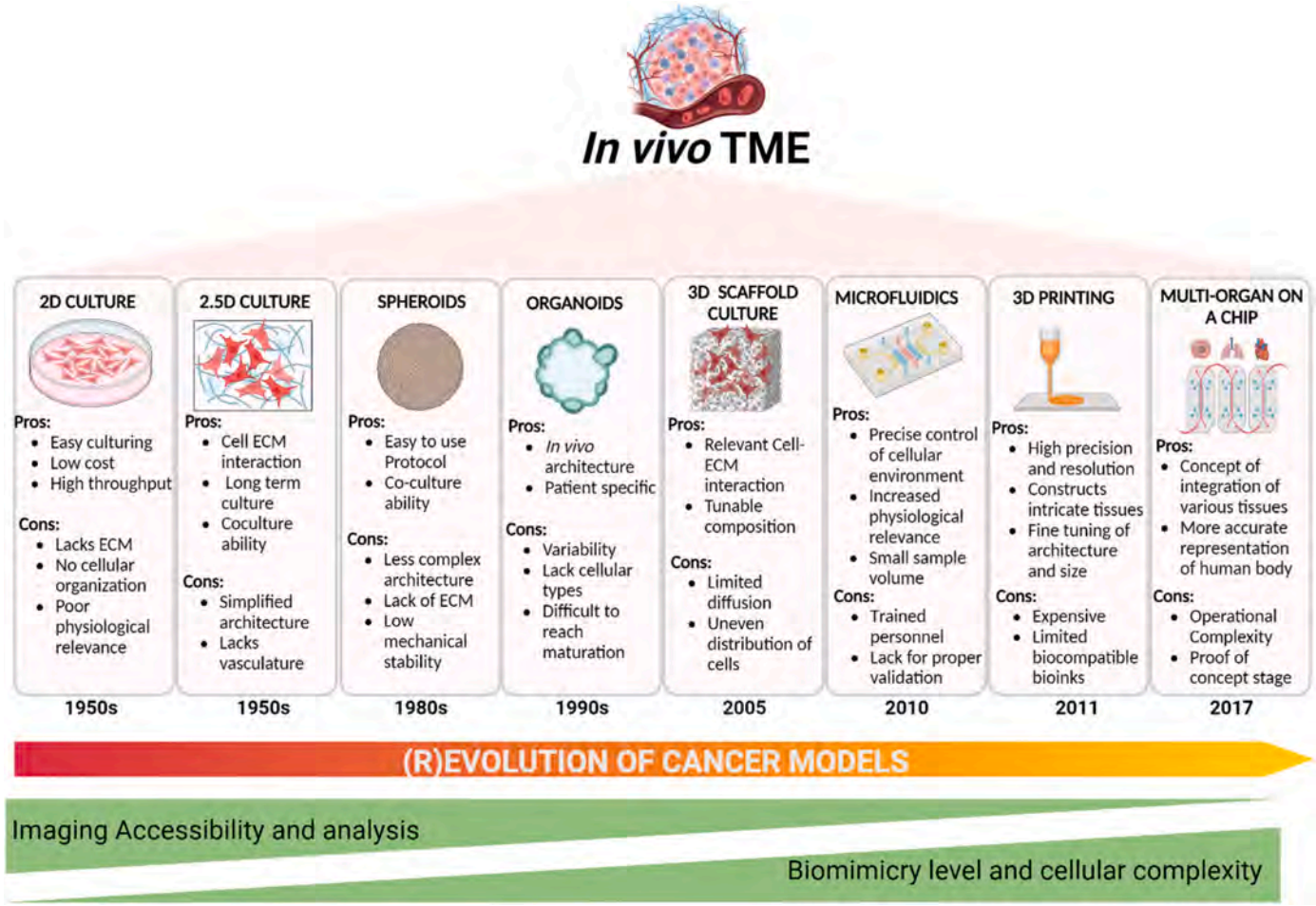

Fig. 2. Evolution of 3D-engineered cancer models. Highlights the evolutionary progression of cancer models, starting from traditional 2D cell cultures towards more sophisticated 3D models. The transition to 3D models, including organoids, spheroids, and microfluidic models, has allowed researchers to capture the complexity of TME more accurately. By incorporating tissue engineering principles and advanced imaging techniques, these models offer a closer representation of *in vivo* tumor behavior, enabling an enhanced understanding of cancer biology and facilitating the development of more effective therapeutic strategies. Created with BioRender.com.

Box 1
Engineered approach for spheroid and organoid fabrication

Spheroid models are typically classified according to the type of cell they contain, and the fabrication technique used. Based on cell type spheroids are categorized as multicellular tumor spheroids (mostly derived from established cell lines), tumorospheres (formed of cancer cells derived from tumor tissue) and heterotypic spheroids (spheroids containing cancer, immune and stromal cells) [257]. Among these heterotypic spheroids are of great interest owing to their close reciprocation of the intricate TME network. Scaffolded and scaffold free spheroids are the most widely used classification based on fabrication technique. Scaffold free method relies on self-organization of cells and spheroids that are cultured without an external matrix. Hanging drop, low-adhesion and magnetic levitation are common scaffold free techniques. On the other hand, in scaffolded techniques, spheroids are cultured in a controlled ECM that are derived from natural or synthetic material. Matrix on top, matrix encapsulated, and spinner flasks are popular technique for scaffolded spheroid generation. Cell source and fabrication method has to be carefully chosen based on the application/model the spheroids are used for [93].

Organoids are similar to spheroids but are superior in such a way that organoids can mimic the function and structure of the tissue better than spheroids. Organoid 3D models are very useful in immunological studies due to their ability to retain the immune cell spectrum. Unlike spheroids, organoids require ECM for their generation. Based on the ECM used for cultivation, organoids are classified as native and reconstituted TME models. Native TME organoids aim to preserve the endogenous immune and stromal cell population. Air Liquid Interface (ALI) and microfluidic organoid cultures are the commonly used native organoid culture methods. Tumor organoids are formed by enzymatically dissociating tumor tissue, and the immune/stromal cells are exogenously added to the formed organoid. Submerged culture is the widely used technique for reconstituted TME spheroid generation [258].

techniques are hanging drop [92,93], liquid overlay [94], and magnetic levitation [95]. Low retention, gravity, and surface tensions are instrumental in forming scaffold-free spheroids. On the other hand, micropatterned plates [96], matrix embedded [97], spinner flasks [98], and microfluidic cultures [99] are the standard methods for scaffold-based spheroid generation. Scaffolds used in these techniques are either a natural hydrogel material like collagen I, Matrigel®, or alginate or a synthetic material like poly (ethylene glycol) or polycarbonate. The scaffold-based approach offers additional advantages of cell-matrix interaction through external cues that support cell adhesion to the hydrogel. Classification of spheroids based on their fabrication method is reviewed in detail elsewhere [91,100–102]. These engineered techniques allow for controlled manipulation of cells to form into spheroids, making them appropriate models for studying tumors.

Cancer spheroids can be established from various cell types, including cell lines, patient-derived cells, stem cells, engineered cells, and co-culturing with other non-cancerous cells. Among various cell sources, the formation of spheroids from cell lines is relatively easy and less complex. Recently, an anti-cancer mitochondrial inhibitor drug was tested on pancreatic cancer spheroids formed from an immortalized pancreatic carcinoma cell line, and the results showed increased effectiveness in inhibiting spheroid growth when combined with radiation therapy [103]. Another study compared the response of bladder cancer cells to doxorubicin treatment under 3D and 2D conditions. Particularly, this study generated spheroids using the hanging drop technique and compared the presence of microvilli with the mono-culture of cells. Findings from imaging-based analysis confirmed the microvilli projections in 3D spheroid cultures as opposed to 2D mono-culture, suggesting the close resemblance of spheroids to *in vivo* tumors. Additionally, the drug response studies showed increased resistance in 3D spheroid culture compared to 2D mono-culture [104]. With the advent of CRISPR/Cas9 technology, genomic mutations can be introduced into cells to replicate the disease phenotypes *in vitro* and *in vivo*. Remarkable engineered models have been reported employing the gene editing tool. For instance, using Cas9 genome editing, a tissue inhibitor of metalloproteinase-2 was inhibited in an ovarian cancer spheroid model. It was observed that tissue inhibitor of metalloproteinase-2 inhibition increased cancer cell proliferation and altered the sensitivity of the spheroids to chemotherapies [105].

To further the research in utilizing spheroid models for cancer genomics studies, a study compared genomic-wide CRISPR screens between 2D culture and 3D spheroid models. This study developed a 3D spheroid system that propagates 200 million lung cancer cells in a single spheroid using low attachment plates for high throughput drug screening. Findings from pathway enrichment and phenotype distribution analyses suggested that 3D spheroid screens closely reflect the features of *in vivo* cancer genes [106]. These studies have enabled the substantial improvement of *in vitro* models and their potential applications for cancer studies. Though all these studies provided valuable information about cancer processes, most studies focused only on cancer cells, isolating them from their environment. Hence, models must be developed to capture the cellular interactions and signaling pathways driving cancer progression. In the following section, we will elaborate on how spheroid models are used to study various tumor-stroma, tumor-immune, and tumor-complex interactions.

3.1.1. Spheroid models for tumor-stromal interactions

Metastasis of cancer cells from the primary tumor to the distant site is among the leading causes of cancer-related death. In this context, numerous groups have utilized 3D heterotypic spheroid models [Box 1] to mechanistically unravel the signaling circuits dictating these processes. For instance, colorectal cancer (CRC) spheroids were co-cultured with fibroblasts to determine the significance of direct contact between CAFs and cancer cells. The analysis revealed that the activation of SRC receptors, triggered by the surface expression of FGF-2 on fibroblasts, promoted cancer cell migration [107]. To better simulate ECM stiffness and cellular interactions in engineered models, a study by Liu et al. devised a tunable hydrogel scaffold using alginate and collagen I. Heterotypic spheroids containing breast cancer cells and mammary fibroblasts were fabricated in a low adhesion 384 well plate (Fig. 3A (i)). Immunofluorescent staining showed that fibroblasts in co-culture were more mobile in tunable hydrogel than the standard collagen I matrix. Building upon these findings, this study assessed the involvement of the CXCL12-CXCR4 axis, which is a known contributor to cancer cell invasion. Two spheroids (fibroblast spheroids expressing CXCL12 and cancer spheroids expressing CXCR4) were embedded in the tunable hydrogel to assess this signaling axis. Using fluorescent microscopic evaluation, it was observed that cells from both spheroids exhibited anisotropic migratory behavior, forming a bridge between them (Fig. 3A (ii)). Surprisingly, spheroids composed of wild-type cells lacking the expression of these signaling molecules had a sun-burst migratory pattern (Fig. 3A (iii)). In sum, this study utilized a novel hydrogel-based 3D invasion model to confirm the directed migration of cancer cells toward a chemotactic gradient [108].

Two studies were conducted to evaluate the impact of ECM stiffness on cancer-stromal crosstalk. The study by Saini et al. utilized a

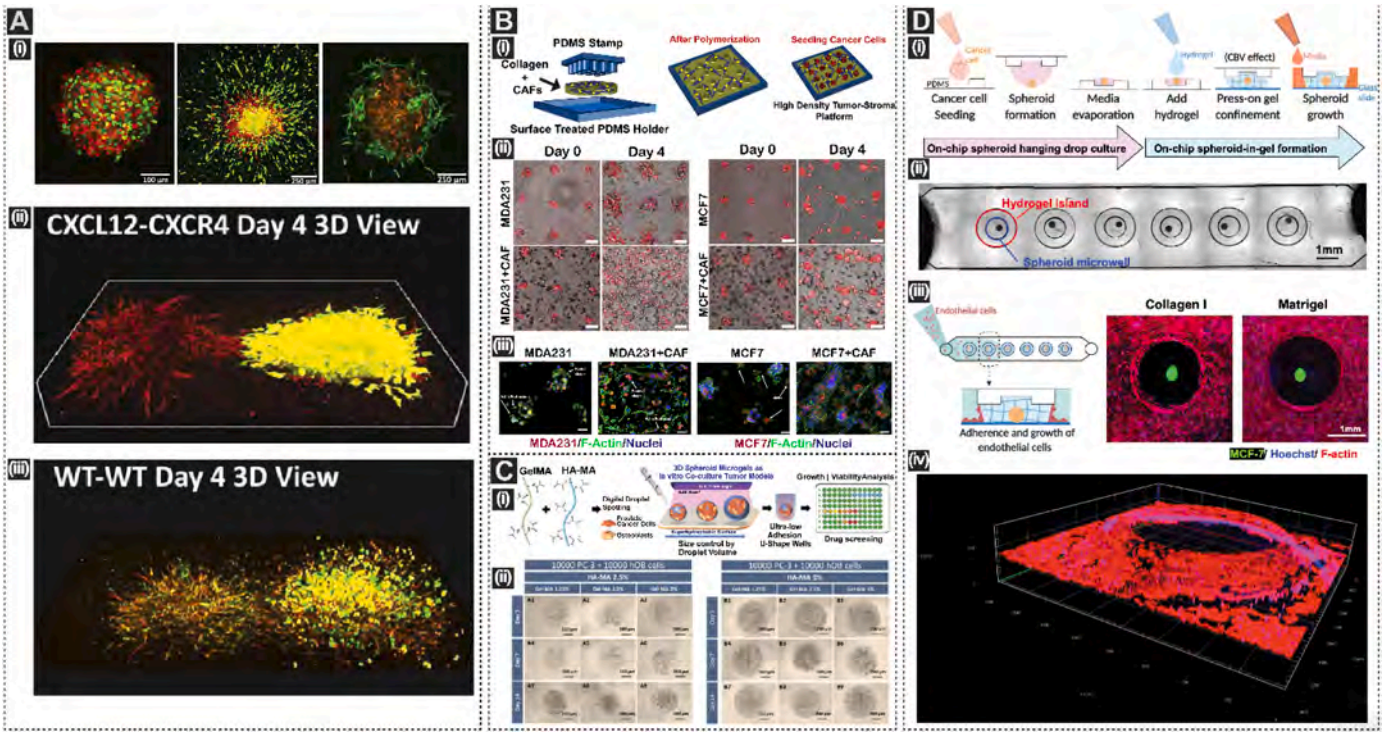

Fig. 3. 3D Spheroid Models to Study Tumor-Stromal Interactions. A) Alginate based 3D invasion model. **(i)** Comparison of invasion of cancer spheroid across three different methods. Cancer spheroids in round bottom plate (left), spheroids in alginate scaffold (middle), and spheroids in collagen I matrix (right). Red – MDA 231 cells, Green – Fibroblasts. **(ii)** 3D view of CXCL2 (red) - CXCR4 (green) driven migration between spheroids embedded in alginate scaffold. **(iii)** Migration of wild type MDA 231 and fibroblast spheroids embedded in the aliginate scaffold. Adapted from Liu. et al. with permission from Elsevier [Acta Biomaterialia], Copyright 2018 [108]. **B)** 3D organotypic tumor-stroma microengineered model. **(i)** Schematic representation of fabrication of 3D spatially organized tumor-stroma model using PDMS stamps and micro-molding technique. **(ii)** Phase contrast images showing the invasion behavior of MCF and MDA-231 cells in the presence and absence of CAFs. Highly invasive MDA-231 cells showed increased single cell migration in the presence of CAFs and less invasive MCF-7 cells showed colony formation in the co-culture condition **(iii)** Immunofluorescent images showing the cytoskeletal organization of spheroids under varying culture conditions. Adapted from Saini. et al. with permission from Elsevier [Biomaterials], Copyright 2020 [109]. **C)** In-air production of 3D microgel-based co-culture spheroid for high throughput drug screening. **(i)** Schematic depicting the generation of 3D photo-crosslinkable heterotypic tumor spheroid assembly using superhydrophobic surfaces. Left – Chemical structure of HA-MA and GelMA hydrogels, Center – Generation and size control of co-culture spheroids using superhydrophobic surface and droplet dispensing. Right- Application of spheroids for drug screening and growth rate monitoring. **(ii)** Optical micrographs of co-cultured prostrate spheroids at two different HA-MA concentrations. Left – Monitoring of spheroid growth in HA-MA 2.5 % and varying GelMA concentrations. Right – Monitoring of spheroid growth in HA-MA 5 % and varying GelMA concentrations. Adapted from Antunes. et al. with permission from Elsevier [Acta Biomaterialia], Copyright 2019 [115]. **D)** Rapid press-on hydrogel-based 3D spheroid generation. **(i)** Schematic representation of on-chip spheroid formation using hanging drop technique followed by generation of spheroid-in-gel formation using press-on patterning. **(ii)** Bright field images of single array of microwells containing spheroids in a collagen I scaffold. Red circle highlights the hydrogel regions and blue circle highlighting the spheroid microwell **(iii)** Left- Schematic representation of co-culture of spheroid with endothelial cells using the spheroid-ingel formation. Right- Immunofluorescent staining of MCF spheroid surrounded by HUVECs. **(iv)** 3D rendered image of vasculature formed inside the microarray chip (Red: Actin, Blue: Hoechst). Adapted from Su. et al. with permission from MDPI [Biosensors], Copyright 2018 [116].

micropatterned tumor model (Fig. 3B (i)) to examine the effect of CAFs on tumor development and stromal desmoplasia **[**Glossary**]**. The study utilized imaging quantification, including real-time imaging and immunofluorescent staining, to demonstrate that CAFs enhanced cancer migration compared to mono-culture conditions (Fig. 3B (ii-iii)). This study also identified that the pro-fibrotic cytokine (PDGFR) produced by tumor cells is a significant contributor to stromal stiffness. Overall, the study provided valuable insights into the biophysical and biochemical cues affecting tumor-stroma interactions and drug responses in the context of TME [109,110]. Another study by Yue et al. evaluated the impact of ECM stiffness on tumor-adipocyte interactions and its influence on adipogenesis **[**Glossary**]** in breast cancer. They used a stromal cell-laden microwell array system with tunable TME composed of gelatin methacrylate (GelMA) to mimic normal and healthy mammary tissue. Nanoindentation studies revealed that breast cancer spheroids increased the surrounding stiffness by activating stromal adipocytes. This study also investigated how tumor spheroid aggressiveness affects adipocyte differentiation, finding that cancer cells influence adipogenesis in an ECM-stiffness-dependent manner. Overall, this research highlighted the crucial role of matrix stiffness in cancer-stromal interactions [111].

Crosstalk between ECs and tumor cells has been critically studied to capture key features of TME, such as angiogenesis. In this context, Shoval et al. conducted a study to investigate the interactions between ECs and tumor cells using a multicellular spheroid model. To account for patient heterogeneity, the authors used different sources of tumor cells to form spheroids, (M21, BR-58 patient-derived spheroids; BxPC3, A375 cell line spheroids), each with different tumor cells to ECs ratios. The study found that the invasiveness of cancer cells was influenced by the origin of the tumor cells, indicating that tumor cells exhibit distinct behaviors depending on their surrounding cellular components [112]. Another independent work utilized a 3D co-culture spheroid model of hepatocellular carcinoma and ECs to investigate a similar question. The co-culture of human umbilical vein endothelial cells (HUVECs) with normal and cancerous cells exhibited inherent variability depending on the type of cancer cell line involved. Confocal imaging of the co-culture spheroids indicated the tube formation of HUVECs, further supporting the liver cancer cells' ability to cause angiogenesis. Western blot analysis of signaling proteins revealed the upregulation of Akt/mTOR signaling in 3D cultures, which is crucial to induce angiogenesis. Finally, using the

3D co-culture model, this study demonstrated the effectiveness of three tyrosine kinase receptor inhibitors under conditions similar to those of the liver TME. Thus, the model shows the system's applicability as a dual-screening tool for comprehending biology and drug screening [113].

In recent years it has become widely recognized that obesity increases the risk of cancer. Currently, a stream of research is focused on understanding how the TME changes during tumor progression in obese patients. In this light, a recent study evaluated the role of breast adipose-derived mesenchymal stromal/stem cells (bASCs) on tumorigenic potential within TME using a spheroid co-culture model. To assess the phenotypic changes of bASCs in obese and lean patients, stromal cells were isolated from primary tissues collected from adjacent and distant tumor sites. Through extensive transcriptomics analysis, this study confirmed the changes in the secretome profiles of lean and obese bASCs, leading them to exhibit characteristics similar to CAFs. These transcriptomic profiles also supported the role of TME in functional changes of bASCs. To corroborate these findings with cancer-stromal crosstalk, hybrid spheroid culture was established. Results from this spheroid model showed that breast cancer-associated bASCs could de-differentiate into CAF-like cells that promoted proliferation, motility, and chemoresistance of tumor cells in the presence of high malignant breast cancer spheroids. These findings highlighted the tumorigenic behavior of bASCs in TME and their phenotypic differences in fueling cancer progression [114].

The use of spheroid models for drug screening has also gained notable momentum due to their ability to resemble critical features of tumors. However, traditional 3D spheroid generation techniques often result in varied size distribution, which is a major limitation. To overcome such limitations various studies have focused on employing and integrating advanced engineering techniques. For instance, a recent study used superhydrophobic surfaces **[**Glossary**]** to rapidly fabricate photo-crosslinkable hyaluronan-methacrylate/gelatin-methacrylate 3D spheroid microgels with precise control over size and co-encapsulation. These microgels were used to create heterotypic spheroids containing prostate cancer cells and human osteoblasts with varying cell densities (Fig. 3C (i)). To establish a relevant prostate-to-bone metastasis model, tumor and osteoblast cells were mixed at 1:1 to form the heterotypic spheroids (Fig. 3C (ii)). Alizarin Red staining for calcium deposition demonstrated the viability and mineralization of encapsulated osteoblasts. Additionally, Cisplatin cytotoxicity evaluation revealed increased resistance of 3D microgel spheroids to chemotherapeutic drugs compared to conventional 3D spheroids. Overall, this study reported a novel technique for the fabrication of reproducible spheroids for anti-cancer drug screening [115]. Leveraging advanced microfabrication techniques, a study by Su et al. demonstrated the encapsulation of individual spheroids into a hydrogel island using a press-on confinement technique (Fig. 3D (i)). To mitigate the need for manual transferring of spheroids onto a hydrogel scaffold, an on-chip spheroid culture was adopted. Briefly, MCF-7 cancer cell suspension was loaded onto the hydrogel confinement and flipped over to initiate spheroid formation. Using this hanging drop technique, spheroids were formed within just two days on-chip (Fig. 3D (ii)). Once spheroids were formed, the hydrogel (Collagen I/Matrigel®) was added directly onto them to create an in-place spheroid-in-gel system (Fig. 3D (iii)). To show the robustness of the proposed model in mimicking the physiological environment, HUVECs were added to the system to form vascularized spheroids (Fig. 3D (iv)). With this co-culture spheroid model, the team of investigators evaluated the system's applicability for drug screening. Overall, this study reported a simple and easy spheroid formation method without manual transferring [116].

It's worth noting that a recent study utilized a microfluidic platform for the formation and maintenance of patient-derived ovarian cancer spheroids. The devised platform consisted of 19 arrays of microwells for spheroid formation. Compared to standard 3D cultures (Matrigel®-based culture), the spheroids generated through microfluidics were reported to be superior, with higher uniformity in size and shape. Leveraging the microfabrication principle of this platform enabled the cultivation of spheroids from cell types that are difficult to culture with minimal number of cells, which helps advance engineered models from fundamental research to translational tools [117].

3.1.2. *Spheroid models for tumor-immune interactions*

Different strategies and techniques have been applied to incorporate and study the immune cell context of TME within spheroids models. In this line, a collagen I embedded spheroid model was developed to incorporate and study the effect of macrophages on synergistic tumor growth and drug treatment. The effect of macrophages on tumor growth was assessed under four different culture conditions where breast cancer spheroids were fabricated initially using agarose microwells and then embedded in a 4 mg/mL collagen I scaffold. It was discovered that the heterospheroid, which contained both macrophages and cancer cells, grew as a solid mass, unlike the other conditions. The cytokine assay revealed that EGF interaction between TAM-cancer cells is partially linked to lower oxygen levels. Moreover, this study emphasizes the significance of tumor cell proximity on TAMs differentiation [118].

Microglia are an essential type of immune cells in the central nervous system. Therefore, studying their interactions with glioma progression is of particular importance. In that line, a study by Wei et al. devised a brain-mimetic hydrogel system to comprehend the crosstalk between microglia on glioblastoma (GBM) progression. GBM spheroids were formed using low binding plates, and the formed spheroids were either mono- or co-cultured in GelMA disks with microglia preventing direct contact. In the presence of GBM cells, microglia showed changes in morphology and activation (Fig. 4A(i)). On the other hand, GBM cells in co-culture conditions were reported to have enhanced proliferation and reduced migration (Fig. 4A(ii)). This observation was consistent among various GBM samples. To couple these findings with the molecular level, transcriptomic studies were performed. Notably, Gene Ontology analyses revealed the upregulation of genes associated with proliferation and the downregulation of genes linked to invasion. These findings emphasized the importance of studying cellular crosstalk and provide valuable insights for screening [119].

The effectiveness of cancer treatments has been dramatically improved with the introduction of immunotherapies, which have become less harmful. Immunotherapy used alongside conventional treatments has emerged as a cornerstone in cancer therapy. Some breakthroughs in the field of immunotherapy include immune checkpoint inhibitors, specifically personalized CAR-T cell therapy. However, ongoing research focus on overcoming immunotherapy resistance and to enhance tumor immunogenicity which creates a need to better understand immune cells involvement and molecular mode of action during therapeutic intervention [120]. In this regard, numerous studies have explored ways to better understand the behavior of immunotherapies through spheroid models. Research in this field can be categorized into two main areas. The first area of focus involves understanding the mechanisms contributing to immune evasion. The second area of focus involves analyzing the participation and reaction of the immune cell populations to immunotherapeutic agents. The following section delves into several of these studies in detail. In the same vein, the study by Jiang et al. developed a high-throughput observation chamber called iHOC to test the effects of immune checkpoint inhibitors on Jurkat T cells and their interaction (Fig. 4B (i)). The iHOC model, which included a 3D printed microwell array for tumor spheroid generation (MDA-MB-231) and a micropillar array coated with a complementary antibody (IL-2) for sampling secreted biomarkers, was used to monitor the effects of *anti*-PD-1 on T cell infiltration into tumor spheroids. The results showed that T cells infiltrated the spheroids more when the *anti*-PD-1 antibody was present, as seen in the confocal microscopic assessment (Fig. 4B (ii-iii)). This study provided a novel model for evaluating immune cell interaction in the presence of immunotherapeutic reagents [121].

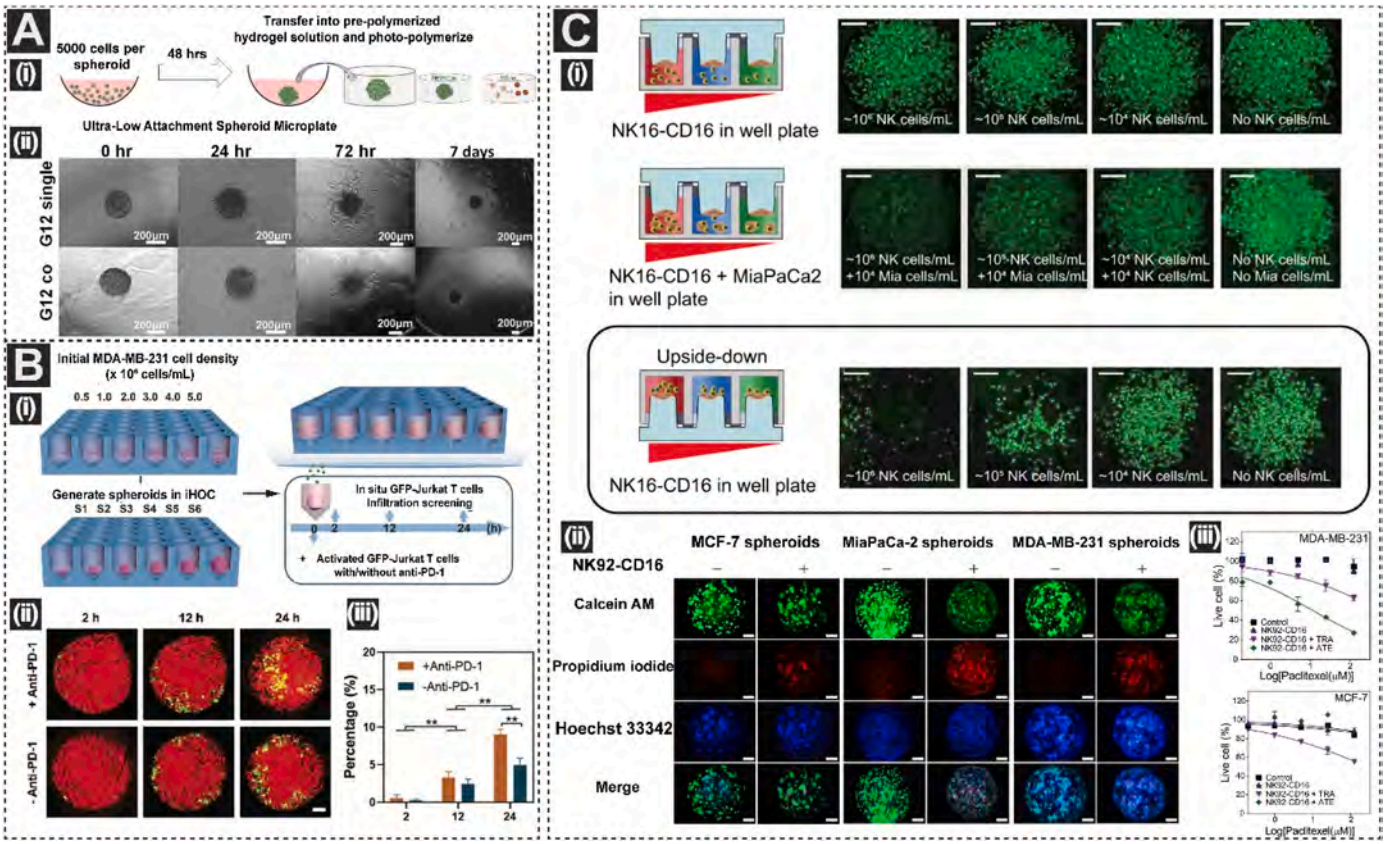

Fig. 4. Spheroid Models to Study Tumor-Immune Interactions. A) Co-culture model of glioma cells with microglia **(i)** Schematic representation of glioma organoid generation and co-culturing with glial cells. **(ii)** Bright-field images of glioma invasion in mono-culture (G12 single) and co-culture condition (G12 co), showing inhibition of glioma migration in the presence of microglia. Adapted from Chen. et al. with permission from BMC [Journal of Neuroinflammation], Copyright 2018 [119]. **B)** High throughput miniaturized bioreactor for modeling immune-tumor interactions. **(i)** Schematic illustration of the immunotherapeutic high-throughput observation chamber (iHOC). Micropillars were generated using a photolithographic technique and used for spheroid generation. Upon spheroid formation, activated T cells are added to the microchambers to initiate T-cell infiltration. **(ii)** Confocal imaging of spheroid in the presence and absence of *anti*-PD-1 antibody. Micrographs show the most profound infiltration of T cells (green) into the spheroid (red) in the presence of anti-PD-1. **(iii)** Quantitative assessment of T-cell infiltration into the spheroid at 2, 12, and 24 h time points. Adapted from Jiang. et al. with permission from Wiley [Small], Copyright 2021 [121]. **C)** High throughput spheroid microarray for NK cell-mediated cytotoxicity study. **(i)** Schematic representation of 384 well plate-based sandwich assay setup alongside immunofluorescent images showing effective capture of NK cells in upside-down technique. **(ii-iii)** NK cell-mediated cytotoxic effect on various cancer spheroids. **(ii)** High content imaging of cancer spheroids showing the live (green) and dead (red) after exposed to NK92-CD16 cells. **(iii)** Dose-dependent responsive curves of MDA-MB-231 (top) and MCF-7 spheroids (bottom) exposed to combinatorial antibodies and NK cells. Adapted from Gopal et al. with permission from Nature [Communications Biology], Copyright 2021 [124].

Alongside T cells, NK cells also possess a remarkable ability to kill cancer cells, making them an important focus in cell-based immunotherapies. Using a co-culture spheroid model, a study by Sarchen et al. investigated NK cell-mediated cytotoxicity. Specifically, spheroids from cancerous cell lines (RH30, Kym-1) and primary neuroblastoma tissue samples were used with activated NK cells to evaluate their ability to infiltrate and kill tumor spheroids. It was observed that NK cells exerted cytotoxic effects on a wide range of cancer spheroids, confirming their role in anti-tumor immunity. To enhance the NK cells ability to kill cancer, this study investigated the impact of BH3 mimetics - compounds that antagonize anti-apoptotic proteins. The results showed that the addition of BH3 mimetics increased the cytotoxic effects of NK cells in destroying a variety of cancer spheroids, confirming a novel approach to increase NK cell-mediated anti-tumor immunity. Together, this study presented a promising approach to induce apoptosis and eliminate tumor cells, potentially offering new strategies for improving therapeutic outcomes [122]. Another study evaluated the interaction of CRC cells with activated NK and T cells using a 3D co-culture spheroid model. Analyzing factors such as spheroid volume and shape showed that activated immune cells can infiltrate tumor cells and induce cell death. The study also revealed that NKG2D-MICA/B engagement is critical in tumor immune surveillance. However, when patient-derived CRC spheroids were co-cultured with enriched autologous lymphocytes, the lymphocyte infiltration potential varied widely. In summary, this study presented a dynamic model that can be used to study anti-tumor immune responses [123].

Along the same line, using rapidly screening drugs in a contextually relevant manner, a recent study reported using a high-throughput micropillar-microwell sandwich platform to assess NK cell-mediated cytotoxicity. Cancer spheroids (breast and pancreatic) were formed by creating a dome of cell-hydrogel mix on the pillar in an upside-down orientation (Fig. 4C (i)). The study showed that the cytotoxicity of NK cells improved when combined with monoclonal antibodies Trastuzumab and Atezolizumab (Fig. 4C (ii-iii)). Additionally, the study used EC50 measurement to confirm the NK cell-mediated apoptosis of the spheroids in the presence of drugs. Finally, researchers found that blocking the PDL-1 receptor with an *anti*-PDL antibody (Atezolizumab) improved NK cell-mediated cytotoxic killing. This platform can be potentially useful for high-content drug screening [124].

3.1.3. Spheroid models for complex TME interactions

The intricate and disordered nature of TME and its elements frequently result in unsuccessful treatments. To combat this, numerous studies are currently concentrating on integrating different aspects of

the TME and enhancing model complexity. For example, a recent study developed a novel high throughput droplet-based platform to generate complex 3D immunogenic tumor spheroids for the assessment of immunomodulatory drug activity for diffuse large B cell lymphoma. Diffuse large B cell lymphoma spheroids consisting of three cell types (cancer cells, fibroblasts, and lymphocytes) embedded in a unique hydrogel combination of alginate and puramatrix. The platform used a microfluidic docking array housing 250 cell-laden microspheres and facilitating the continuous perfusion of spheroids with drugs (Fig. 5A (i-ii)). Quantitative analysis of cell proliferation and viability under the treatment regime and control (without drug) clearly showed the difference between 2D mono-cultured cells and 3D microspheres, where cells encapsulated inside a 3D hydrogel exhibited greater resistance to the drug treatment (Fig. 5A (iii)). Additionally, it was shown that the anti-cancer drug-Lenalidomide, showed enhanced cancer cell death that was mediated through increased proliferation of the immune cells. Finally, through proteomics analysis, this study profiled the secretome from the spheroid array. As expected, they observed downregulation of pro-inflammatory cytokines like IL-6 and IL-8. Overall, this study reported a platform that can be used for multiparametric assessment of cellular interaction [125]. In par with this study, another group devised a multicellular spheroid model that incorporated fibroblast, breast cancer cells, and monocytes to evaluate multidimensional interactions in a hot and cold TME scenarios **[**Glossary**]**. Spheroids were fabricated using MDA-MB-231 (hot) and MCF7 (cold) cancer subtypes to represent hot and cold tumors. To generate co-culture or tri-culture spheroids cancer cells, stromal, and immune cells were seeded at 1:1:1 ratio. During the initial screening of spheroids, it was observed that the expression of immunosuppressive modulators like PDL-1 and IDO-1 differed among cancer subtypes in response to doxorubicin. This implies that immunosuppression may play a role in chemotherapeutic resistance. Next, spheroids were co-cultured with dermal fibroblasts to evaluate how the stromal cells mediate in creating an immunosuppressive environment. Screening for CAF-associated markers including **α**-SMA, CXCL2, FAP showed significant upregulation in MDA spheroids as opposed to MCF7 spheroids. Subsequently, THP-1 and peripheral blood mononuclear cells were incorporated into the model (tri-culture spheroid) to assess the influence of CAFs on immune cell infiltration. As expected, the study reported a higher infiltration of immune cells in the presence of MDA spheroids compared to the other condition, accompanied by a significant differentiation of macrophages to M2 phenotype in the MDA condition. Overall, through this study, two things can be inferred. First, findings from flow cytometry and gene expression analyses revealed the correlation between stromal-immune crosstalk to establish an immune suppressive environment. Secondly, this study also highlighted the inherent variation that could potentially arise from cancer subtypes [126]. To recapitulate the diverse cellular composition of TME, Berger et al. developed a high throughput droplet-based microfluidic system that utilized alginate (Alg) or alginate-alginate sulfate (Alg/Alg-S) hydrogels along with breast cancer cells to create tumor-stroma scaffolds, simulating the breast cancer TME. Breast cancer along with fibroblasts and epithelial cells to mimic other stromal cells were assessed in the presence of two TME scaffold types– proinflammatory microenvironment (M1 macrophages and activated T cells) and immunosuppressive microenvironment (M2 macrophages and non-activated T cells). Proteomic analysis of tumor cells in Alg/Alg-S

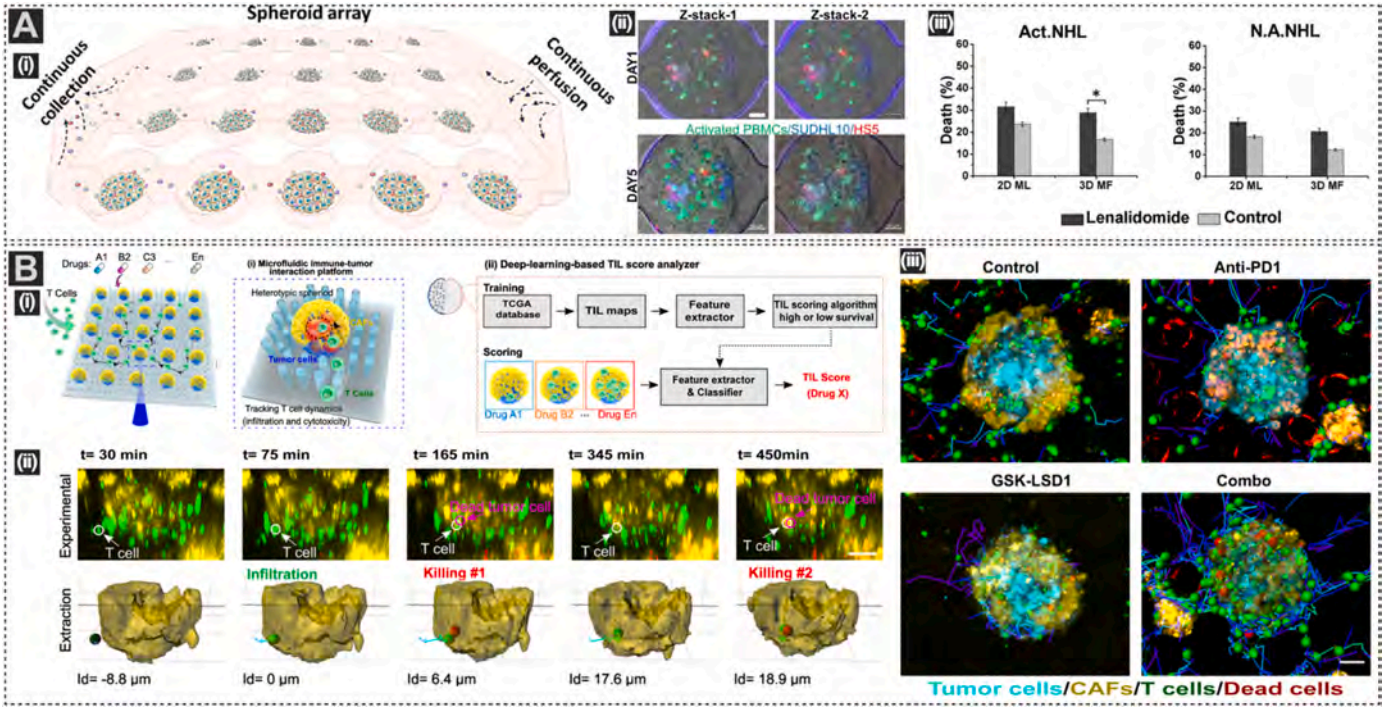

Fig. 5. Spheroid Models to Study Complex TME Interactions. A) Microfluidic array system for the assembly of immunogenic spheroids. **(i)** Schematic of spheroid array system housing 250 cell-laden spheroids generated using a droplet-based microfluidic system. **(ii)** Overlay image of spheroids in the array containing different cells such as peripheral blood mononuclear cells, lymph node cells, etc. **(iii)** Bar graph showing the percentage of cell death in spheroids vs 2D model, with and without drug. Both in the presence and absence of drugs overall cell death in the 3D platform was less when compared to 2D system. Adapted from Pooja. et al. with permission from Elsevier [Journal of Controlled Release], Copyright 2019 [125]. **B)** High-content microarray platform coupled with deep learning for immunotherapeutic screening. **(i)** Graphical representation of spheroid generation, drug screening, and deep learning technique to assess drug candidates. Microfluidic-based fabrication of core-shell spheroids (core-tumor; shell-CAFs)-right, microfluidic immune-tumor interaction platform for assessing T cell infiltration pattern – middle, and deep learning analyzer for image processing and T cell infiltration scoring. **(ii)** Time-lapse image showing T cell killing dynamics within the spheroid at various time points. **(iii)** Simultaneous tracking of T cell infiltration and cytotoxicity within the heterotypic tumor spheroid. 3D projections highlighting the position and trajectory plots of T cells under different treatment regime namely untreated, Anti-PD1, GSK-LSD1, and combo, suggesting the highest infiltration in the combinatorial therapies. Adapted from Ao. et al. with permission from PNAS [Communications Biology], Copyright 2021 [128].

scaffolds showed an increase in proteins involved in cell-cell interactions. Additionally, macrophages shifted from a proinflammatory to an immunosuppressive phenotype when cultured in Alg/Alg-S hydrogel. This study is significant in understanding the complexity of the TME and its role in cancer progression [127].

Another recent study examined the behavior of T cells for effective immunotherapeutic outcomes using a high throughput screening model for pancreatic cancer. The proposed model consisted of a pillar-lattice-array-based microfluidic system that enabled the heterotypic formation of uniform spheroids (Fig. 5B(i)). Through imaging analysis, it was shown that stromal components within the tumor spheroid hindered the infiltration capabilities of the T cells. Furthermore, it was reported that the speed of cytotoxic T cells was slower than non-cytotoxic T cells. To automate the screening process, the study created a deep learning-based analyzer to screen drugs for reversing T-cell exhaustion (Fig. 5B(ii-iii)). Drug library screening identified an epigenetic drug, lysine-specific histone demethylase one inhibitor as the top drug candidate promoting T cell tumor infiltration. Cross-validation of the drug using *in vivo* studies further confirmed the efficacy of lysine-specific histone demethylase one inhibitor in T cell infiltration. This unique study showed the integration of engineered models and machine learning methods for discovering effective immune and combination therapies [128].

Although all the suggested platforms have great advantages, above reported spheroid systems may not be ideal for solid tumors with leaky blood vessels. However, this limitation has been resolved with advanced micro-engineered models such as microfluidic platforms and vascularized spheroid models. In this effort, a study reported a vascularized tumor model, which aims to stimulate the early stages of solid tumor progression. This model consisted of spheroids with both endothelial and tumor cells within a fibrin matrix along with fibroblasts. The amenability of the proposed platform was confirmed by adapting the system to other non-cancerous cell types. When assessing capillary network growth among different cell types, irregular and more branched capillaries were formed in the presence of colon cancer spheroids. In contrast, dense capillary formation occurred when breast tumor cells were co-cultured. These results clearly demonstrated the differences among various cancer cell types. Furthermore, this established model evaluated the potential of cancer cell extravasation (i.e., exit of cancer cells from circulation) under different oxygen rates. CRC cells were found to have double the potential for extravasation under lower oxygen rates, and this process was dependent on the epithelial to mesenchymal (EMT) transcription factor slug. Overall, this model allowed understanding of cancer cells intravascular migration through lumenized vessels, and the fundamental processes involved in cancer progression [129].

Another recent study aimed to closely monitor the behavior and infiltration of immune cells by creating a microfluidics-based tumor model with perfusable vascular networks. Perfusable multi-cellular tumor spheroids (MCTS) was established inside a microfluidic platform by co-culturing pre-formed MCTS with ECs inside a fibrin hydrogel. The study established three spheroid conditions: Mono-, Co-, and Tri-culture (Fibroblasts, Cancer cells, and Endothelium) and assessed the spheroids morphology. Secretome analysis revealed increased expression of angiogenic factors confirming the initiation and maintenance of vasculature. Furthermore, tri-culture spheroids on a vascular bed showed a two-fold increase in growth with the anastomosis of vascular bed cells with the endothelial spheroid cells. Together, these findings confirmed the formation of perfusable vascular networks within the spheroids. Finally, evaluation of the cytotoxic drug Cisplatin showed varying penetration patterns across different spheroid conditions. It was reported that the accumulation of drugs in mono-culture was observed to be on the periphery of the tumor spheroids and required higher dosing of the drug to reach enough penetration. On the other hand, penetration of the drug was observed to be higher in the core of the spheroid in case of tri-culture condition. These findings underpin the role and need for inclusion of varying cellular compositions of TME to take these *in vitro* models further toward the personalized medicine screening [130].

Owing to the intermediate complexity between traditional 2D monolayers and *in vivo* tumors, spheroid models have garnered considerable recognition as appropriate engineered models for basic tumor biological studies and drug screening. Despite their advantages, a set of constraints impedes the seamless integration of spheroids into preclinical testing models. A pivotal but intricate aspect that poses a critical challenge is the consistent formation of spheroids. The size of the spheroids is intricately linked to seeding densities, and their dimensions can vary substantially across different cancer types, adding a layer of complexity to the standardization process [131]. Furthermore, while spheroids are favored as culture models for drug screening, assays predominantly evaluate the efficacy of the drug based on the size and volume of the spheroids [102]. However, relying solely on these criteria poses challenges, as the variability in size and shape mentioned earlier undermines the appropriateness of such assessments. Thus, there is a pressing need to establish more accurate evaluation methods tailored to the unique characteristics of spheroids to ensure the reliability of spheroids-based assays.

3.2. Organoid models

Organoids are self-organized 3D clusters of cells that sustain long-term culture with increased stability [132,133]. Organoids are derived exclusively from primary tissue samples, embryonic stem cells, or induced pluripotent stem cells [134–138]. Organoids has a unique ability to retain intra and intertumoral heterogeneity with spatial organization mirroring the physiological architecture [139]. Additionally, patient-derived organoid (PDO) models help preserve the T cell spectrum, cancer-specific mutation and capture the epigenetic alternation complementing the pathological condition [140]. These features make organoid models functionally suitable for *in vitro* drug screening, personalized medicine, and are currently being tested in real-time clinical decision-making [141,142].

Various strategies have been adopted for generating tumor organoids to retain the TME architecture [Box 1]. Among those, submerged organoid cultures **[**Glossary**]** are commonly used. For instance, 3D breast cancer organoids were developed to dissect the invasive behavior of cancer cells that leads to metastasis. Organoids were established using combinatorial (both mechanical and enzymatic) digestion of primary tumor tissue and encapsulating the cells in collagen I matrix. This study revealed that leader cells expressing epithelial genes K14 and p63 were crucial for collective migration [143]. In another study, researchers utilized primary human liver organoids collected from various patients to predict their response to chemotherapeutic drugs like plicamycin and idarubicin. The results of the study showed diverse responses to these drugs due to the presence of intratumor heterogeneity, while emphasizing the usefulness of organoid models in personalized drug testing [144]. While it is relatively easy to create organoids using the submerged method and scale up the process, these organoids lack other non-epithelial cell types found in the tumor environment [145].

To address the limitations of epithelial-based organoid culture, researchers have also developed new methods that incorporate non-cancerous cellular components. Two commonly used methods for generating tumor organoids that can incorporate other cellular components of TME are the reconstituted TME model and the native TME model. In the reconstituted TME model, immune and/or stromal components of the TME from the same tissue sample or exogenous cells are added to the organoid culture. While, the native TME model aims to preserve the TME component of the native tissues. An air-liquid interphase (ALI) technique has shown a great promise in generating PDOs while maintaining their natural structural environment. These models are widely used to study TME processes, as they retain the pathophysiology of tumors. As in the previous section, we have categorized organoid models based on their cellular interactions.

3.2.1. Organoid models for tumor-stromal interactions

Organoids are considered a suitable platform for studying tumor-nonimmune cell interactions. As CAFs are an important stromal component of the TME, their role in carcinogenesis has been investigated by many studies. Accumulating evidence has revealed the activated state of CAFs to be strikingly different from that of myofibroblasts [146]. This conversion of normal fibroblast to CAFs is partially associated with CAF-cancer cell interactions [147]. In the same line, another study utilized 3D co-culture liver tumor organoid to functionally investigate tumor-CAFs interactions and their response to drug treatment. Confocal imaging confirmed the presence of CAFs surrounding the organoids, and immunofluorescent imaging revealed their role in promoting organoid growth. This study also found that secreted factors released by tumor cells affected CAFs physiology. Additionally, the study assessed the response of organoids to clinically used anti-cancer drugs (sorafenib and regorafenib) in the presence and absence of CAFs, which demonstrated the role of CAFs in contributing to treatment resistance [148]. In a different approach, hyaluronan-gelatin-based co-culture model was proposed to establish an organotypic CRC organoid system (Fig. 6A (i)). Notably, this study

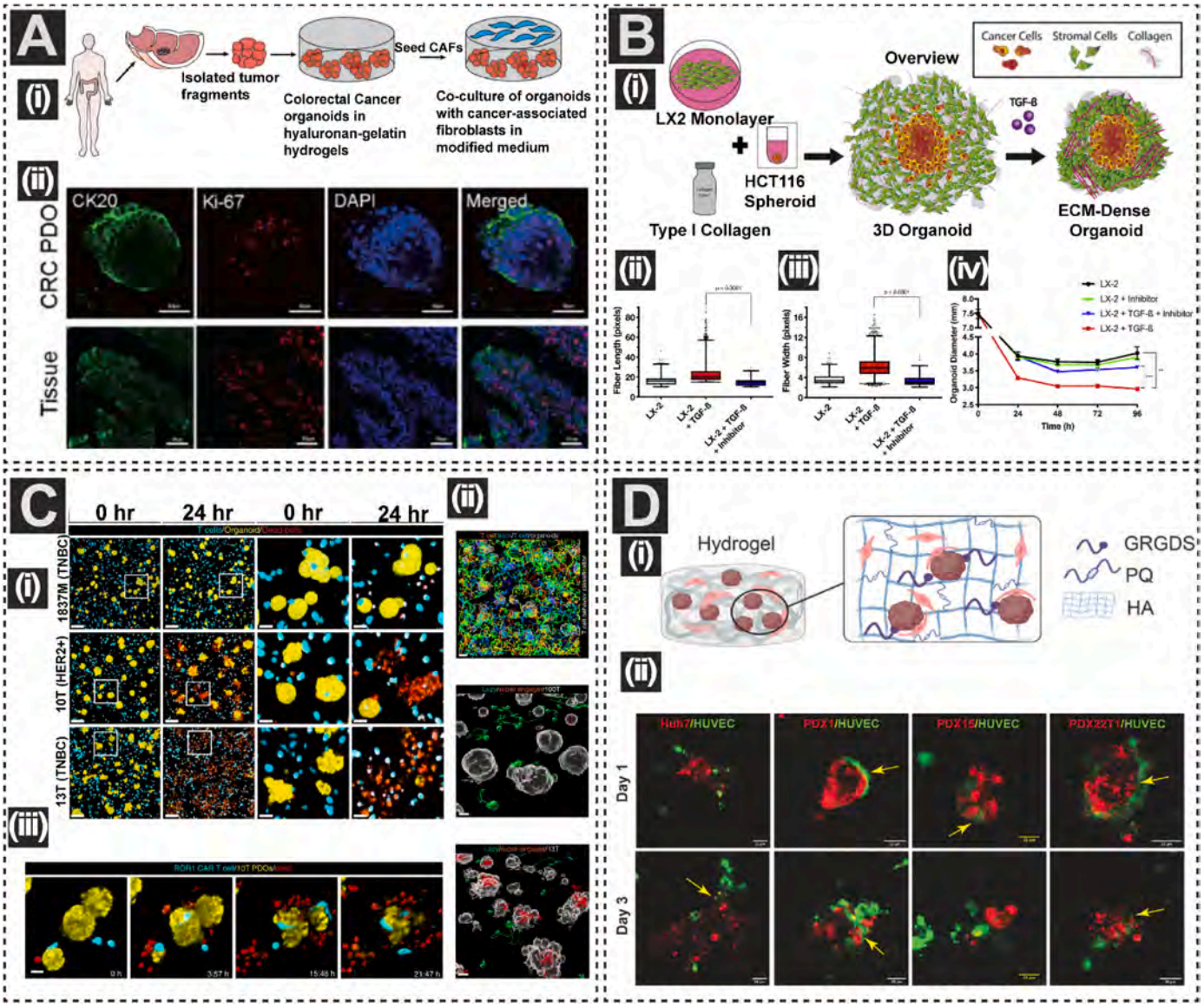

Fig. 6. Organoid Models A) Hyaluronic and gelatin-based cancer organoid model. **(i)** Schematic representation of isolation and establishment of patient-derived organoid and fibroblast co-culture system. **(ii)** Characterization of hydrogel-embedded organoids (CRC PDO) with original patient tissue, confirming the maintenance of actual tissue features in the hydrogel system. Adapted from Luo. et al. with permission from Elsevier [Acta Biomaterialia], Copyright 2021 [149]. **B)** Tumor organoid model for modulating TME stiffness and chemotherapeutic studies. **(i)** Schematic representation of establishing a CRC organoid model with dense ECM. **(ii-iii)** Characterization of structural changes of the ECM fibers upon exposure of the organoids to TGF-β. **(ii)** Box and whisker plot diagrams show wider and elongated fiber length in organoids exposed to TGF-β compared to control organoids. **(iii)** Inhibition of TGF- β using SB 431542 showed a reduction in organoid contraction, confirming TGF-β's role on ECM modulation. Adapted from Dominijanni. et al. with permission from Elsevier [iScience], Copyright 2020 [152]. **C)** Patient-derived organoid model to discover engineered T cell mode of action. **(i)** Multispectral 3D images of breast cancer PDOs (yellow) co-cultured with TEGs (blue) showing the killing of TEGs: Slow (1837), intermediate (10t), and high (13 T) at indicated time points. **(ii)** 3D rendered image showing the tracks of T cells in two different breast cancer organoid subtypes. **(iii)** 3D multispectral images of CART (blue) cell mode of killing within the co-culture spheroid system. Adapted from Dekkers, J.F. et al. with permission from Springer Nature [Nature Biotechnology], Copyright 2022 [159]. **D)** Co-culture organoid model to mimic angiogenic crosstalk **(i)** Graphical representation of pancreatic organoid co-cultured with endothelial cells inside a hyaluronic acid based hydrogel scaffold. **(ii)** Confocal images of co-culture organoids on day 1 and day 3. Adapted from Lim. et al. with permission from Elsevier [Biomaterial], Copyright 2022 [160].

reported the negative impact of organoid culture medium (advanced DMEM/F12 medium with 5 % Fetal Bovine Serum, growth factors, and small molecules) on CAFs viability. Through RNA- and whole-exome sequencing, this study confirmed that the proposed CRC organoids maintained molecular traits similar to those of original patient tumors (Fig. 6A (ii)). Additionally, results from RNA-sequencing showed increased upregulation of focal adhesion-related genes, confirming the recapitulation of ECM-mediated CAF-cancer crosstalk [149]. Overall, this study reported an engineered hydrogel system for culturing both CAFs and CRC organoids. In another hybrid cancer organoid model, the effect of podoplanin-positive CAFs (a subtype of CAFs) on lung adenocarcinoma was studied. Results from this study showed the supportive role of CAFs in organoid formation and provided insights about the effect of CAFs subtype on lung cancer cell proliferation [150]. Additionally, some other studies have also focused on evaluating the effect of matrix stiffness on treatment outcomes. A study conducted by Xiao and colleagues illustrated the creation of co-culture pancreatic organoids with corresponding CAF populations by utilizing advanced biomaterial that simulates the fibrotic stiffness. To construct a physiologically relevant microenvironment, the proposed study developed a tunable matrix by integrating collagen-I into Matrigel®. Precise adjustments to the collagen I matrix led to heightened activation and exosome secretion of CAFs. These findings not only emphasized the pivotal role of matrix stiffness but also highlighted it as one of the fundamental mechanisms driving CAF activation. This studies innovative use of biomaterials, to recreate the fibrotic context of pancreatic organoids, represents a promising stride towards enhancing the physiological relevance of *in vitro* models for studying cancer biology [151].

The ECM surrounding the solid tumors is mostly stiffer and denser compared to the healthy counterparts. These altered ECM depositions have confounding effects on the surrounding cells. Among various cell types, stellate cells are quiescent fibroblast cell types that are mostly involved in collagen I synthesis. Unfortunately, the exact mechanism by which the stromal components impact the acellular ECM deposition is not completely understood. Utilizing advanced bio-fabrication techniques, various efforts have been taken to characterize the ECM deposition and its effect on the cellular population. In a proof-of-concept study, tumor organoid model embedded in collagen I was established to study the effect of cytokines TGF-β on stellate cell activation (Fig. 6B (i)). In the underlying approach, CRC organoids were formed by embedding CRC spheroids within stellate cells using polydimethyl siloxane (PDMS) microwell. Stellate cells were induced to myofibroblast-like phenotype when the organoid culture was exogenously exposed to TGF-β. Furthermore, immunohistochemistry quantification showed a 2-fold increase in fibroblast-associated markers (**α**-SMA and FAP) in the presence of TGF-β. To corroborate these findings with change in ECM organization, structural and morphological changes (diameter change and matrix stiffness) under different culture condition were assessed. It was observed that organoids cultured in TGF-β-containing media showed more diameter reduction than those cultured in control media (without TGF-β). Furthermore, the characterization of organoids for collagen I fiber distribution using immunofluorescent staining showed wider and denser collagen I fiber in organoids exposed to TGF-β (Fig. 6B (ii-iii)). Together, these results confirmed cytokine-mediated alteration of ECM through fibroblasts-like cells. Next, to probe if this cytokine-exerted stiffness can be reversed, TGF-β inhibitor- SB 431542 was added to the system. Evaluation of the inhibitor to modulate stiffness at different time points clearly showed time-dependent reversal (Fig. 6B (iv)) [152].

3.2.2. Organoid models for tumor-immune interactions

Countless tumor immunological studies have highlighted the crucial impact of the immune landscape on tumor growth and treatment outcomes [153]. A major limitation in the clinical success of immunotherapies lies in the poor response from the patients. Various underlying mechanisms that are involved in immune evasion have been proposed [154,155]. In this context, a multitude of studies have focused on evaluating the T-cell-mediated anti-tumor immune response. For instance, a proof-of-concept study was conducted to evaluate T-cell--mediated tumor recognition using a patient-derived organoid model. The co-culture organoid model was established from tissue and peripheral blood lymphocytes obtained from the same patient samples. Flow cytometric analysis for IFN-ɣ and CD107 expression confirmed the induction of tumor reactivity in T-cell. Next, the ability of autologous T-cell-mediated organoid killing was assessed using live-cell imaging and cytotoxicity assay. Findings from this study showed the effective killing of organoids by T cells. Interestingly, T cells did not show detrimental effects on non-tumorigenic organoids. Overall, this study provided a model that allowed the assessment of T-cell mediated sensitivity on tumor cell killing [156]. In the same vein, another proof-of-concept study evaluated the soluble factors mediated cytotoxic effect of T cells. Patient-derived Cholangiocarcinoma (type of primary liver cancer) organoids were co-cultured with either PMBCs or T cells obtained from healthy donors. Increased effector cytokine expression was detected in T cells co-cultured with the organoid samples. Additionally, quantitative analysis of confocal imaging revealed increased apoptotic cells in organoids co-cultured with T cells as compared to mono-culture organoids. Furthermore, the viability of organoids cultured in an immune cell-conditioned medium confirmed the in-direct effect of T-cell-mediated killing. Intriguingly, only one PDO was susceptible to cell death, making these effects organoid-specific [157]. These two studies presented organoid models as a screening tool to predict individual patient responses to immune cell-based therapies. In another study, Marcon et al. evaluated NK cells functional and phenotypic features within the pancreatic TME using tumor organoids. Flow cytometric and qPCR analyses showed downregulation of CD16 and CD57 expression for NK cells co-cultured with tumor organoids. Observation of activation receptor expression showed no change in culture, suggesting impairment of NK cell function within the TME. Additionally, functional profiling of peripheral blood-derived NK cells further confirmed the modulation of NK cell cytokine profile by disease progression. Taken together, these findings suggest an immune evasion mechanism within NK cells and provide insight into potential approaches to target similar mechanisms used by other immune cells within the TME [158].

Dekkers et al. created an imaging-based platform to investigate the interaction between engineered T cells and breast cancer PDOs with the aim of expanding the use of engineered cell-based immunotherapies for solid tumors. The study found that cancer metabolite sensing engineered T cells (TEGs) co-cultured with different subtypes of breast cancer organoids displayed higher diversity in killing potential (Fig. 6C (i-ii)). The study also revealed two behavioral patterns of the TEGs, inactive and active motility, suggesting the heterogenous TEGs behavior (Fig. 6C (iii)). The universal solid tumor-targeting efficacy of TEGs was confirmed by extending this assessment to other organoids such as head and neck and glioma with similar results. Transcriptomics profiling of TEGs post-PDO exposure identified differentially expressed genes that are involved in tumor killing [159]. The study introduced a distinctive approach to examining the interactions between immune cells and cancer cells, with a focus on evaluating the effects on a patient-specific basis. Using imaging capabilities in conjunction with the engineered model will create new opportunities to better understand cellular interaction dynamics in complex 3D systems.

3.2.3. Organoid models for complex TME interactions

Lim et al. conducted a study to investigate the communication between hepatocellular carcinoma (HCC) and ECs. The co-culture model was established by combining HUVECs and HCC patient xenograft-derived organoids in hyaluronan hydrogel (Fig. 6D (i)). The angiogenesis array revealed an increase in angiocrine factors, such as MCP-1 and CXCL16, in co-culture organoids, indicating the impact of direct cell-cell contact on mediating angiogenic factors. Furthermore, confocal imaging confirmed the establishment of perfusable organoids (Fig. 6D (ii)). Bulk

RNA-sequencing revealed upregulation of genes related to the TNF cascade, indicating an inflammatory response of HCC cells. The study further investigated the polarization ability of macrophages due to the upregulation of inflammatory-mediated genes in co-culture conditions. qPCR analysis confirmed the potential capabilities of ECs on macrophage polarization. Overall, this study highlights the importance of stromal and cancer interplay [160].

Apart from delineating the underlying cell-cell and cell-ECM interactions, organoids have served as a preclinical tool for cancer immunotherapeutic research. A recent study investigated melanoma organoids as a potent tool for cancer immunotherapeutic research. Organoids established from melanoma tissue obtained from 30 different patients and maintained in advanced DMEM/F12 medium were subjected to various immune checkpoint, cellular, and targeted therapies. The study employed different methods for organoid formation, including embedding them in a collagen I scaffold similar to ALI and laying them in Matrigel®. In-depth characterization of various markers such as **α**-SMA, vimentin, and ICAM-1 (adhesion molecule) revealed that the PDOs were able to successfully preserve the tumor stroma, including fibroblasts (**α**-SMA), mesenchymal cell (vimentin), and T cells (ICAM-1). Fluorescent-activated sorting revealed the preservation of diverse immune cell populations ($CD4^+$, $CD8^+$, and $CD11b^+$). The study concluded by highlighting the potential efficacy of combining small molecules and tertiary lymphoid srructures **[**Glossary**]** therapies, showcasing the utility of engineered organoid models in precision medicine [161].

In another approach, multi-cellular organotypic pancreatic co-culture model was developed and characterized. Patient-specific pancreatic organoids were grown with stromal cells (i.e., CAFs) using a submerged culture system. $CD3^+$ T lymphocytes isolated from the buffy coat were then added to the growth medium in the organoid dome culture. It was shown that CAFs co-cultured with organoids were activated to a myofibroblast state with **α**-SMA-positive expression. Additionally, it was reported that T cells in the liquid phase showed tumor-dependent infiltration [162]. Overall, this study offers a unique approach to studying the impact of heterogeneous cellular compartments within the TME and brings us closer to meeting some of the unmet needs of 2D-based assays.

While the organoid model effectively preserves the architecture of *in vivo* tumors, establishing organoids from tissue samples often encounters challenges related to suboptimal culture conditions. These culture conditions may not meet the diverse cellular requirements of various cellular components within the model, leading to the deterioration of the unique *in vivo* microenvironment [163]. This necessitates the use of special media composition to maintain their viability for an extended period of time. Consequently, the expense associated with organoids poses a barrier to large scale production and the translation potential of these models. Furthermore, the lack of vasculature presents a technical challenge, limiting the model's ability to fully emulate the physiological conditions of the tumor [164].

3.3. Microfluidic models

Microfluidics are cutting-edge technologies that enables precise manipulation of minuscule amounts of fluids that ranges from 10^{-9} to 10^{-18} L within channels measuring tens to hundreds of micrometers in height [165,166]. A distinctive feature of these technologies is efficient operation at low Reynolds numbers (Re), which signifies the presence of laminar flow in microfluidic systems. At low Reynolds numbers, the influence of inertial forces is greatly diminished compared to the dominant viscous forces acting on the fluid, implying that mass transfer primarily occurs through diffusion rather than fluid motion [167]. Another key feature is providing exceptional spatial control for the distribution of cells, thus creating a well-defined microenvironment [168]. Furthermore, since microfluidic channels are small, they require a small amount of reagents and cells that reduce the cost of study.

The initial fabrication technique in the development of microfluidics involved photolithography etching, adapted from the fabrication processes of electronic microchips, which enables control over the feature shape and size to control cell-cell, cell-ECM, and cell-soluble factors interaction [169–174]. Apart from etching, the other employed fabrication methods of microfluidic devices include molding, lithography, and 3D printing [Box 2] [175,176]. Microfluidic systems are often made using the soft lithography technique **[**Glossary**]** which utilizes an optically clear polymer known as PDMS which has become a staple for the field of microfluidics because of its ease in the fabrication process as well as for its material attributes such as biocompatibility, cost-effectiveness, elasticity as well as gas permeability. Furthermore, its non-toxic characteristics make PDMS ideal for biological applications, and its optically transparent property makes it feasible for real-time analysis [177]. Besides PDMS, rigid thermoplastic polymers such as polycarbonate and cyclic olefin copolymer have been also widely used [168].

Microfluidics are rapidly expanding technologies that allow precise control over the cellular, physical, and biochemical environment, striking a unique balance between *in vivo* and other *in vitro* models. In this regard, microfluidic models have gained significant prominence as an essential tool in cancer modeling research which includes studying metastatic cascades [178,179], tumor-stroma interactions [180,181], cancer extravasation [182,183], cancer migration, modeling cancer-immune interactions [165] and personalized cancer therapy [184]. The evolution of multichannel microfluidic platforms has facilitated the study of complex biological events within defined spatial environments [175]. One key aspect of microfluidics in cancer modeling and bioengineering is the ability to recreate TME, which comprises of cancer cells and various stromal cells such as fibroblasts, immune cells, as well as ECs in an appropriate 3D matrix in a spatial compartment, allowing us to study their interactions and impact on tumor growth, invasion, and response to therapies [175]. Apart from this, it also allows studying other fundamental biological processes within the TME. For instance, hypoxia, a common characteristic of tumors, is a known driver of migration and invasion [185]. In this regard, a study by Grist et al. utilized a droplet-based microfluidic system to generate breast cancer spheroids with spatiotemporal oxygen controls. Two-photon microscopy showed that spheroids in different oxygenated regimes (normoxia, hypoxia) have varying swelling dynamics. Furthermore, spheroid monitored using sectional microscopy showed the correlation between cyclic hypoxia and penetration of anti-cancer drugs [186]. The integration of multiple 3D culture systems, such as the 'organoid-on-chip' technology, has also demonstrated enormous potential in cancer research. These advanced platforms combine the benefits of 3D organoids with the microfluidic capabilities of chips, enabling precise control over the culture conditions and facilitating dynamic interactions within the TME [187]. By incorporating vascular networks, immune cell infiltration, and the ability to mimic physiological fluid flow, organoid-on-chip systems offer a more realistic representation of tumor behavior and response to therapies [188]. This approach holds great promise for accelerating drug discovery, personalized medicine, and our overall understanding of cancer biology. In the recent years, microfluidic platforms have been also used for several immunotherapeutic applications, such as improving immune checkpoint blockade therapies, understanding immune cell dynamics and the process of immune evasion, and evaluating the cytotoxic potential of engineered immune cells. Also, cancer immunotherapeutic gene targets such as PD-L/PD-L1 [189], CXCR2 CD71 [190], and EpCAM [191] have been studied to identify potential biomarkers in various types of cancer using microfluidic platforms, which is a promising approach for gene-based therapy development.

A critical perspective on utilization of microfluidic models to recapitulate the complex multicellular interactions is still emerging and will be discussed in the coming sections. In this section, we will delve into the application of microfluidic platforms in exploring the interactions between cancer cells and the stroma and the interactions between cancer

Box 2
Microfabrication technique for microfluidics and bioprinting

Microfabrication techniques play a crucial role in the fabrication of microfluidic devices, which are used for precise manipulation of fluids at the microscale. Common microfabrication techniques combine the use of soft lithography, where elastomeric materials like PDMS are molded to create microfluidic channels, and photolithography, which uses light-sensitive materials and masks to create patterns on substrates [259]. Recent research has advanced to create more complex multicellular channels within microfluidic platforms to study multicellular interaction withing the TME in a reductionist and controlled manner and to understand the role of cellular/noncellular components role on tumor progression. Apart from soft and photolithography, laser micromachining, 3D printing, Electron beam lithography allows for high-resolution fabrication of intricate features. These techniques enable the creation of microfluidic devices with precise geometries and functional components, facilitating various applications.

One of the prominent microfabrication techniques utilized for 3D bioprinting is called extrusion-based bioprinting. In extrusion-based bioprinting, a bioink containing living cells and a supportive biomaterial is extruded through a nozzle or needle to create a 3D structure layer by layer. The bioink can be composed of hydrogels, such as alginate, collagen I, or gelatin, which provide a scaffold for cell growth and tissue formation. The extrusion process is controlled by a computer-aided design (CAD) model, allowing precise deposition of the bioink to create complex tissue-like structures [241]. Other techniques used in 3D bioprinting include inkjet bioprinting, which uses droplet ejection to deposit cells and biomaterials, and laser-assisted bioprinting, which employs lasers to precisely position cells and biomaterials. These microfabrication techniques enable creation of 3D biological constructs with defined spatial organization, mimicking the complexity of native tissues and organs for applications in tissue engineering and regenerative medicine.

cells and the immune system. Lastly, we will provide an in-depth review of microfluidic platforms designed to simulate and understand the complexities of multicellular interactions within TME.

3.3.1. *Microfluidic models for tumor-stromal interactions*

Having the advantage of including multiple cell types to analyze specific interactions in appropriate spatial confinement, microfluidics has gained much thrust in investigating tumor-stromal crosstalk. For instance, cancer and EC interaction plays a vital role in tumorigenesis. This interplay supports tumor growth characterized by leaky, chaotic, and heterogeneous vessel networks [178]. Several microfluidic platforms have focused on this cancer-EC interactions using hydrogel matrices to better understand the metastatic cascade, which includes the process of invasion, intravasation (entry of cancer cells into circulation), and extravasation [192]. A study by Zhang et al. highlighted the process of *trans*-endothelial invasion of ACC (Salivary gland Adenoid Cystic Carcinoma) tumor aggregates to the endothelial layer when induced with CXCL12. Briefly, the design of the platform consisted of a main channel that served as blood vessel cavity and the side channels mimicking the perivascular ECM. Once the endothelial layer was established on the surface of the side channels, tumor aggregates were injected into the main channels with different concentrations of CXCL12. The absence of CXCL12 prevented tumor aggregates from invading into the blood vessels [193]. Lee et al. reported similar studies to study cancer intravasation that allowed lung fibroblasts to stimulate EC to become differentiated microvessels, followed by cancer cell (MDA-MB-231) introduction to study cancer-endothelial interaction. By treating the microvessels with TNF-α prior to introduction of cancer aggregates, it was evident that cancer cells invaded three times more than without TNF-α [194]. Nagaraju et al. studied the tumor-vascular crosstalk in breast cancer using a three-layer organotypic microfluidic platform that incorporated tumor-stroma-vasculature, layer by layer separated by microposts that permitted interconnectivity between channels, while maintaining spatial confinement along with flanking media channel (Fig. 7A (i)). It was apparent that the invasion of MBA-MB-231 breast tumor cells was pronounced in the presence of ECs; the tumor cells intravasated the endothelial layer on Day 6 (Fig. 7A (ii & iii)). The vascular networks were thinner with higher permeability in the presence of MDA-MB-231 cells [195]. In another study which utilized the same platform as [195], Truong et al. established a 3D microfluidic model to study glioma invasion influenced by microvascular networks using a patient-derived xenograft model. A significant invasion of Glioma Stem Cells (GSCs) was observed in the presence of microvascular networks. In this study, the authors assessed the influence of three medium compositions (NSC, NSC+, and EGM-2 media) on tumor invasion. It was evident that in EGM-2 media, the GSCs invasion was more pronounced regardless of the presence of HUVECs, suggesting that the cytokines in EGM-2 media could shield the influence of HUVECs. However, a significant difference was observed between the mono-culture and co-culture groups in NSC and NSC + media, signifying the role of HUVECs in GSC invasion. The authors hypothesized that CXCR4-CXCL12 might play a significant role in the migration of glioma cells; using AMD3100 to inhibit the CXCR4 pathway, it was evident that there was a decreasing trend in the invasion distance of glioma cells with increasing concentration of AMD3100 in the presence of HUVECs [196].

The role of fibroblasts has significant implications for cancer progression, contributing to tumor growth and angiogenesis. As one of the predominant cell types in TME, they are associated with all stages of cancer, which are investigated using engineered microfluidic platforms. For instance, Truong et al. developed a two-layer tumor-stroma organotypic microfluidic platform that enabled the spatial organization of tumor and stromal entities to study breast cancer invasion using SUM159 cells - a Triple Negative Breast Cancer cell line (Fig. 7B (i)). The complexity of the model was further increased by incorporating patient-derived CAFs. The invasion of SUM159 cells was significantly higher in the presence of CAFs compared to normal fibroblasts. Further molecular analysis revealed that glycoprotein nonmetastatic b (GPNMB) knockdown, inhibited the potential of CAFs in regulating the invasiveness of cancer cells (Fig. 7B (ii-iii)) [197,198]. A similar study focused on examining the CAFs in the CRC spheroid model to investigate multicellular interaction within the TME in a microfluidic platform using an appropriate 3D matrix by Jeong et al. The platform contained four units comprising seven cell/media loading channels. In co-culture with fibroblasts, the fibroblasts acquired an elongated morphology with increased expression of fibroblast activation marker α-SMA. In addition, the migration ability of fibroblast towards the tumor channel was pronounced in co-culture conditions [199]. Lugo-Cintron et al. established a microfluidic device to mimic the interaction between breast cancer cells and normal fibroblasts/CAFs (Fig. 7C (i-ii)). The device consisted of lumens filled with a mixture of breast cancer cells encapsulated in collagen I, surrounded by a collagen I matrix containing fibroblasts. In this study, it was observed that the migration of MDA-MB-231 cells was considerably enhanced when cocultured with CAFs compared to normal fibroblasts. However, in fibronectin-rich collagen I, there was an increased migration of cancer cells in the presence of normal fibroblast, indicating the tumor-promoting capabilities of the fibronectin matrix

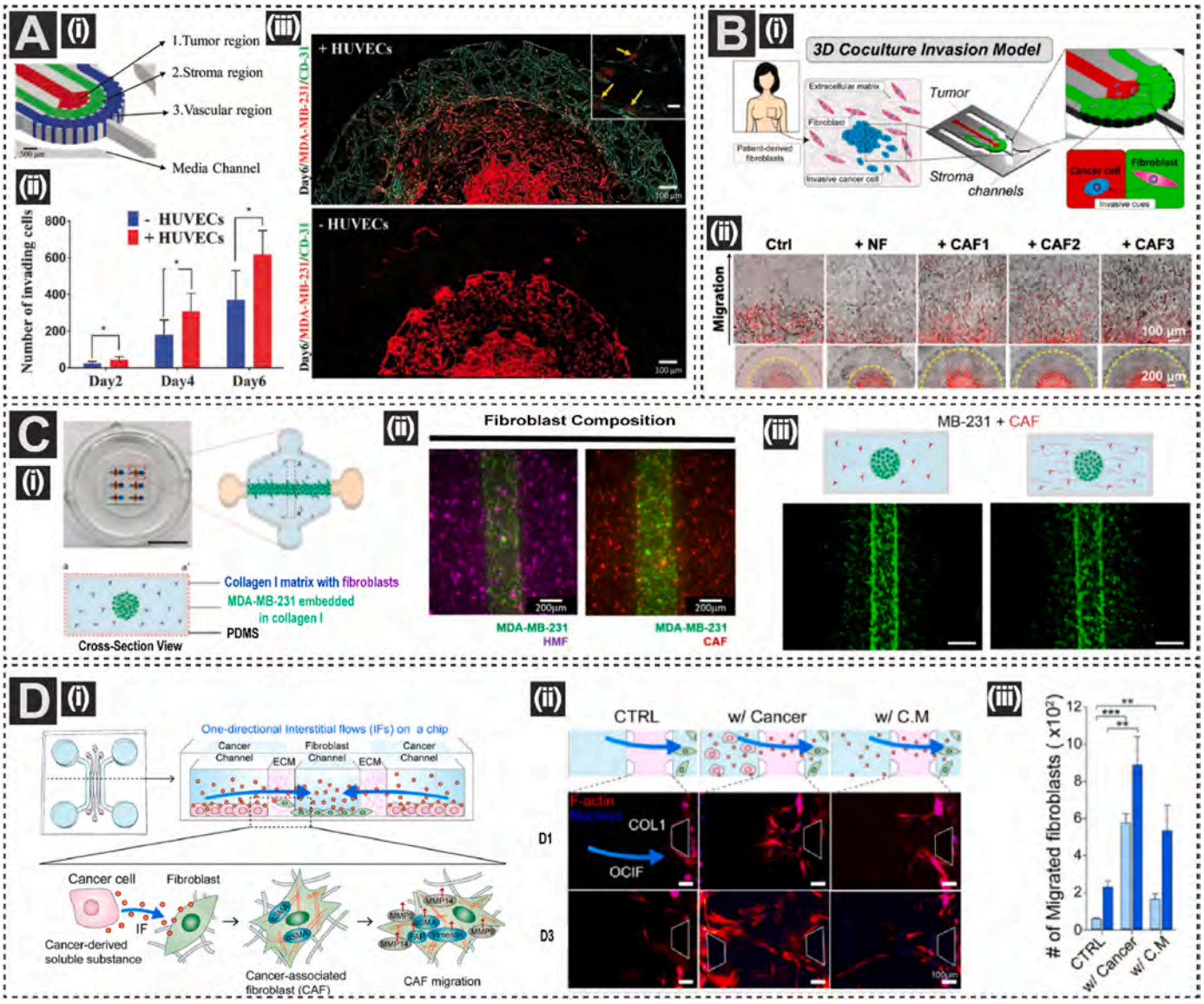

Fig. 7. Microfluidic Models to Study Tumor-Stromal Interactions A) Microfluidic model to study vascular-tumor crosstalk **(i)** Depiction of the three-layered model to study tumor-vascular crosstalk **(ii)** Quantification of the invading cancer cells in presence/absence of HUVECs **(iii)** Fluorescent images of cancer cells (red) intravasation into the vascular network on day 6 in presence or absence of HUVECs. Adapted from Nagaraju et al. with permission from Wiley Online Library [Advanced Healthcare Materials], Copyright (2018) [195]. **B)** Microfluidic model to study fibroblast-tumor interaction **(i)** Diagrammatic illustration of microfluidic platform with distinct tumor and stromal entities to study CAF-Cancer interactions. **(ii)** Migration of SUM159 in the presence of CAF/normal fibroblast. Adapted from Truong et al. with permission from American Association for Cancer Research [Cancer Research], Copyright (2019) [198]. **C)** Microfluidic model to study fibroblast and ECM influence of cancer progression **(i)** Representative image of the microfluidic co-culture model to recapitulate the TME. **(ii)** Fluorescent images of MDA-MB-231 (green) with normal fibroblast (purple) and Cancer-Associated-Fibroblast (red) **(iii)** Presence of fibronectin rich matrix shows higher invasion of cancer cells (right). Adapted from Lugo et al. with permission from MDPI [Cancers (Basel)], Copyrights (2020) [200]. **D)** Microfluidic model to study the influence of fibroblast and interstitial flow on cancer progression **(i)** Schematic of the model to study the role of interstitial flow on cancer-CAF interaction **(ii)** Fluorescent images of migrated fibroblasts in three different conditions: mono-culture, co-culture with cancer as well as mono-culture treated by conditioned media (CM) from cancer **(iii)** Quantification of number of migrated fibroblasts cell which clearly depicts the direct influence of cancer cells significantly increase the migration of fibroblasts. Adapted from Kim et al. with permission from Elsevier [Acta Biomaterialia], Copyright (2022) [201].

(Fig. 7C (iii)) [200]. In a recent study, Kim and his research group developed a microfluidic platform to generate a one-directional flow in the device to investigate if the soluble substance delivered by the interstitial flow from cancer cells could activate the fibroblasts. In the presence of interstitial flow, there was increased fibroblast migration in the presence of NCI–H28 cells (Fig. 7D (i & iii)). Further, the migrating fibroblasts had enhanced expression of **α**-SMA and ECM remodeling proteins [201]. In a study by Lee et al. a microfluidic co-culture system with multiple channels was utilized to investigate the impact of pancreatic stellate cells (PSCs) on human pancreatic cancer cells. Specifically, PANC-1 cells (human pancreatic cancer cells) were co-cultured with PSCs. PSCs primarily comprise CAFs and are typically found within the stroma of pancreatic ductal adenocarcinoma. The cancer cells were embedded in collagen I and placed in a central channel, while two adjacent channels contained collagen I-embedded PSCs. In the presence of PSCs, the cancer cells exhibited enhanced migration, proliferation, EMT, and drug resistance [202].

Although many microfluidic models incorporate nonimmune components to study the mechanisms of tumor progression, the crosstalk between the immune cells and its role in cancer would pave the way for a

better understanding of dynamic TME. Therefore, the following section will explain the complex interaction between immune components and tumors in detail.

3.3.2. *Microfluidic models for tumor-immune interactions*

Modeling immune cell migration is crucial to understand the tumor-immune dynamic interaction; combining microscopy with a microfluidic model to visualize cell migration using time-lapse imaging can provide insights into the dynamics of immune cells and open much scope in the field of immunotherapy [203]. This section will explore the available microfluidic platforms employed to investigate the tumor-immune crosstalk. It mainly focuses on evaluating how this dynamic interaction influences the migratory behavior of both cancer and immune cells. Additionally it discusses the application of microfluidics in testing current immunotherapeuties as well as in evaluating the cytotoxic potential of immune cells towards cancer. However, as far as our understanding goes, fewer microfluidic platforms are utilized for studying the interactions between cancer and the immune system [204,

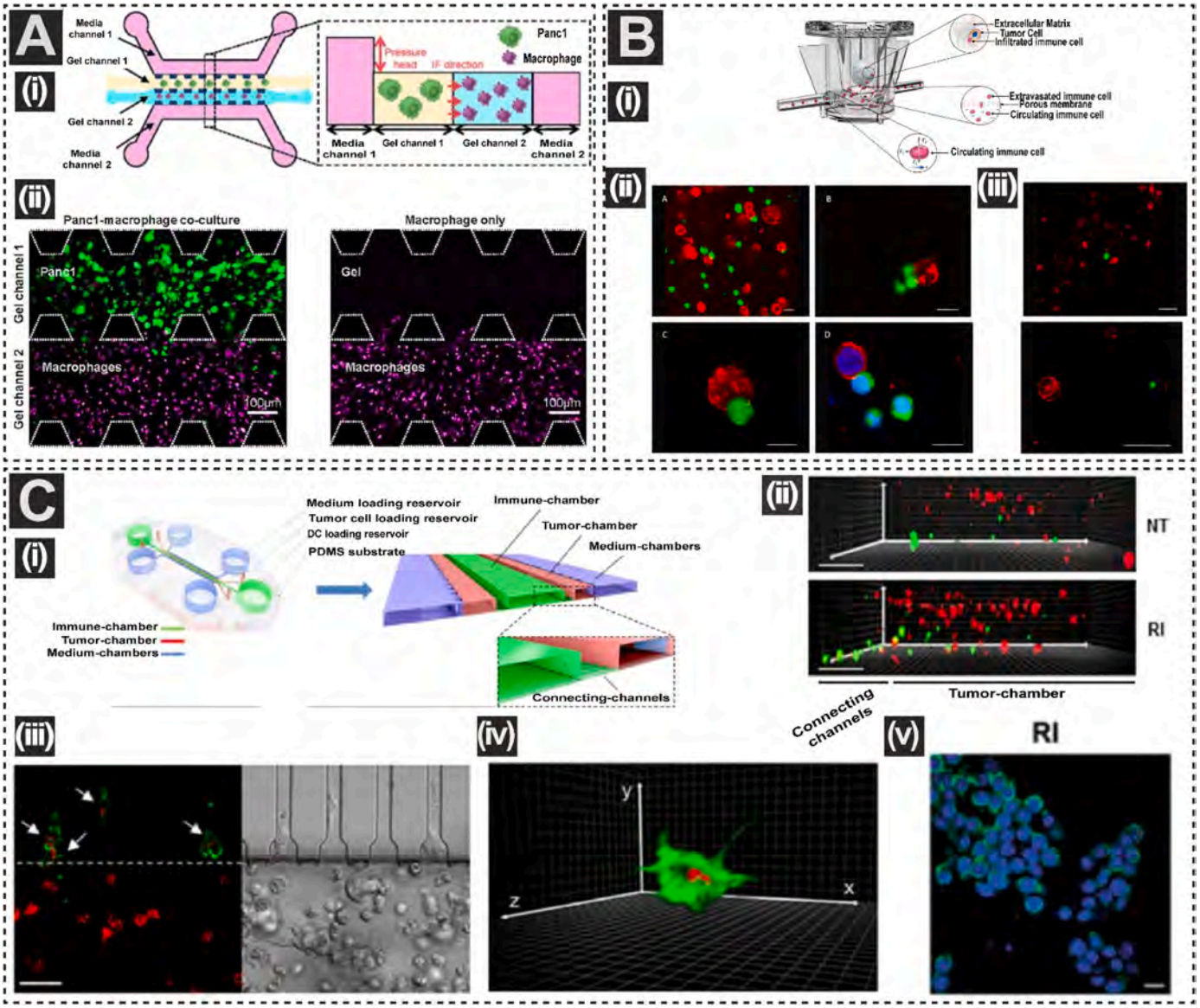

Fig. 8. Microfluidic Models to Study Tumor-Immune Interactions A) Model to evaluate tumor secreted factors on macrophage migration **(i)** Schematic of microfluidic platform to study the Panc 1 – macrophage crosstalk with the incorporation of interstitial flow **(ii)** Confocal image to depict macrophages with/without tumor cells in gel channel. Adapted from Lee et al. with permission from Oxford University Press [Integrative Biology] Copyright (2020) [206]. **B)** Microfluidic model to study NK cell extravasation **(i)** Schematic of the organ-on-chip platform where HTLA-230 cells were incorporated into a 3D alginate scaffold and cultured alongside a microcirculation of NK cells. **(ii)** NK cells (green) and NB cells (red) co-embedded in a 3D alginate scaffold to depict NK cell infiltration in tumor compartment (static culture) (blue - DAPI). **(iii)** Confocal images of NB cells embedded in 3D alginate scaffolds and subjected to 4 h of dynamic flow revealing successful infiltration of NK cells into the gel. Adapted from Marzagalli et al. with permission from Frontiers [Frontiers in Bioengineering and Biotechnology], Copyright, 2022 [209]. **C)** Model to assess DC-Cancer interaction **(i)** Schematic of the microfluidic device to track DC-cancer cells dialogue that has immune and tumor spaces connected by connecting chambers to understand the motion of migrating DCs **(ii)** 3D reconstructed image made from confocal images showing connecting-channels and tumor-chambers. IFN-DCs (green) are observed actively migrating in three directions within the non-treated (NI) (top) and the drug-treated (RI) spaces (bottom). However, they are more prevalent within the 3D tumor space containing drug treated cancer cells (red) (bottom). **(iii)** Fluorescence image displays IFN-DCs spanning connecting-channels towards the RI space after phagocytizing SW620 cells (bottom). **(iv)** 3D representation depicts the engulfment of SW620 cells (red) by IFN-DC. **(v)** Immunofluorescence of CXCL12 expression in RI-treated SW620. Adapted from Parlato et al. with permission from Springer Nature [Scientific Reports], Copyright (2017) [210].

205]. Therefore, there is a pressing need to develop a 3D microfluidic platform to understand the involvement of immune cells in tumor progression comprehensively. Such platforms would provide a reductionist and controlled approach to evaluate the precise role of immune cells in the TME.

Macrophages, being an abundant population in the TME, contribute to 5–50 % of the tumor mass. To better understand the role of macrophages, Lee's group focused on the co-culture of human blood monocyte-derived macrophages with human pancreatic adenocarcinoma to evaluate how interstitial flow and tumor-secreted factors that affect macrophage migration and cancer progression (Fig. 8A (i)). It was established that there was increased macrophage migration in the presence of cancer cells or interstitial flow, but no significant difference was observed when both factors were included. The secretion of cytokines IL8 and CCL2 secreted by tumor cells enhances the migration of macrophages. The migration was inhibited by blocking antibodies for IL8 and CCL2 and restored by interstitial flow, indicating cytokine-independent migration induction [206]. Hebert et al. discovered that when macrophages and MDA-MB-231 cells were co-cultured in a 3D microfluidic chip, macrophages were found to enhance the migration of MDA-MB-231 cells by releasing TNF-α and TGF-β1 via NF-kB dependent MMP1 expression [207]. A similar observation was made in the case of ovarian tumor cells co-cultured with neutrophils in a microfluidic device, where neutrophils facilitated the invasion of ovarian tumor cells by producing neutrophil extracellular traps [208]. Current promising immunotherapy target utilizes NK cells for their capability to cause cytotoxicity in cancer cells. Marzagalli et al. utilized a humanized and immunocompetent organ-on-chip technology designed to mimic the behavior of NK cells in a 3D alginate-based neuroblastoma tumor model. Briefly the design has two compartments, where the tumor cells are separated from the fluid flow compartment using a porous membrane, where the devices are connected to a pumping system capable of generating fluid flow, that closely mimics the microcirculation of NK cells within TME (Fig. 8B (i)). The researchers observed a significant increase in NK cell extravasation in the presence of tumor cells. (Fig. 8B (ii-iii)). By comparing the standard NK cells with infiltrated NK cells recovered from the alginate hydrogel, it was evident that infiltrated NK cells had reduced $CD16^+$ NK cells, where $CD16^+$ NK cells represent the NK cell population that have high cytotoxic potential. Overall, the multi-organ-on-chip system provided a novel and promising tool for studying the complex behavior of NK cells within the context of tumor infiltration and cytotoxicity in a more physiologically relevant setting [209]. Parlato et al. conducted another study to assess how dendritic cells (DCs) migrate within a 3D tumor environment in response to anti-cancer treatment. The researchers utilized a device featuring five parallel channels. The middle channel was loaded with human monocyte-derived DCs. The two adjoining channels contained human CRC cells encapsulated in a collagen I matrix connected by microchannels. The tumor channels were supported by two additional channels that supplied nutrients and facilitated gas exchange (Fig. 8C (i)). The CRC cells were treated with a synergis blend of epigenetic drugs - histone deacetylase inhibitor romidepsin (R) and immune-modulator cytokine IFN-α (I), which is known to induce immune-mediated cancer cell death. Results from time-lapse analysis revealed that compared to the control group, the treatment enhanced DC migration through the activation of CXCR-4/CXCL12 axis (Fig. 8C (ii-iv)) [210].

Microfluidic platforms are also used as a preclinical tool for testing immunotherapeutic strategies. For instance, Patient-derived organotypic tumor spheroids (PDOTS), which harbors autologous tumor-infiltrating PD-1 blockade-sensitive immune cells, were cultured within the central gel region of a 3D microfluidic chamber. This gel region was physically separated from the side channels that were perfused with medium and antibodies by a series of posts. Through live imaging analysis, researchers were able to observe and track fluorescently labeled immune and cancer cells within the PDOTS. They also assessed the cell viability in the presence of *anti*-CTLA-4 and/or *anti*-PD-1 antibodies. This experimental setup provided the advantage of evaluating the dynamic responses to immune checkpoint inhibitors, allowing for a better understanding of the effectiveness of these treatments [211]. Pavesi et al. utilized a platform that contained a central gel channel with cancer cells embedded in collagen I connected to two adjacent media channels by trapezoidal spacing posts to investigate the efficacy of T cell receptor-engineered-T cells (TCRe-T Cell) in combating HCC. The HCC cells were confined within a microenvironment embodied by hypoxia and inflammation. One of the media channels was filled with TCRe-T cells labeled with fluorescent dye. Through live-cell imaging, the researchers assessed the migration of TCRe-T cells into the 3D hydrogel matrix and their ability to eliminate tumor cells in the presence of inflammatory cytokines and elevated oxygen levels. Moreover, this device proved beneficial in demonstrating that TCRe-T cells maintained their cytotoxic potential even in the presence of immunosuppressive drugs, to better predict the success of immunotherapy in specific scenarios, such as organ transplant patients [212]. With research advancements, microfluidic models to study the bidirectional crosstalk between immune components and other stromal components are gaining much interest to identify novel mechanisms that could have better physiological mimicry and develop effective therapeutics. The following section will, in detail, discuss the microfluidic platform integrating complex multicellular interactions within the TME.

3.3.3. *Microfluidic models for complex TME interactions*

Recent research has been centered on incorporating more intricate TME models, including 3D models that contain innate/adaptive immune cells with other stromal cells to add more complexity as well as to understand the synergistic crosstalk between various cell types in tumor progression. Immune components such as TAMs, T cells, and NK cells are recruited from the bloodstream through chemokine/cytokine gradient [213], which can be precisely modeled using microfluidic platforms by controlling the fluid flow in these miniature devices. Also, incorporating vascularized networks to mimic *in vivo* physiological systems to study the immune cell recruitment to primary or metastatic sites via *trans*--endothelial migration can be feasible through microfluidic platforms. Luuk de Haan et al. studied *trans*-endothelial migration of T cells in both healthy and diseased states. Briefly, the propsoed microfluidic model comprised of perfusable blood vessels that allowed to study the extravasation and migration of T cells into 3D ECM. By co-culturing melanoma cancer cells with ECs, it was evident that the vascular permeability was increased with increased T cell migration towards the tumor cells. However, in the absence of cancer cells, the migration of T cells extravasating the endothelium was low [214]. Zervasantonakis et al. recreated the tumor vasculature and investigated the role of immune modulation on the process of intravasation across the endothelium. The device consisted of two independent microchannels that were seeded with tumor cells on one side and ECs on the other side. They were interconnected by a central hydrogel region, creating the tumor-vascular interface. To assess the influence of macrophages on cancer cell intravasation, macrophages were added to the central hydrogel channel. It was observed that there was significantly higher number of intravasating cancer cells in the presence of macrophages. To test whether macrophage induced permeability increases the intravasation of cancer cells across the endothelium, the ECs were treated with TNF-α (a vital cytokine secreted by macrophages). It was found that the permeability of vascular network as well the number of intravasating cancer cells were pronounced with TNF-α treatment. Furthermore, in presence of macrophages, alongside neutralizing TNF-α with an antibody, reduced the leakiness of the endothelium, suggesting that TNF-α signaling by macrophages is vital for maintaining barrier function [215]. Song et al. engineered an intricate *in vitro* vascularized model to mimic the TME. The platform had three parallel microchannels where the central channel was loaded with HUVECs, fibroblasts, and CRC cells. The side channels were populated with HUVECs. Following the establishment of the vascular networks, NK cells were loaded into the vessel

via the side channel. The study yielded intriguing results, indicating that NK cells exhibited notable cytotoxicity against CRC cells within this simulated tumor vasculature framework [216]. Studies also investigated the role of more than two stromal cells with immune cells in a single platform. For instance, Liu et al. used a microfluidic platform to mimic the bladder cancer microenvironment, with four cell types that include bladder cancer cells along with fibroblasts, ECs and macrophages that permitted culturing in four intersecting cell culture chambers, which allowed for paracrine interactions along with the ability to assess cell motility in the TME. In addition, each chamber was separated by a barrier of Matrigel® that facilitated cell interaction through the exchange of biochemical factors as well as metabolites. Consequently, macrophages displayed migratory behavior directed towards cancer cells, mirroring the process of macrophage recruitment into the TME. This platform also allowed testing neo-adjuvant chemotherapy, laying a foundation for individual therapy [217]. Aung et al. developed a tumor-on-chip platform to study the heterogeneous mix of cells (i.e., cancer cells, ECs, monocytes, T cells) and noncellular components to study the role of TME in examining the infiltration of T cells. It was established that the presence of monocytes along with cancer cells in the form of spheroids/dispersed cells and a hypoxic environment increased the recruitment of T cells into the TME [218]. Lee et al. conducted a study to assess engineered T cells (i.e., TCRe-T cells) to discern hepatitis B antigen-expressing hepatocellular carcinoma cells (HBV–HCCs) using a 3D TME model. Within this setup, the central gel channel was loaded with human monocytes and HBV-HCC aggregates encapsulated in a collagen I matrix with an adjacent fluidic channel to load TCRe-T cells. The presence of monocytes substantially reduced the cytotoxicity of

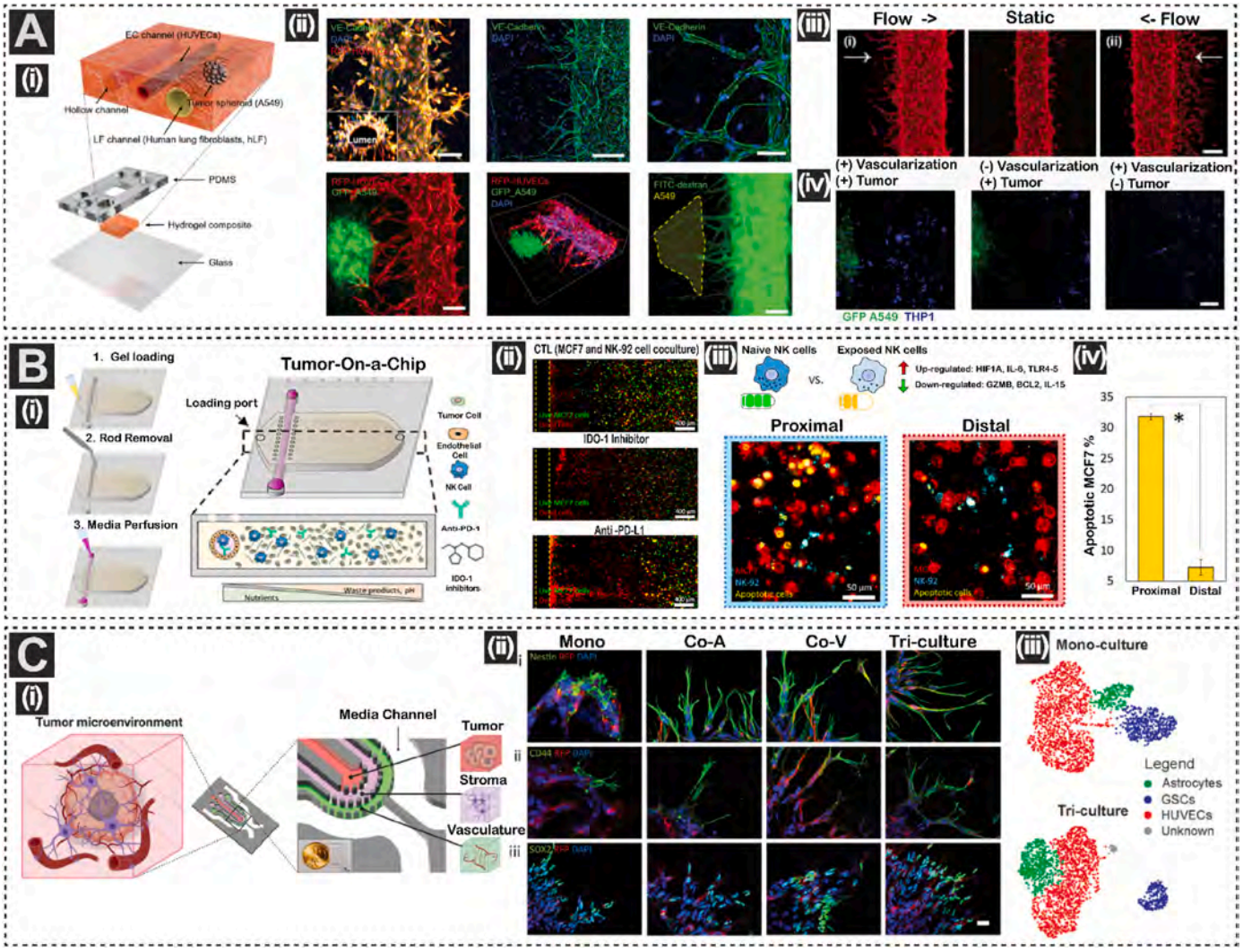

Fig. 9. Microfluidic Models to Study Complex TME Interactions A) Vascularized model to assess immune cell infiltration **(i)** Design of the vascularized microfluidic tumor model **(ii)** Fluorescence image depicting the vascularized lung cancer model. **(iii)** Growth patterns of HUVECs (RFP expressing) vary depending on the flow directions. **(iv)** Delivery of THP1 cells to the tumor spheroid via the microvessels on the vascularized tumor chip, leading to the conspicuous presence of numerous THP1 cells (blue) in close proximity to the tumor spheroid (green). Adapted from Kim et al. with permission from Wiley Online Library, [Advanced Healthcare Materials], Copyright (2022) [221]. **B)** Microfluidic model to assess NK Cell exhaustion **(i)** Schematic representing the tumor-on-a-chip system. The interior lumen is coated with HUVECs to create surrogate blood vessels **(ii)** The influence of an *anti*-PD-L1 antibody and IDO-1 inhibitor was assessed using TOC (Live cells: green and Dead Cells: Red). **(iii)** Recovered NK Cells, continued to display numerous changes in gene expression (top). Fluorescent image to depict majority of the apoptotic cells were MCF7 cancer cells (bottom) **(iv)** Quantification of apoptotic MCF7 cells which indicates majority of the apoptotic cells are in the proximal area of the devices. Adapted from Ayuso et al. with permission from American Association for the Advancement of Science [Scientific Reports], Copyright (2021) [223]. **C)** Recapitulating complex GBM vascular niche using microfluidics **(i)** Schematic of three layered GBM-perivascular niche microfluidic chip. **(ii)** Positive immunostaining for Nestin, CD44, and SOX2 markers was observed in GB3-RFP cells. **(iii)** Through clustering of scRNA-seq profiles and analysis of cell-specific marker genes, distinct clusters were identified for ECs, astrocytes, and GB3-RFP cells in mono-culture and triculture. Adapted from Adhei et al. with permission from Wiley VCH GmbH [Advanced Sciences], Copyright (2022) [225].

TCRe-T cells. However, this reduction was reversed when *anti*-PD-L1/PD-1 antibodies were administered. Overall, it is suggested that this microfluidic models can be a reliable pre-clinical testing platform for evaluating the efficacy of TCRe-T cell therapy [219].

Another study employed a microfluidic device to investigate angiogenesis in liquid tumors, explicitly focusing on leukemia. The microfluidic 3D angiogenesis chip offered a practical approach to enhance and observe the initial stages of angiogenesis triggered by leukemic cells and bone marrow stromal cells. Briefly, leukemic cells and HUVECs were introduced into two parallel microchannels, separated by an acellular channel filled with collagen I gel. When the microchannel designated for leukemic cells was kept acellular, only a small number of ECs invaded the collagen I matrix that separated the two channels. However, in the presence of leukemic cells and bone fibroblasts, the ECs exhibited invasion into the collagen I matrix, forming sprouts and new blood vessels. This study also evaluated quantitative assessments of angiogenic factors released by mono-cultures and cocultures of leukemic cells with fibroblasts derived bone marrow that revealed a synergistic interplay among ECs, leukemic cells, and fibroblasts [220]. Kim et al. developed an alternative model of vascularized tumor-on-a-chip, where they placed ECs and fibroblasts in adjacent prepatterned channels. To simulate the high pressure of interstitial fluid similar to tumors, they introduced interstitial flow in a direction that facilitated the transfer of molecules secreted by fibroblasts towards the EC channel after which the lung spheroids (A549 cells) were introduced on Day 4 (Fig. 9A (i) & (ii)). This arrangement promoted the formation of new blood vessels towards the fibroblast channel along with tumor spheroids through angiogenic sprouting. Further transport of immune cells through the tumor-associated blood vessels was investigated using THP1 cells, in the vascularized tumor model there was increased immune cells around the proximity of tumor spheroids (Fig. 9A (iii)) [221]. Mollica et al. conducted a study to investigate the infiltration of T cells into the TME of pancreatic cancer. They employed a microfluidic model comprising separate channels for Panc-1 cells, PSCs, and HUVECs. The model successfully replicated the increased permeability of blood vessels in the presence of T cells. Furthermore, the activated T cells (stimulated through CD3/CD28) exhibited enhanced infiltration toward the pancreatic ductal adenocarcinoma (PDAC) compartment. Through cytokine analysis, the researchers observed that the co-culture of pancreatic cancer cells and stellate cells led to stronger activation of T cells, indicated by higher levels of IL-2 and IFN-γ as measured by a multiplex immunoassay. The study also claimed that activated T cells displayed increased cytotoxicity compared to non-activated T cells in the presence of HUVECs and Panc-1 cells, as evidenced by the upregulation of genes associated with cytotoxicity (granzyme B, perforin, and Fas). Interestingly, in the tri-culture group involving PSCs, lower levels of these genes were observed, indicating that PSCs dampened the inflammatory response and supported tumor growth [222].

To evaluate the influence of TME stress on NK cell function, a tumor-on-chip model was utilized where breast cancer cells (MCF7) and NK cells were coembedded in a 3D matrix. The other end of the microchamber contained lumen with HUVECs (Fig. 9B (i)). Through the presence of lumen in one end of the platform, the researchers were able to mimic 3 distinct zones of the solid tumor namely 1) Proximal 2) Central and 3) Distal end. It was found that most of the apoptotic cancer cells were within the proximal end in comparison to the distal end, meaning that the cytotoxic potential of NK cells in distal end is diminished. This clearly indicated the role of TME stress on NK cell exhaustion (Fig. 9B (iii-iv)). The research group also tested anti PD-L1 and IDO-1 inhibitor in the device, however live cells were found in the distal end (Fig. 9B (ii)). The study showed that prolonged exposure of NK cells to high levels of tumor stress led to their exhaustion, characterized by decreased NK cell cytotoxicity and cytokine production [223]. Wimalachandra et al. co-cultured ECs and ovarian cancer cells with the main objective to explore the potential of chemokine-functionalized nanoparticles in the process of recruitment of T cells and DCs to the site of the tumor. Their experimental configuration consisted of a microfluidic platform with a central channel with ovarian cancer cells embedded in fibrin. The two flanking parallel channels were seeded with ECs. These channels were linked through 37 interpost regions. By employing image analysis techniques, the researchers observed that the nanoparticles loaded in the vascular channels effectively traversed the endothelial barrier and accumulated at the interface between the tumor and endothelium, reaching the tumor site. This orchestrated chemokine regulated migration of DCs and T cells from the vascular channel towards the ovarian cancer cells was pronounced potentially showcasing the anti-tumor response against the tumor [224]. In another study by Adjei et al., the complexity of the model was increased by incorporating astrocytes, an important stromal component in gliomas; the tri-culture platform with GSCs + ECs + Astrocytes significantly increased the invasion distance of cancer cells with a change in its morphology (Fig. 9C (i) & (ii)). Using sc-RNAseq, 15 ligand-receptors that were upregulated were identified, and it was found that the Serum Amyloid A (SAA1) ligand protein led to the significant chemotactic invasion of GSCs (Fig. 9C (iii)) [225]. In another study, Muhammad R. Haque et al. developed a tumor microarray device to study the TME of pancreatic ductal adenocarcinoma using patient-derived cells (PCCs). They incorporated pancreatic stellate cells and U937 monocytes. In the presence of stromal cells, the PCCs grew significantly faster. In addition, macrophages showed relatively increased pro-tumorigenic (M2 phenotype) marker expression in co-culture conditions [226]. A study by Hu et al. developed vascularized tumor-spheroid-on-a-chip to mimic TME and to find the role of Prolyl hydroxylases (PHD) inhibitors known as DMOG (Dimethylallyl glycine) role in enhancing the anticancer drug i.e., paclitaxel activity. Briefly, the device consists of 5 parallel channels to assemble fibroblast, HUVECs and human esophageal carcinoma (Eca-109) cells. Based on their studies from assessing the vessel size, permeability it was established that the presence of DMOG increased the delivery of drug to the tumor spheroids with increased effectiveness for paclitaxel as well as cisplatin in killing cancer cells [227]. In a very recent study by Geyer et al., the authors established a microfluidic-based PDAC organoid system to study the role of PSCs in pancreatic cancer under both hypoxic and normoxic conditions. Under hypoxia and normoxic conditions, both mono-culture and co-culture of pancreatic organoids with PSCs were exposed to *gemcitabine* in conjunction with other chemotherapeutic drugs. The findings provide substantial evidence that hypoxia serves as a distinct molecular programs in PDAC organoids that affect the responses to different classes of drugs [228]. To end, the investigation of complex spatial multicellular cancer interactions in microfluidics has provided invaluable insights and remarkable prospects within the realm of cancer research, thus driving further groundbreaking discoveries.

By leveraging microscale platforms, researchers have gained a deeper understanding of the intricate interplay between cancer cells, their surrounding microenvironment, and therapeutic agents. However, there are drawbacks that limit the overall implementation and impact of microfluidics in this domain. Scalability, particularly concerning downstream analysis necessitating specific cell volumes or quantities, poses a challenge that may be demanding with microfluidic systems. Moreover, the technology demands specialized expertise, requiring trained personnel proficient in both microfabrication techniques and biological research. Additionally, the lack of proper validation of the model in comparison to *in vivo* TME remains elusive [229,230]. As exploration of spatial multicellular cancer interactions in microfluidics continues to evolve, we anticipate its continued contribution to advancements in cancer diagnostics, treatment optimization, and ultimately, improved patient outcomes.

3.4. 3D printed models

3D bioprinting, a technological breakthrough, entails the precise and regulated deposition of bioinks, including tissue spheroids, cell pellets, ECM components, and cell-laden hydrogels. These bioinks are

strategically deposited in a layer-by-layer fashion, following a computer-generated design. This design process results in the creation of 3D structures with intricate and functional counterparts, which have gained significant progress over the past few decades. Currently, natural biomaterials such as alginate, gelatin, collagen I as well as hyaluronic acid are widely used in bioprinting [231–233]. Also, combination of synthetic and natural polymers such as gelatin methacryloyl are also used to print robust scaffolds. To produce stable physiological scaffolds, crosslinking is a crucial factor to stabilize as well as strengthen the printed constructs. Two modes of crosslinking include chemical (enzymes, tannic acid, or calcium ions) and physical crosslinking (ultraviolet treatment) [234].

The primary modalities used in bioprinting include extrusion-based bioprinting (EBB), laser-based bioprinting (LBB), and droplet-based bioprinting (DBB) [235,236]. EBB, one of the most common methods of fabrication, involves using robotic or pneumatic-driven forces to dispense bioinks, and its main idea is to replace the ink as liquid/melt through the nozzle and solidify. It's printing accuracy and feasibility depend on the printing material chosen [237]. Some of the critical parameters to optimize would be the printing speed, diameter of the nozzle, mechanical force or dispensing pressure, and distance from the printhead [238]. DBB, also known as 'inkjet bioprinting,' is a non-contact printing method that relies on the precise deposition of droplets through mechanical actuation methods like thermal, solenoid-based, or piezoelectric mechanisms. The viscosity of the ink and the surface tension are the essential properties of the ink that must be considered. The motive force of this bioprinting modality highly lies in the spatial resolution, that is, proper placement of the droplets. Some notable advantages encompass high printing speed, fine resolution, and the ability to create intricate patterns as well as complex and heterogeneous structures. LBB is a technique that involves depositing bioinks in a predetermined pattern defined by the path of a laser. Briefly, a laser beam is focused onto a layer of bioink coated on a target surface. The laser energy is absorbed by bioink which locally increases the temperature and forms vapor bubbles. This rapid bubble expansion and collapse generate droplets on the target surface, allowing precise printing. One advantage of this modality is having high-resolution printing and allowing multiple cell types or bioinks to be printed simultaneously, thereby creating more complex structures. Some aspects affecting printability include laser fluence, substrate humidity, sample viscosity, and surface density.

Bioprinting can also be classified based on scaffold-free and scaffold-based approaches. In scaffold-free approaches, the bioink, i.e., the cell pellets, are printed on the sacrificial mold that is later sacrificed once the tissue matures and deposits its own ECM. In a scaffold-based approach, the bioink is encapsulated in a hydrogel. This method relies on the degradation kinetics of the material as well as the cell-hydrogel interaction to guide tissue growth [235,239–241]. In the recent past, 3D printing has shown great promises in cancer research, especially in tumor modeling, drug testing, personalized medicine, and metastatic research. One advantage of bioprinting to reconstitute TME is controlling the spatial distribution of matrix properties. For instance, the mechanical properties of ECM, including matrix stiffness, significantly influence cancer cells' metastatic behavior, which can be integrated into the 3D-printed tumor model [242]. The spatial arrangement of biochemical factors can also be modulated to replicate the characteristics of the native TME within bioprinted models. Bioprinting has been utilized to create blood vessels and vascularized tissues, employing the scaffold-based or scaffold-free methodology.

3.4.1. 3D printing models for tumor-stromal interactions

In recent years, brain tumor physiology has been mimicked using 3D printed tumor on chip. A model of GBM was fabricated by Lee et al. using the extrusion-based bioprinting method. GSCs derived from patients were used for the study, along with HUVECs. Gelatin was used as the sacrificial material, where a 3D collagen I matrix with different laminin concentrations was used to create a vascular channel. GSCs were injected either during the printing process/or once the vascular channel was established. In collagen I with a higher concentration of laminin, higher invasion, and proliferation of GSCs was observed [243].

Yi et al. recapitulated the cancer stroma of GBM on a silicon-based 3D-printed chip. The chip had two concentric circles: an inner core with patient-specific cancer cells encapsulated in porcine decellularized brain matrix and an outer core with ECs in GelMA hydrogel that closely mimicked the *in vivo* hypoxic tumors. The model also proved that GBM-on-a-chip reproduces clinically observed patient-specific resistance to treatments with chemoradiation and temozolomide [244]. Chaji et al. studied the role of pre-differentiated adipose-derived mesenchymal stem cells in breast cancer using a low-cost extrusion printer with various alginate/gelatin composites. A bioink with 3:2.5 % alginate and gelatin was determined to mimic the breast TME. The authors chose DMEM-complete medium for 3D bioprinted cell-laden hydrogels after a preliminary screening of culture media. Direct printing resulted in morphological changes with most of the cells migrating towards the center of the construct. Overall, this study reported the reconstruction of multicellular breast cancer TME using a 3D printing technique with optimal media composition for maintaining the viability of various cell types [245]. Tang et al. developed a tri-regional GBM model with varying stiffness in different regions representing GBM stroma, diseased or healthy brain tissue, and brain capillaries using patient-derived GBM cells and hyaluronic acid derivatives through the process of digital light processing-based bioprinting. Two varied ECM stiffness with a constant HA concentration were assessed: (i) Glycidyl Methacrylate Hayaluronic Acid (stiff) (ii) GelMA (soft) bioinks. The stiff culture increased the expression of genes associated with mesenchymal subtypes that is often linked to poorest treatment outcomes. The inclusion of HUVECs within the stiff model gave rise to extensions resembling blood vessels that closely interacted with SOX2+ TS576 cells. Moreover, these ECs triggered varying drug responses within the GBM model [246]. To study patient derived CRC-CAF interaction, Chen et al. utilized acoustic bioprinting strategy to assess the role of CAFs in cancer invasion and migration. A model with cancerous microtissues surrounded by fibroblast was constructed in GelMA to mimic the *in vivo* TME. On day 2, CAFs stretched the microtissues outwards, treatment with 5-fluorouracil (5-FU), showed tendency of not much invasion. By analyzing the invasive potential of fibroblasts along with protein expression, it was established that the model mimicked the key features reported in clinical data based on immunohistochemistry, magnetic resonance imaging, and H&E staining [247]. To model early stages of migration of cancer cells from the primary site to the secondary site, the study by Cui et al. used a stereolithographic 3D printing technique. The complex dissemination process was simplified into a single 3D vascularized tissue construct made from biocompatible photo-crosslinkable ink. 3D printed tissue structure had three distinct regions namely bone, endothelial, and tumor region. To recapitulate the bone micro vascularized microenvironment, mineralized bone scaffold containing 10 % GelMA, 10 % polyethylene glycol diacrylate (PEGDA) and hydroxyapatite (major bone mineral) was used. 10 % GelMA and 10 % PEGDA ink was used for establishing the tumor region containing two distinct breast cancer cells (MDA-MB 231 and MCF-7). Finally using pure GelMA the vascular region was printed. Through IF staining it was shown that highly metastatic MDA-231 cells successfully colonized into the bone region through *trans*-endothelial migration after 2 weeks of culture [248].

3.4.2. 3D printed models for tumor-immune interactions

A study conducted by Heinrich et al. investigated the interaction between glioma-associated macrophages and GBM cells utilizing a mini 3D-printed brain model. Using a two-step printing strategy this study evaluated the cellular crosstalk based on paracrine and juxtracrine signaling. In the paracrine model, where GBM cells GL261 and macrophages RAW264.7 cells were printed separately and cultured together (Fig. 10A (i)). On the other hand, in the juxtracrine model, both cell

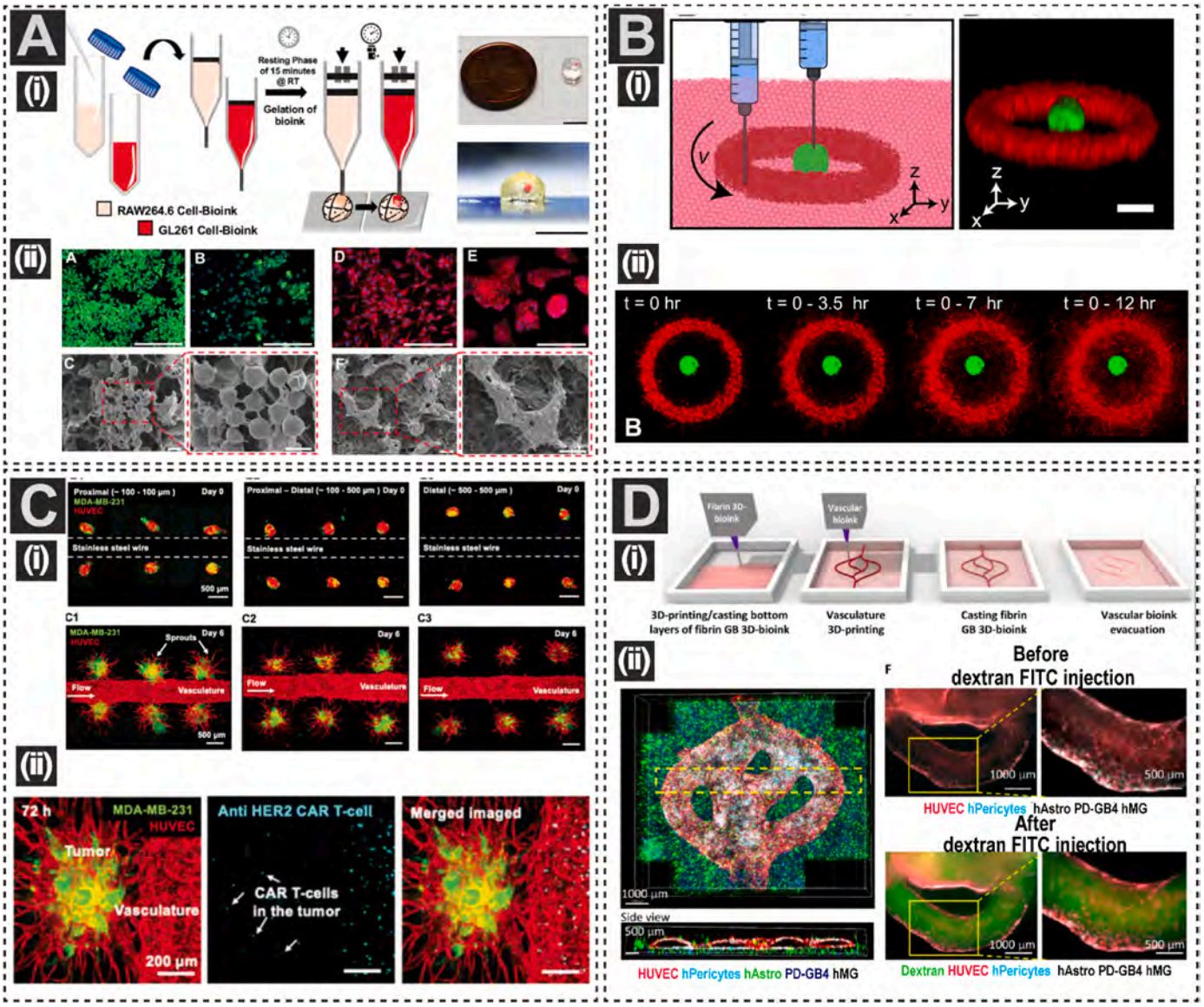

Fig. 10. 3D printed Models A) 3D printed mini-brain GBM model **(i)** Schematic representation of the two-step 3D printing process. The larger brain encapsulating macrophages (RAW264.7) with a cavity are printed followed by the filling of GBM cells (GL261) into the cavity (left). Glioma cells within the 3D printed model are highlighted in red alongside the cross-sectional image (right). **(ii)** SEM and F-actin verification of attachment of RAW264.7 (left) and GL261 (right) on to the bioink matrix in comparison to conventional well plate. Adapted from Heinrich et al. with permission from Wiley [Advanced Materials] Copyright (2019) [249]. **B)** Immunotherapy model to access T cell dynamics **(i)** Schematic representation of the 3D printed adoptive cell transfer model with spatially organized tumor spheroid (green) surrounded by CAR-T cells (red). **(ii)** 3D rendered image of adoptive cell transfer model. **(iii)** Maximum intensity projection images for monitoring the migration pattern of T cells from the printed ring. Adapted with permission from Elsevier [Bioprinting], Copyright (2022) [252]. **C)** Dynamic flow based multi-scale vascularized breast tumor model. **(i)** Confocal images of breast tumor spheroids (green) printed at three different locations [(i) proximal, (ii) proximal-distal, and (iii) distal location] from the central (red) perfusable vasculature. Images obtained after 6 days of perfusion exhibit tumor angiogenesis. **(ii)** Immunofluorescent images of CAR-T cells (labeled with cell tracker violet) showing the infiltration into the 3D printed spheroids at 24 h and 72 h time points. Adapted from Dey et al. with permission from AFM [Advanced Functional Materials], Copyright (2022) [253]. **D)** 3D GBM TME model **(i)** Illustrative diagram depicting the multi-stage process of the 3D bioprinting model. **(ii)** Confocal microscopy tiled Z-stack images showcasing the 3D-printed vascularized GBM model with a penta-culture composition. The blood vessels are enveloped by pericytes labeled with iRFP (cyan) and accompanied by HUVECs labeled with mCherry (red). Surrounding this arrangement are PD-GB4 cells labeled with azurite (blue), while hAstro cells labeled with GFP (green) and nonlabelled hMG (left), and images obtained through fluorescence microscopy depict the 3D-bioprinted vascularized GBM model, captured both prior (upper section) and subsequent (lower section) to the infusion of 70-kDa dextran-FITC (right image) Adapted from Neufeld et al. with permission from American Association for the Advancement of Science [Science Advances] Copyright (2021) [254].

types were printed together to enable direct cell-cell interactions. Assessment of the paracrine model showed increased expression of genes involved in macrophage recruitment (CCL2) and matrix remodeling (i.e., MMP9, MMP8). Furthermore, through scanning electron microscopy and immunofluroscent staining, the attachment of RAW264.7 and GL261was verified (Fig. 10A (ii)). Next, evaluation of direct cellular interactions through transcriptomic analysis showed higher upregulation of macrophage-specific markers (Nos 2, IL10) in the juxtacrine model than in the paracrine model. Findings from this study showed a resemblance of the proposed model to the *in vivo* system to a great extent [249].

The efficacy of CAR-T cells in treating solid tumors is still challenging mainly due to the limitation of 3D model that can better recapitulate the 3D microenvironmental aspect. L1 is an adhesion molecule that is

strongly expressed by tumor cells. L1 targeting CAR-T cells are in clinical trials for neuroblastoma studies [250]. In those efforts, a large-scale neuroblastoma bioprinted model was employed for testing the CAR-T performance in targeting the L1 adhesion molecule. The final 3D architecture was a 4 mm diameter and 500 μm deep disc that was printed using a stereolithographic bioprinter. Uniform distribution of cells within the 3D structure was achieved through layer-by-layer printing of GelMA scaffold and reported the extended viability of the cells within the model during long-term culture. Using two-photon and confocal microscopic techniques, the infiltration of CAR-T cells within the co-culture model was demonstrated. Functional evaluation of CAR-T cells using flow cytometry showed more activation of T-cell (positive for CD25 and CD137) in 3D printed neuroblastoma model as compared to the 2D model. This study showed the potential applicability of these engineered models as a preselection tool for assessing CAR-T cells efficacy as compared to simplified 2D models [251].

In adoptive immunotherapies, tumor-reactive T cells are activated *in vitro* and introduced back into the host system. Though this is a promising technique, the efficacy of this treatment remains unresolved. Using a spatiotemporal model that allows precise control over cell type organization, 3D printed adoptive immunotherapy model of glioma cancer was proposed. The architecture of the proposed study contains tumor spheroid surrounded by 2 mm T cell ring (Fig. 10B (i)). Confocal time-lapse imaging analysis showed migration of T cells to the spheroid region and using non-tumor specific T cells (control group) it further confirmed the influence of tumor factors on T-cell migration (Fig. 10B (ii)). Furthermore, transcriptomic analysis of cells from the platform revealed the influence of crosstalk between cancer and stromal cells on immune cell migration. Thus, the reported work provided a spatiotemporal model that allowed real time assessment of T cell dynamics in a complex microenvironment [252].

3.4.3. 3D printed models for complex TME interactions

Though in the previous section 3D printed models are used for immunotherapeutic studies, those models evaluated the effect without a proper vascular network. In an attempt to model CAR-T interactions in a physiological environment, a recent study reported the development of 3D flow-based 3D-vascularized breast tumor model. Vascularized tissue construct was formed in 7 sequential steps as shown in (Fig. 10C (i)). Using aspiration-assisted bioprinting. Heterotypic tumor spheroids containing MDA-MB-231 breast cancer cells and human dermal fibroblast were bioprinted at proximal or distal locations from the main perfusable vasculature. 3D printed spheroids at varying locations from the vasculature showed optimal sprout formation and endothelial barrier expression (Fig. 10C (ii)). Intriguingly, tumors located at proximal distance showed longer vessels and it was attributed that direct diffusion from the main vasculature influenced the growth of the tumor angiogenesis. The established platform was validated for use in drug studies by evaluating the efficacy of chemotherapeutic and immunotherapeutic agents. For the chemotherapeutic evaluation, doxorubicin was perfused through the main vasculature at concentrations ranging from 0 to 100 μm and these studies were conducted in spheroids located at proximal distance from the vasculature. Under perfusion condition, this study observed dose dependent reduction of the tumor volume. Similarly, CAR-T cells that are specific to HER2 receptor were used for immunotherapeutic screening. Visualization of CAR-T migration into the tumor spheroid showed increased infiltration of CAR-T HER2 as compared to CAR-T CD19 cells. This clearly highlights antigen specific activation of CAR-T cells in cytotoxic effects. Overall, this study set a framework for developing more physiologically relevant TME models [253].

Neufeld et al. developed a sophisticated model of GBM with a bioink made of fibrin (Fig. 10D (i)), which contained GBM cells obtained from patients, along with human astrocytes, human microglia, and HUVECs with human pericytes. The vascular network within the construct was created by sacrificial printing, and then HUVECs and human microvascular brain pericytes were added to line the vessels (Fig. 10D (ii)). The PD-GB cells proliferated and invaded higher in co-culture with human astrocytes. By comparing the transcriptional profiles of cells cultured in 2D, 3D-printed, and murine *in vivo* models, the group found striking similarities in gene expression between cells cultured in the 3D bioprinted system and *in vivo* murine model [254].

In another study, Lesile group devised a GBM model using a modified scaffold made of alginate, collagen I, and hyaluronic acid. This scaffold was printed using a multi-nozzle extrusion printer. This study aimed to study the influence of stromal population on tumor cell signaling and its impact on glioma treatment outcomes. To achieve a complex TME of GBM using the co-printing technique, GBM cells alongside fibroblasts and macrophages were encapsulated within the modified alginate bioink. Firstly, through immunofluorescent staining for viability and neural stem markers the authors showed that bioprinting did not affect the viability of the embedded cells and the cells were able to maintain their stem properties in the modified scaffold. Next, the effect of stromal and immune cells on drug sensitivity was studied. Intriguingly, the response of the model to commonly used GBM drugs (temozolomide) in the presence or absence of macrophages showed not much of a difference in their viability. These findings clearly suggested the need to incorporate relevant stromal cellular components for better screening. Lastly, using fluorescent protein kinase receptors signaling at single cell level, it was observed that stromal cells are involved in cell signaling activation which was evident with more fluorescent activation of cells in 3D conditions [255]. Overall, this 3D printed strategy outlined in this study act as a valuable tool for drug screening as well as to understand the dynamic influence of TME.

The advent of 3D bioprinting in cancer research, facilitating precise deposition of bioinks to create intricate and functional 3D structures, has led to significant advancements in this area. However, this innovative technology is not without challenges. The complexity and cost associated with fabrication and maintenance, demanding specialized expertise in both biological and engineering domains, could limit accessibility. Additionally, there are challenges related to the limited availability of suitable printing materials, impacting the diversity of constructs that can be produced depending on the type of 3D printer. Addressing these limitations is pivotal for harnessing the full potential of 3D bioprinting in cancer research, and enhancing its utility in tumor modeling, drug testing, personalized medicine, and metastatic studies [256].

4. Conclusion and future perspectives

Developing effective treatment strategies for cancer requires a deep understanding of the complex interactions between cancer cells and the surrounding stromal and immune components. Research over the past decade has highlighted the critical importance of TME interactions in cancer progression, metastasis, and drug resistance. The goal is to gain a deep understanding of these crosstalk at the molecular level, in order to reverse the tumor-supporting effects of the TME.

Models that replicate the TME, including blood vessels and immune cells, are best portrayed *in vivo*. However, these models are expensive, time consuming and can raise ethical concerns. In addition, animal models have different physiology than humans and it is challenging to dissect the specific role of stromal or immune components on disease progression. The reemergence of 3D-engineered *ex vivo* tumor models are rapidly improving and gaining momentum in replicating the TME landscape. Incorporating patient-derived cells into 3D models enhances physiological relevance but may entail higher costs and clinical coordinations, however the translational relevance is higher when compared to animal models. Engineered models, from spheroids and organoids to more complex tumor-on-a-chip and 3D bioprinted models, have enabled mimicking the tumor microstructure with high precision and controllability. The current ability to model cancer *ex vivo* has reached unprecedented heights, providing valuable insights into the molecular and cellular pathways associated with tumor malignancy. The use of 3D models are more advantageous in comparison to humanized

animal models (animals that are genetically modified or treated to incorporate human cells, tissues or genes) in terms of scalability, cost, and ethical considerations. The controlled and reproducible nature of 3D cultures enables high throughput screening of drugs which might be a demanding process using humanized animal models.

Despite the notable advancements, a realm of unanswered questions and challenges persist in the field of 3D-engineered cancer models. Foremost among these challenges is the imperative need to sustain the viability and functionality of various cell types within the 3D-engineered constructs. Continuous perfusion of tailored media, enriched with essential growth factors, emerges as a key strategy to mitigate this challenge. Alternatively, nanocarrier-mediated growth factor release offers another avenue to improve the cellular viability.

The immune system, with its inordinate complexity and various cellular components, presents a frontier of exploration. While 3D *in vitro* models have provided a versatile platform for manipulating primary cells and advancing tumor immunology research, there exists a substantial scope for enhancing clinical translational research. A significant challenge in immunological inquiry revolves around comprehending the impact of lymphatic drainage of immune cells originating from TME and its consequential effect on antigen presentation. Specifically, the mechanisms underlying the migration and antigen presentation of DCs in the lymph node remain inadequately elucidated. By harnessing biofabrication techniques, it is possible to integrate multiple model systems, offering a precise understanding of antigen presentation in the lymph node. Such integrated studies hold great potential to augment our fundamental understanding of how the immune system surveys our body in normal and pathological conditions. This nuanced understanding of intricate interplay between immune cells, lymphatic drainage, and antigen presentation is poised to contribute significantly to the development of more effective immunotherapeutic strategies.

A secondary imperative lies in the standardization of these *ex vivo* models, critical for transistioning the engineered models from bench side to clinical application. Presently, the reliance of many microfluidic models on PDMS raises concerns related to drug adsorption. Overcoming this challenge necessitates the rapid prototyping of novel materials that are less prone to drug and protein adsorption. Furthermore, concentrated efforts must be made to process the large voluminous data generated by these engineered models, emphasizing the integration of imaging and computational modeling to gain meaningful insights. Finally, it is worth exploring the possibility of combining spatial RNA-seq with 3D-engineered models to gain better understanding of the TME influences on cancer progression. Obtaining information on the polarized state of different cells in proximal and distal locations within the developed model can provide valuable insight into cellular crosstalk. Moreover, this spatial information can help us direct TME microenvironmental components for better tumor therapies.

In summary, this review highlighted the impressive progress that has been made in developing bioengineered *ex vivo* TME models for advanced cancer research. Despite facing several challenges in accurately reflecting patients' physiology, the past few decades have seen significant breakthroughs in this area. As the scientific community continues to advance research in this avenue, we are steadily approaching a point where we can create highly sophisticated models that replicate the human body with exceptional accuracy. These systems will be instrumental in conducting fundamental cancer biology and drug responsiveness research in a highly effective manner.

CRediT authorship contribution statement

Kalpana Ravi: Conceptualization, Writing - original draft, Writing - review & editing. **Twinkle Jina Minette Manoharan:** Conceptualization, Writing - original draft, Writing - review & editing. **Kuei-Chun Wang:** Writing - review & editing. **Barbara Pockaj:** Writing - review & editing. **Mehdi Nikkhah:** Conceptualization, Funding acquisition, Writing - review & editing.

Declaration of competing interest

The authors declare the following financial interests/personal relationships which may be considered as potential competing interests: Mehdi Nikkhah reports financial support was provided by National Science Foundation (NSF) and National Institutes of Health (NIH) as acknowledged in the manuscript.

Data availability

No data was used for the research described in the article.

Acknowledgments

MN would like to acknowledge the NSF Award #1914680 and NIH-NINDS Award #1R01NS123038-01.

Glossary.

Extracellular matrix (ECM)- The ECM is a 3D network of structural proteins along with adhesive proteins and glycoproteins, glycosaminoglycans, as well as growth factors that provides structural support to tissues. It surrounds cells, and the basement membrane, a specialized ECM layer separating epithelial cells from the stroma.

Hot tumor - Hot tumors are rich in antitumor cells and respond well to immunotherapy which are characterized by increased immune cell infiltration especially CD8+ T cells with high levels of immune activity.

Cold tumor - Cold tumors lack T cells infiltration and are characterized "non-inflamed". They are limited by immune cell infiltration, low levels of immune activity, and poor response to immunotherapies, often resulting in a lack of effective antitumor immune response.

Immune Checkpoint Inhibitor – A type of immunotherapy that aims at targeting the immune checkpoints such as PD-1, CTLA-4, which are the key regulators of immune system that helps keeping the immune responses in check.

Chimeric Antigen Receptor (CAR) - CAR is a synthetic receptor engineered to combine an extracellular antigen recognition domain, typically derived from an antibody, with intracellular T-cell signaling domains, enabling T cells to specifically recognize and target cancer cells expressing the corresponding antigen, thereby enhancing the antitumor immune response.

Cytotoxic T Lymphocyte - Known as CD8+ T cells, are a subset of T lymphocytes that recognize and eliminate target cells displaying specific antigens through the release of cytotoxic granules.

Infiltrating T Lymphocytes - Infiltrating T lymphocytes are T cells that migrate into and accumulate within tissues, such as tumors, where they play a role in immune surveillance and response against abnormal cells.

Antigen Presenting Cells (APCs) - APCs, in general, are defined as the cells that can uptake, process, and present various antigens, including but not limited to tumor antigens to the naïve T cells.

Desmoplasia- Growth of connective fibrous tissue due to increased proliferation of SMA-positive fibroblast. Desmoplasia is a common pathological characteristic of breast and pancreatic cancer.

Adipogenesis – Process of differentiation of pre-adipocytes into adipocytes.

Superhydrophobic surfaces- Surfaces that are extremely difficult to wet.

Air Liquid Interface - Organoid generation technique where tumor and/or immune-stromal cells are encapsulated in a collagen I matrix inside a trans well chamber and media from outside diffuses inside the gel. The top of the culture system is exposed to air.

Submerged Culture - Another method for organoid generation where tumor cells are mixed with ECM to form dome like structures and submerged inside culture media. Culture media typically contains exogenous immune-stromal cell types.

Tertiary Lymphoid Structures – TLS are ectopic lymphoid formation found in non-lymphatic tissues.

Photolithography- A microfabrication technique that utilizes ultraviolet light to transfer patterns from mask onto a photosensitive substrate which undergoes chemical changes when exposed to light, allowing the pattern to be etched or deposited onto the substrate, enabling the precise fabrication of micro- and nano-scale structures.

Soft lithography- A method of replicating structures using elastomeric materials such as PDMS to create patterns or structures.

3D bioprinting - 3D bioprinting is a subset of additive manufacturing that involves the layer-by-layer fabrication of living 3D structures using viable cells and biomaterials.

References

[1] A.K. Palucka, L.M. Coussens, The basis of oncoimmunology, Cell 164 (6) (2016) 1233–1247.
[2] F.R. Balkwill, M. Capasso, T. Hagemann, The tumor microenvironment at a glance, J. Cell Sci. 125 (23) (2012) 5591–5596.
[3] D.F. Quail, J.A. Joyce, Microenvironmental regulation of tumor progression and metastasis, Nat. Med. 19 (11) (2013) 1423–1437.
[4] C. Walker, E. Mojares, A. del Río Hernández, Role of extracellular matrix in development and cancer progression, Int. J. Mol. Sci. 19 (10) (2018) 3028.
[5] S. Guo, C.-X. Deng, Effect of stromal cells in tumor microenvironment on metastasis initiation, Int. J. Biol. Sci. 14 (14) (2018) 2083.
[6] J. Rodrigues, et al., 3D in vitro model (R) evolution: unveiling tumor–stroma interactions, Trends Cancer 7 (3) (2021) 249–264.
[7] M. Simian, M.J. Bissell, Organoids: a historical perspective of thinking in three dimensions, JCB (J. Cell Biol.) 216 (1) (2017) 31–40.
[8] K. Stock, et al., Capturing tumor complexity in vitro: comparative analysis of 2D and 3D tumor models for drug discovery, Sci. Rep. 6 (1) (2016) 28951.
[9] K. Kersten, et al., Genetically engineered mouse models in oncology research and cancer medicine, EMBO Mol. Med. 9 (2) (2017) 137–153.
[10] W.-C. Son, C. Gopinath, Early occurrence of spontaneous tumors in CD-1 mice and sprague—dawley rats, Toxicol. Pathol. 32 (4) (2004) 371–374.
[11] M.C. Cox, et al., Toward the broad adoption of 3D tumor models in the cancer drug pipeline, ACS Biomater. Sci. Eng. 1 (10) (2015) 877–894.
[12] I. Kola, J. Landis, Can the pharmaceutical industry reduce attrition rates? Nat. Rev. Drug Discov. 3 (8) (2004) 711–716.
[13] A. Letai, P. Bhola, A.L. Welm, Functional precision oncology: testing tumors with drugs to identify vulnerabilities and novel combinations, Cancer Cell 40 (1) (2022) 26–35.
[14] E.L. Fong, et al., Heralding a new paradigm in 3D tumor modeling, Biomaterials 108 (2016) 197–213.
[15] K. Chwalek, L.J. Bray, C. Werner, Tissue-engineered 3D tumor angiogenesis models: potential technologies for anti-cancer drug discovery, Adv. Drug Deliv. Rev. 79 (2014) 30–39.
[16] G. Bahcecioglu, et al., Breast cancer models: Engineering the tumor microenvironment, Acta Biomater. 106 (2020) 1–21.
[17] F. Amirghasemi, et al., Microengineered 3D tumor Models for anti-cancer drug Discovery in female-related cancers, Ann. Biomed. Eng. 49 (8) (2021) 1943–1972.
[18] S.A. Langhans, Three-dimensional in vitro cell culture models in drug discovery and drug repositioning, Front. Pharmacol. 9 (2018) 6.
[19] T. Osaki, V. Sivathanu, R.D. Kamm, Vascularized microfluidic organ-chips for drug screening, disease models and tissue engineering, Curr. Opin. Biotechnol. 52 (2018) 116–123.
[20] W.J. Wulftange, et al., Spatial control of oxygen delivery to three-dimensional cultures alters cancer cell growth and gene expression, J. Cell. Physiol. 234 (11) (2019) 20608–20622.
[21] M. Mao, et al., Human-on-leaf-chip: a biomimetic vascular system integrated with chamber-specific organs, Small 16 (22) (2020) 2000546.
[22] J. Thiele, et al., 25th anniversary article: designer hydrogels for cell cultures: a materials selection guide, Adv. Mater. 26 (1) (2014) 125–148.
[23] S.N. Bhatia, D.E. Ingber, Microfluidic organs-on-chips, Nat. Biotechnol. 32 (8) (2014) 760–772.
[24] X. Liu, J. Fang, S. Huang, et al., Tumor-on-a-chip: from bioinspired design to biomedical application, Microsyst. Nanoeng. 7 (2021) 50. https://doi.org/10.1038/s41378-021-00277-8.
[25] Z. Baka, et al., Cancer-on-chip technology: current applications in major cancer types, challenges and future prospects, Prog. Biomed. Eng. 4 (3) (2022) 032001.
[26] Y.A. Jodat, et al., Human-derived organ-on-a-chip for personalized drug development, Curr. Pharmaceut. Des. 24 (45) (2018) 5471–5486.
[27] A. Prina-Mello, et al., Use of 3D models in drug development and precision medicine-advances and outlook, Front. Media SA (2021) 658941.
[28] W. Li, et al., 3D biomimetic Models to reconstitute tumor microenvironment in vitro: spheroids, organoids, and tumor-on-a-chip, Adv. Healthcare Mater. 12 (18) (2023) 2202609.
[29] O. Habanjar, et al., 3D cell culture systems: tumor application, advantages, and disadvantages, Int. J. Mol. Sci. 22 (22) (2021).
[30] S.D. Soysal, A. Tzankov, S.E. Muenst, Role of the tumor microenvironment in breast cancer, Pathobiology 82 (3–4) (2015) 142–152.
[31] S. Gupta, A. Roy, B.S. Dwarakanath, Metabolic cooperation and competition in the tumor microenvironment: implications for therapy [review], Front. Oncol. 7 (2017). https://doi.org/10.3389/fonc.2017.00068.
[32] A. Adamo, et al., Role of mesenchymal stromal cell-derived extracellular vesicles in tumour microenvironment, Biochim. Biophys. Acta Rev. Canc 1871 (1) (2019) 192–198.
[33] H. Choi, A. Moon, Crosstalk between cancer cells and endothelial cells: implications for tumor progression and intervention, Arch Pharm. Res. (Seoul) 41 (2018) 711–724.
[34] S.-R. Woo, L. Corrales, T.F. Gajewski, Innate immune recognition of cancer, Annu. Rev. Immunol. 33 (1) (2015) 445–474.
[35] C.D. Mills, et al., M-1/M-2 macrophages and the Th1/Th2 paradigm, J. Immunol. 164 (12) (2000) 6166–6173.
[36] J.W. Pollard, Tumour-educated macrophages promote tumour progression and metastasis, Nat. Rev. Cancer 4 (1) (2004) 71–78.
[37] R.T. Netea-Maier, J.W. Smit, M.G. Netea, Metabolic changes in tumor cells and tumor-associated macrophages: a mutual relationship, Cancer Lett. 413 (2018) 102–109.
[38] G. Landskron, et al., Chronic inflammation and cytokines in the tumor microenvironment, J. Immunol. Res. 2014 (2014) 149185.
[39] J.N. Amens, G. Bahçecioglu, P. Zorlutuna, Immune system effects on breast cancer, Cell. Mol. Bioeng. 14 (4) (2021) 279–292.
[40] R. Noy, J.W. Pollard, Tumor-associated macrophages: from mechanisms to therapy, Immunity 41 (1) (2014) 49–61.
[41] M.R. Shurin, Dendritic cells presenting tumor antigen. Cancer immunology, Immunotherapy 43 (1996) 158–164.
[42] M. Collin, V. Bigley, Human dendritic cell subsets: an update, Immunology 154 (1) (2018) 3–20.
[43] F. Veglia, D.I. Gabrilovich, Dendritic cells in cancer: the role revisited, Curr. Opin. Immunol. 45 (2017) 43–51.
[44] G. Nizzoli, et al., *Human CD1c+ dendritic cells secrete high levels of IL-12 and potently prime cytotoxic T-cell responses.* Blood, J. Ame. Soc. Hematol. 122 (6) (2013) 932–942.
[45] Frasca, L., C. Piazza, and E. Piccolella, CD4* T Cells Orchestrate Both Amplification and.
[46] J.P. Böttcher, et al., NK cells stimulate recruitment of cDC 1 into the tumor microenvironment promoting cancer immune control, Cell 172 (5) (2018) 1022–1037, e14.
[47] C.-H. Chang, et al., Metabolic competition in the tumor microenvironment is a driver of cancer progression, Cell 162 (6) (2015) 1229–1241.
[48] M. Hashimoto, et al., CD8 T cell exhaustion in chronic infection and cancer: opportunities for interventions, Annu. Rev. Med. 69 (2018) 301–318.
[49] B. Molon, B. Calì, A. Viola, T cells and cancer: how metabolism shapes immunity, Front. Immunol. 7 (2016) 20.
[50] B.T. Fife, J.A. Bluestone, Control of peripheral T-cell tolerance and autoimmunity via the CTLA-4 and PD-1 pathways, Immunol. Rev. 224 (1) (2008) 166–182.
[51] A. Kano, Tumor cell secretion of soluble factor (s) for specific immunosuppression, Sci. Rep. 5 (1) (2015) 8913.
[52] D.A. Vignali, L.W. Collison, C.J. Workman, How regulatory T cells work, Nat. Rev. Immunol. 8 (7) (2008) 523–532.
[53] E.J. Wherry, M. Kurachi, Molecular and cellular insights into T cell exhaustion, Nat. Rev. Immunol. 15 (8) (2015) 486–499.
[54] A. Taylor, et al., Mechanisms of immune suppression by interleukin-10 and transforming growth factor-beta: the role of T regulatory cells, Immunology 117 (4) (2006) 433–442.
[55] T. Komai, et al., Transforming growth factor-β and interleukin-10 synergistically regulate humoral immunity via modulating metabolic signals, Front. Immunol. 9 (2018) 1364.
[56] R.A.M. Rossetti, et al., B lymphocytes can be activated to act as antigen presenting cells to promote anti-tumor responses, PLoS One 13 (7) (2018), e0199034.
[57] G.V. Sharonov, et al., B cells, plasma cells and antibody repertoires in the tumour microenvironment, Nat. Rev. Immunol. 20 (5) (2020) 294–307.
[58] R. Cabrita, et al., Tertiary lymphoid structures improve immunotherapy and survival in melanoma, Nature 577 (7791) (2020) 561–565.
[59] L. Zhang, et al., Regulatory B cell-myeloma cell interaction confers immunosuppression and promotes their survival in the bone marrow milieu, Blood Cancer J. 7 (3) (2017) e547, e547.
[60] P.B. Olkhanud, et al., Tumor-evoked regulatory B cells promote breast cancer metastasis by converting resting CD4+ T cells to T-regulatory cells, Cancer Res. 71 (10) (2011) 3505–3515.
[61] S. Shalapour, et al., Author Correction: inflammation-induced IgA+ cells dismantle anti-liver cancer immunity, Nature 561 (7721) (2018) E1. E1.
[62] A.D. Barrow, C.J. Martin, M. Colonna, The natural cytotoxicity receptors in health and disease, Front. Immunol. 10 (2019) 909.
[63] H. Arase, et al., Direct recognition of cytomegalovirus by activating and inhibitory NK cell receptors, Science 296 (5571) (2002) 1323–1326.
[64] P. Carrega, et al., Natural killer cells infiltrating human nonsmall-cell lung cancer are enriched in CD56brightCD16− cells and display an impaired capability to kill tumor cells, Cancer 112 (4) (2008) 863–875.
[65] A. Stiff, et al., Nitric oxide production by myeloid-derived suppressor cells plays a role in impairing Fc receptor–mediated natural killer cell function, Clin. Cancer Res. 24 (8) (2018) 1891–1904.
[66] L. Bu, et al., Biological heterogeneity and versatility of cancer-associated fibroblasts in the tumor microenvironment, Oncogene 38 (25) (2019) 4887–4901.

[67] D. Öhlund, et al., Distinct populations of inflammatory fibroblasts and myofibroblasts in pancreatic cancer, J. Exp. Med. 214 (3) (2017) 579–596.
[68] T. Liu, et al., Cancer-associated fibroblasts: an emerging target of anti-cancer immunotherapy, J. Hematol. Oncol. 12 (1) (2019) 1–15.
[69] J. Harper, R.C. Sainson, Regulation of the anti-tumour immune response by cancer-associated fibroblasts, in: Seminars in Cancer Biology, Elsevier, 2014.
[70] E. Elyada, et al., Cross-species single-cell analysis of pancreatic ductal adenocarcinoma reveals antigen-presenting cancer-associated fibroblasts, Cancer Discov. 9 (8) (2019) 1102–1123.
[71] Q. Wu, et al., Unraveling adipocytes and Cancer links: is there a role for senescence? Front. Cell Dev. Biol. 8 (2020) 282.
[72] S. Morikawa, et al., Abnormalities in pericytes on blood vessels and endothelial sprouts in tumors, Am. J. Pathol. 160 (3) (2002) 985–1000.
[73] L. Nagl, et al., Tumor endothelial cells (TECs) as potential immune directors of the tumor microenvironment–new findings and future perspectives, Front. Cell Dev. Biol. 8 (2020) 766.
[74] J. Kalucka, et al., Single-cell transcriptome Atlas of murine endothelial cells, Cell 180 (4) (2020) 764–779, e20.
[75] D. Ferland-McCollough, et al., Pericytes, an overlooked player in vascular pathobiology, Pharmacol. Therapeut. 171 (2017) 30–42.
[76] M. Hellström, et al., Lack of pericytes leads to endothelial hyperplasia and abnormal vascular morphogenesis, JCB (J. Cell Biol.) 153 (3) (2001) 543–553.
[77] S. Song, et al., PDGFRbeta+ perivascular progenitor cells in tumours regulate pericyte differentiation and vascular survival, Nat. Cell Biol. 7 (9) (2005) 870–879.
[78] R. Navarro, et al., Immune regulation by pericytes: modulating innate and adaptive immunity, Front. Immunol. 7 (2016) 480.
[79] C. Zhu, et al., CECR1-mediated cross talk between macrophages and vascular mural cells promotes neovascularization in malignant glioma, Oncogene 36 (38) (2017) 5356–5368.
[80] A.T. Henze, M. Mazzone, The impact of hypoxia on tumor-associated macrophages, J. Clin. Invest. 126 (10) (2016) 3672–3679.
[81] C.H. Wong, K.W. Siah, A.W. Lo, Estimation of clinical trial success rates and related parameters, Biostatistics 20 (2) (2019) 273–286.
[82] C.M. Neophytou, et al., The role of tumor microenvironment in cancer metastasis: molecular mechanisms and therapeutic opportunities, Cancers 13 (9) (2021) 2053.
[83] L.A. Hapach, et al., Engineered models to parse apart the metastatic cascade, npj Precis. Oncol. 3 (2019) 20.
[84] V. Brancato, et al., Could 3D models of cancer enhance drug screening? Biomaterials 232 (2020) 119744.
[85] N. Peela, et al., Effect of suberoylanilide hydroxamic acid (SAHA) on breast cancer cells within a tumor–stroma microfluidic model, Integr. Biol. 9 (12) (2017) 988–999.
[86] A. Villasante, G. Vunjak-Novakovic, Tissue-engineered models of human tumors for cancer research, Expet Opin. Drug Discov. 10 (3) (2015) 257–268.
[87] N. Peela, et al., Advanced biomaterials and microengineering technologies to recapitulate the stepwise process of cancer metastasis, Biomaterials 133 (2017) 176–207.
[88] E.C. Costa, et al., 3D tumor spheroids: an overview on the tools and techniques used for their analysis, Biotechnol. Adv. 34 (8) (2016) 1427–1441.
[89] P.S. Thakuri, et al., Quantitative size-based Analysis of tumor Spheroids and Responses to therapeutics, Assay Drug Dev. Technol. 17 (3) (2019) 140–149.
[90] K.H. Lee, T.H. Kim, Recent advances in multicellular tumor spheroid generation for drug screening, Biosensors 11 (11) (2021). Basel.
[91] S. Sant, P.A. Johnston, The production of 3D tumor spheroids for cancer drug discovery, Drug Discov. Today Technol. 23 (2017) 27–36.
[92] N.E. Timmins, L.K. Nielsen, Generation of multicellular tumor spheroids by the hanging-drop method, Methods Mol. Med. 140 (2007) 141–151.
[93] S. Nath, G.R. Devi, Three-dimensional culture systems in cancer research: focus on tumor spheroid model, Pharmacol. Ther. 163 (2016) 94–108.
[94] E.C. Costa, et al., Spheroids Formation on non-adhesive surfaces by liquid overlay technique: considerations and practical approaches, Biotechnol. J. 13 (1) (2018).
[95] F. Leonard, B. Godin, 3D in vitro Model for breast cancer research using magnetic Levitation and bioprinting method, Methods Mol. Biol. 1406 (2016) 239–251.
[96] Y. Liu, et al., Promoting hepatocyte spheroid formation and functions by coculture with fibroblasts on micropatterned electrospun fibrous scaffolds, J. Mater. Chem. B 2 (20) (2014) 3029–3040.
[97] K.M. Tevis, Y.L. Colson, M.W. Grinstaff, Embedded spheroids as models of the cancer microenvironment, Adv. Biosyst. 1 (10) (2017).
[98] T.M. Achilli, J. Meyer, J.R. Morgan, Advances in the formation, use and understanding of multi-cellular spheroids, Expet Opin. Biol. Ther. 12 (10) (2012) 1347–1360.
[99] S.I. Lee, et al., 3D multicellular tumor Spheroids in a microfluidic droplet System for Investigation of drug resistance, Polymers 14 (18) (2022).
[100] N.D. Caprio, J.A. Burdick, Engineered biomaterials to guide spheroid formation, function, and fabrication into 3D tissue constructs, Acta Biomater. 165 (2023) 4–18.
[101] S.Y. Lee, et al., In Vitro three-dimensional (3D) cell culture tools for spheroid and organoid models, SLAS Discov. 28 (4) (2023) 119–137.
[102] S.J. Han, S. Kwon, K.S. Kim, Challenges of applying multicellular tumor spheroids in preclinical phase, Cancer Cell. Int. 21 (2021) 152. https://doi.org/10.1186/s12935-021-01853-8.
[103] H.Y. Khan, et al., Targeting cellular metabolism with CPI-613 sensitizes pancreatic cancer cells to radiation therapy, Adv. Radiat. Oncol. 8 (1) (2023) 101122.
[104] R.L.F. Amaral, et al., Comparative analysis of 3D bladder tumor spheroids obtained by forced floating and hanging drop methods for drug screening, Front. Physiol. 8 (2017) 605.
[105] R.M. Escalona, et al., Knock down of TIMP-2 by siRNA and CRISPR/Cas9 mediates diverse cellular reprogramming of metastasis and chemosensitivity in ovarian cancer, Cancer Cell Int. 22 (1) (2022) 422.
[106] K. Han, et al., CRISPR screens in cancer spheroids identify 3D growth-specific vulnerabilities, Nature 580 (7801) (2020) 136–141.
[107] S. Knuchel, et al., Fibroblast surface-associated FGF-2 promotes contact-dependent colorectal cancer cell migration and invasion through FGFR-SRC signaling and integrin αvβ5-mediated adhesion, Oncotarget 6 (16) (2015) 14300–14317.
[108] C. Liu, D. Lewin Mejia, B. Chiang, K.E. Luker, G.D. Luker, Hybrid collagen alginate hydrogel as a platform for 3D tumor spheroid invasion, Acta Biomater. 75 (2018) 213–225. https://doi.org/10.1016/j.actbio.2018.06.003.
[109] H. Saini, et al., The role of tumor-stroma interactions on desmoplasia and tumorigenicity within a microengineered 3D platform, Biomaterials 247 (2020) 119975.
[110] H. Saini, et al., The role of desmoplasia and stromal fibroblasts on anti-cancer drug resistance in a microengineered tumor model, Cell. Mol. Bioeng. 11 (5) (2018) 419–433.
[111] X. Yue, et al., Stromal cell-laden 3D hydrogel microwell arrays as tumor microenvironment model for studying stiffness dependent stromal cell-cancer interactions, Biomaterials 170 (2018) 37–48.
[112] H. Shoval, et al., Tumor cells and their crosstalk with endothelial cells in 3D spheroids, Sci. Rep. 7 (1) (2017) 10428.
[113] G.G.Y. Chiew, et al., Bioengineered three-dimensional co-culture of cancer cells and endothelial cells: a model system for dual analysis of tumor growth and angiogenesis, Biotechnol. Bioeng. 114 (8) (2017) 1865–1877.
[114] A. Ritter, et al., Cancer-educated mammary adipose tissue-derived stromal/stem cells in obesity and breast cancer: spatial regulation and function, J. Exp. Clin. Cancer Res. 42 (1) (2023) 35.
[115] J. Antunes, et al., In-air production of 3D co-culture tumor spheroid hydrogels for expedited drug screening, Acta Biomater. 94 (2019) 392–409.
[116] C. Su, et al., A Facile and scalable hydrogel patterning Method for microfluidic 3D cell Culture and spheroid-in-gel culture array, Biosensors 11 (12) (2021) 509.
[117] N. Dadgar, et al., A microfluidic platform for cultivating ovarian cancer spheroids and testing their responses to chemotherapies, Microsyst. Nanoeng. 6 (1) (2020) 93.
[118] K.M. Tevis, et al., Mimicking the tumor microenvironment to regulate macrophage phenotype and assessing chemotherapeutic efficacy in embedded cancer cell/macrophage spheroid models, Acta Biomater. 50 (2017) 271–279.
[119] J.E. Chen, et al., Crosstalk between microglia and patient-derived glioblastoma cells inhibit invasion in a three-dimensional gelatin hydrogel model, J. Neuroinflammation 17 (1) (2020) 346.
[120] M. Abbott, Y. Ustoyev, Cancer and the immune system: the history and background of immunotherapy, Semin. Oncol. Nurs. 35 (5) (2019) 150923.
[121] X. Jiang, L. Ren, P. Tebon, C. Wang, X. Zhou, M. Qu, J. Zhu, H. Ling, S. Zhang, Y. Xue, Q. Wu, P. Bandaru, J. Lee, H.J. Kim, S. Ahadian, N. Ashammakhi, M. R. Dokmeci, J. Wu, Z. Gu, A. Khademhosseini, Cancer-on-a-chip for modeling immune checkpoint inhibitor and tumor interactions, Small 17 (7) (2021), e2004282. https://doi.org/10.1002/smll.202004282.
[122] V. Särchen, et al., Pediatric multicellular tumor spheroid models illustrate a therapeutic potential by combining BH3 mimetics with Natural Killer (NK) cell-based immunotherapy, Cell Death Discov. 8 (2022) 11, https://doi.org/10.1038/s41420-021-00812-6.
[123] T. Courau, et al., Cocultures of human colorectal tumor spheroids with immune cells reveal the therapeutic potential of MICA/B and NKG2A targeting for cancer treatment, J. ImmunoTherap. Cancer 7 (1) (2019) 74.
[124] S. Gopal, et al., 3D tumor spheroid microarray for high-throughput, high-content natural killer cell-mediated cytotoxicity, Commun. Biol. 4 (1) (2021) 893.
[125] P. Sabhachandani, et al., Microfluidic assembly of hydrogel-based immunogenic tumor spheroids for evaluation of anticancer therapies and biomarker release, J. Contr. Release 295 (2019) 21–30.
[126] H. Dhandapani, et al., In vitro 3D spheroid model preserves tumor Microenvironment of Hot and cold breast cancer subtypes, Adv. Healthcare Mater. (2023), e2300164.
[127] I. Berger Fridman, et al., High-throughput microfluidic 3D biomimetic model enabling quantitative description of the human breast tumor microenvironment, Acta Biomater. 132 (2021) 473–488.
[128] Z. Ao, et al., Microfluidics guided by deep learning for cancer immunotherapy screening, in: Proceedings of the National Academy of Sciences vol. 119, 2022, e2214569119, 46.
[129] S.M. Ehsan, et al., A three-dimensional in vitro model of tumor cell intravasation, Integr. Biol.: Quant. Biosci. Nano Macro 6 (6) (2014) 603–610.
[130] J. Park, et al., Enabling perfusion through multicellular tumor spheroids promoting lumenization in a vascularized cancer model, Lab Chip 22 (22) (2022) 4335–4348.
[131] E.M. Tosca, et al., Replacement, reduction, and Refinement of animal Experiments in anticancer drug development: the Contribution of 3D in vitro cancer Models in the drug efficacy assessment, Biomedicines 11 (4) (2023).
[132] M. Fujii, et al., Human intestinal organoids maintain self-renewal capacity and cellular diversity in niche-inspired culture condition, Cell Stem Cell 23 (6) (2018) 787–793, e6.
[133] A. Ootani, et al., Sustained in vitro intestinal epithelial culture within a Wnt-dependent stem cell niche, Nat. Med. 15 (6) (2009) 701–706.

[134] N. Sachs, et al., A living Biobank of breast cancer organoids captures disease heterogeneity, Cell 172 (1–2) (2018) 373–386, e10.
[135] X. Li, et al., Oncogenic transformation of diverse gastrointestinal tissues in primary organoid culture, Nat. Med. 20 (7) (2014) 769–777.
[136] M. Matano, et al., Modeling colorectal cancer using CRISPR-Cas9-mediated engineering of human intestinal organoids, Nat. Med. 21 (3) (2015) 256–262.
[137] H.H.N. Yan, et al., A comprehensive human gastric cancer organoid biobank captures tumor subtype Heterogeneity and enables therapeutic screening, Cell Stem Cell 23 (6) (2018) 882–897, e11.
[138] A. Linkous, et al., Modeling patient-derived Glioblastoma with cerebral organoids, Cell Rep. 26 (12) (2019) 3203–3211, e5.
[139] A. Fatehullah, S.H. Tan, N. Barker, Organoids as an in vitro model of human development and disease, Nat. Cell Biol. 18 (3) (2016) 246–254.
[140] H. Garner, K.E. de Visser, Immune crosstalk in cancer progression and metastatic spread: a complex conversation, Nat. Rev. Immunol. 20 (8) (2020) 483–497.
[141] Y. Yao, et al., Patient-derived organoids predict chemoradiation Responses of locally advanced rectal cancer, Cell Stem Cell 26 (1) (2020) 17–26, e6.
[142] Q. Meng, et al., Empirical identification and validation of tumor-targeting T cell receptors from circulation using autologous pancreatic tumor organoids, J. Immunother. Cancer 9 (11) (2021), e003213.
[143] K.J. Cheung, et al., Collective invasion in breast cancer requires a conserved basal epithelial program, Cell 155 (7) (2013) 1639–1651.
[144] L. Li, et al., Human primary liver cancer organoids reveal intratumor and interpatient drug response heterogeneity, JCI Insight 4 (2) (2019).
[145] T. Sato, et al., Single Lgr5 stem cells build crypt-villus structures in vitro without a mesenchymal niche, Nature 459 (7244) (2009) 262–265.
[146] E. Sahai, et al., A framework for advancing our understanding of cancer-associated fibroblasts, Nat. Rev. Cancer 20 (3) (2020) 174–186.
[147] M.I. Koukourakis, et al., Metabolic cooperation between co-cultured lung cancer cells and lung fibroblasts, Lab. Invest. 97 (11) (2017) 1321–1331.
[148] J. Liu, et al., Cancer-associated fibroblasts Provide a stromal Niche for liver cancer organoids that confers trophic Effects and therapy resistance, Cell. Mol. Gastroenterol. Hepatol. 11 (2) (2021) 407–431.
[149] X. Luo, et al., Hydrogel-based colorectal cancer organoid co-culture models, Acta Biomater. 132 (2021) 461–472.
[150] H. Nakamura, et al., Organoid culture containing cancer cells and stromal cells reveals that podoplanin-positive cancer-associated fibroblasts enhance proliferation of lung cancer cells, Lung Cancer 134 (2019) 100–107.
[151] W. Xiao, et al., Matrix stiffness mediates pancreatic cancer chemoresistance through induction of exosome hypersecretion in a cancer associated fibroblasts-tumor organoid biomimetic model, Matrix Biol. 14 (2022) 100111.
[152] A. Dominijanni, M. Devarasetty, S. Soker, Manipulating the tumor microenvironment in tumor organoids induces phenotypic changes and chemoresistance, iScience 23 (12) (2020) 101851.
[153] T. Kitamura, B.Z. Qian, J.W. Pollard, Immune cell promotion of metastasis, Nat. Rev. Immunol. 15 (2) (2015) 73–86.
[154] K.K. Dijkstra, et al., Genomics- and transcriptomics-based patient Selection for cancer treatment with immune checkpoint inhibitors: a review, JAMA Oncol. 2 (11) (2016) 1490–1495.
[155] P. Sharma, et al., Primary, adaptive, and acquired Resistance to cancer immunotherapy, Cell 168 (4) (2017) 707–723.
[156] K.K. Dijkstra, C.M. Cattaneo, F. Weeber, M. Chalabi, J. van de Haar, L.F. Fanchi, M. Slagter, van der Velden, S. Kaing, S. Kelderman, N. van Rooij, van Leerdam, A. Depla, E.F. Smit, K.J. Hartemink, R. de Groot, M.C. Wolkers, N. Sachs, P. Snaebjornsson, E.E. Voest, Generation of tumor-reactive T cells by co-culture of peripheral blood lymphocytes and tumor organoids, Cell 174 (6) (2018) 1586–1598.e1512. https://doi.org/10.1016/j.cell.2018.07.009.
[157] G. Zhou, et al., Modelling immune cytotoxicity for cholangiocarcinoma with tumour-derived organoids and effector T cells, Br. J. Cancer 127 (4) (2022) 649–660.
[158] F. Marcon, et al., NK cells in pancreatic cancer demonstrate impaired cytotoxicity and a regulatory IL-10 phenotype, OncoImmunology 9 (1) (2020) 1845424.
[159] J.F. Dekkers, et al., Uncovering the mode of action of engineered T cells in patient cancer organoids, Nat. Biotechnol. 41 (1) (2023) 60–69.
[160] J.T.C. Lim, et al., Hepatocellular carcinoma organoid co-cultures mimic angiocrine crosstalk to generate inflammatory tumor microenvironment, Biomaterials 284 (2022) 121527.
[161] L. Ou, et al., Patient-derived melanoma organoid models facilitate the assessment of immunotherapies, EBioMedicine (2023) 92.
[162] S. Tsai, et al., Development of primary human pancreatic cancer organoids, matched stromal and immune cells and 3D tumor microenvironment models, BMC Cancer 18 (1) (2018) 335.
[163] J. Qu, et al., Tumor organoids: synergistic applications, current challenges, and future prospects in cancer therapy, Cancer Commun. 41 (12) (2021) 1331–1353.
[164] M.A. Foo, et al., Clinical translation of patient-derived tumour organoids-bottlenecks and strategies, Biomark. Res. 10 (1) (2022) 10.
[165] A. Boussommier-Calleja, et al., Microfluidics: a new tool for modeling cancer–immune interactions, Trends Cancer 2 (1) (2016) 6–19.
[166] E.K. Sackmann, A.L. Fulton, D.J. Beebe, The present and future role of microfluidics in biomedical research, Nature 507 (7491) (2014) 181–189.
[167] M.H. Wu, S.B. Huang, G.B. Lee, Microfluidic cell culture systems for drug research, Lab Chip 10 (8) (2010) 939–956.
[168] K.J. Regehr, et al., Biological implications of polydimethylsiloxane-based microfluidic cell culture, Lab Chip 9 (15) (2009) 2132–2139.
[169] M. Nikkhah, J.S. Strobl, M. Agah, Attachment and response of human fibroblast and breast cancer cells to three dimensional silicon microstructures of different geometries, Biomed. Microdevices 11 (2) (2009) 429–441.
[170] M. Nikkhah, et al., Engineering microscale topographies to control the cell-substrate interface, Biomaterials 33 (21) (2012) 5230–5246.
[171] M. Nikkhah, et al., Cytoskeletal role in differential adhesion patterns of normal fibroblasts and breast cancer cells inside silicon microenvironments, Biomed. Microdevices 11 (3) (2009) 585–595.
[172] M. Nikkhah, et al., The cytoskeletal organization of breast carcinoma and fibroblast cells inside three dimensional (3-D) isotropic silicon microstructures, Biomaterials 31 (16) (2010) 4552–4561.
[173] M. Nikkhah, et al., Evaluation of the influence of growth medium composition on cell elasticity, J. Biomech. 44 (4) (2011) 762–766.
[174] M. Nikkhah, et al., MCF10A and MDA-MB-231 human breast basal epithelial cell co-culture in silicon micro-arrays, Biomaterials 32 (30) (2011) 7625–7632.
[175] S. Regmi, et al., Applications of microfluidics and organ-on-a-chip in cancer research, Biosensors 12 (7) (2022) 459.
[176] N. Peela, et al., A three dimensional micropatterned tumor model for breast cancer cell migration studies, Biomaterials 81 (2016) 72–83.
[177] M.K. Raj, S. Chakraborty, PDMS microfluidics: a mini review, J. Appl. Polym. Sci. 137 (27) (2020) 48958.
[178] J.J.F. Sleeboom, et al., Metastasis in context: modeling the tumor microenvironment with cancer-on-a-chip approaches, Dis. Model. Mech. 11 (3) (2018).
[179] Z. Lin, et al., Recent advances in microfluidic platforms applied in cancer metastasis: circulating tumor cells' (CTCs) isolation and tumor-on-A-chip, Small 16 (9) (2020) 1903899.
[180] J. Rodrigues, et al., 3D in vitro model (R)evolution: unveiling tumor-stroma interactions, Trends Cancer 7 (3) (2021) 249–264.
[181] H.F. Tsai, et al., Tumour-on-a-chip: microfluidic models of tumour morphology, growth and microenvironment, J. R. Soc. Interface 14 (131) (2017).
[182] Y.-H.V. Ma, et al., A review of microfluidic approaches for investigating cancer extravasation during metastasis, Microsyst. Nanoeng. 4 (1) (2018) 17104.
[183] M.F. Coughlin, R.D. Kamm, The use of microfluidic platforms to probe the mechanism of cancer cell extravasation, Adv. Healthcare Mater. 9 (8) (2020), e1901410.
[184] D. Caballero, et al., Organ-on-chip models of cancer metastasis for future personalized medicine: from chip to the patient, Biomaterials 149 (2017) 98–115.
[185] V. Aggarwal, et al., Three dimensional engineered models to study hypoxia biology in breast cancer, Cancer Lett. 490 (2020) 124–142.
[186] S.M. Grist, et al., Long-term monitoring in a microfluidic system to study tumour spheroid response to chronic and cycling hypoxia, Sci. Rep. 9 (1) (2019) 17782.
[187] F. Duzagac, et al., Microfluidic organoids-on-a-chip: quantum Leap in cancer research, Cancers 13 (4) (2021).
[188] S.E. Park, A. Georgescu, D. Huh, Organoids-on-a-chip, Science 364 (6444) (2019) 960–965.
[189] X. Wang, et al., PD-L1 expression in human cancers and its association with clinical outcomes, OncoTargets Ther. 9 (2016) 5023–5039.
[190] V.J. Lyons, A. Helms, D. Pappas, The effect of protein expression on cancer cell capture using the Human Transferrin Receptor (CD71) as an affinity ligand, Anal. Chim. Acta 1076 (2019) 154–161.
[191] M. Czaplicka, et al., Effect of varying expression of EpCAM on the efficiency of CTCs detection by SERS-based immunomagnetic optofluidic device, Cancers 12 (11) (2020).
[192] S.P. Chiang, R.M. Cabrera, J.E. Segall, Tumor cell intravasation, Am. J. Physiol.: Cell Physiol. 311 (1) (2016) C1–c14.
[193] Q. Zhang, T. Liu, J. Qin, A microfluidic-based device for study of transendothelial invasion of tumor aggregates in realtime, Lab Chip 12 (16) (2012) 2837–2842.
[194] H. Lee, et al., A microfluidic platform for quantitative analysis of cancer angiogenesis and intravasation, Biomicrofluidics 8 (5) (2014) 54102.
[195] S. Nagaraju, et al., Microfluidic tumor-vascular Model to study breast cancer cell Invasion and intravasation, Adv. Healthcare Mater. 7 (9) (2018), e1701257.
[196] D. Truong, et al., A three-dimensional (3D) organotypic microfluidic model for glioma stem cells - Vascular interactions, Biomaterials 198 (2019) 63–77.
[197] D. Truong, et al., Breast cancer cell invasion into a three dimensional tumor-stroma microenvironment, Sci. Rep. 6 (1) (2016) 34094.
[198] D.D. Truong, et al., A human organotypic microfluidic tumor model permits Investigation of the Interplay between patient-derived Fibroblasts and breast cancer cells, Cancer Res. 79 (12) (2019) 3139–3151.
[199] S.Y. Jeong, et al., Co-Culture of tumor Spheroids and Fibroblasts in a collagen matrix-incorporated microfluidic chip mimics reciprocal Activation in solid tumor microenvironment, PLoS One 11 (7) (2016), e0159013.
[200] K.M. Lugo-Cintrón, et al., Breast fibroblasts and ECM components modulate breast cancer cell migration through the secretion of MMPs in a 3D microfluidic Co-culture model, Cancers 12 (5) (2020).
[201] J. Kim, et al., Microfluidic one-directional interstitial flow generation from cancer to cancer associated fibroblast, Acta Biomater. 144 (2022) 258–265.
[202] J.H. Lee, S.K. Kim, I.A. Khawar, S.Y. Jeong, S. Chung, H.J. Kuh, Microfluidic co-culture of pancreatic tumor spheroids with stellate cells as a novel 3D model for investigation of stroma-mediated cell motility and drug resistance, J. Exp. Clin. Cancer Res. 37 (1) (2018) 4. https://doi.org/10.1186/s13046-017-0654-6.
[203] H. Xie, J.W. Appelt, R.W. Jenkins, Going with the flow: modeling the tumor microenvironment using microfluidic technology, Cancers 13 (23) (2021).
[204] L. Businaro, et al., Cross talk between cancer and immune cells: exploring complex dynamics in a microfluidic environment, Lab Chip 13 (2) (2013) 229–239.

[205] F. Mattei, et al., A multidisciplinary study using in vivo tumor models and microfluidic cell-on-chip approach to explore the cross-talk between cancer and immune cells, J. Immunot. 11 (4) (2014) 337–346.
[206] S.W.L. Lee, R.J. Seager, F. Litvak, F. Spill, J.L. Sieow, P.H. Leong, D. Kumar, A.S. M. Tan, S.C. Wong, G. Adriani, M.H. Zaman, A.R.D. Kamm, Integrated in silico and 3D in vitro model of macrophage migration in response to physical and chemical factors in the tumor microenvironment, Integr. Biol. (Camb) 12 (4) (2020) 90–108. https://doi.org/10.1093/intbio/zyaa007.
[207] R. Li, et al., Macrophage-secreted TNFα and TGFβ1 influence migration Speed and Persistence of cancer Cells in 3D tissue Culture via independent pathways, Cancer Res. 77 (2) (2017) 279–290.
[208] V. Surendran, et al., A novel tumor-immune microenvironment (TIME)-on-Chip mimics three dimensional neutrophil-tumor dynamics and neutrophil extracellular traps (NETs)-mediated collective tumor invasion, Biofabrication 13 (3) (2021).
[209] M. Marzagalli, et al., A multi-organ-on-chip to recapitulate the infiltration and the cytotoxic activity of circulating NK cells in 3D matrix-based tumor model, Front. Bioeng. Biotechnol. 10 (2022) 945149.
[210] S. Parlato, et al., 3D Microfluidic model for evaluating immunotherapy efficacy by tracking dendritic cell behaviour toward tumor cells, Sci. Rep. 7 (1) (2017) 1093.
[211] R.W. Jenkins, et al., Ex vivo profiling of PD-1 blockade using organotypic tumor spheroids, Cancer Discov. 8 (2) (2018) 196–215.
[212] A. Pavesi, et al., A 3D microfluidic model for preclinical evaluation of TCR-engineered T cells against solid tumors, JCI Insight 2 (12) (2017).
[213] B. Moser, K. Willimann, Chemokines: role in inflammation and immune surveillance, Ann. Rheum. Dis. 63 (Suppl 2) (2004) ii84–ii89. Suppl 2.
[214] L. de Haan, et al., A microfluidic 3D endothelium-on-a-chip Model to study transendothelial Migration of T Cells in Health and disease, Int. J. Mol. Sci. 22 (15) (2021).
[215] I.K. Zervantonakis, et al., Three-dimensional microfluidic model for tumor cell intravasation and endothelial barrier function, in: Proceedings of the National Academy of Sciences vol. 109, 2012, pp. 13515–13520, 34.
[216] J. Song, et al., High-throughput 3D in vitro tumor vasculature Model for real-time Monitoring of immune cell Infiltration and cytotoxicity, Front. Immunol. 12 (2021) 733317.
[217] P.F. Liu, et al., A bladder cancer microenvironment simulation system based on a microfluidic co-culture model, Oncotarget 6 (35) (2015) 37695–37705.
[218] A. Aung, et al., An engineered tumor-on-a-chip Device with breast cancer-immune cell Interactions for assessing T-cell recruitment, Cancer Res. 80 (2) (2020) 263–275.
[219] S.W.L. Lee, G. Adriani, E. Ceccarello, A. Pavesi, A.T. Tan, A. Bertoletti, R. D. Kamm, S.C. Wong, Characterizing the role of monocytes in T cell cancer immunotherapy using a 3D microfluidic model [original research], Front. Immunol. 9 (2018). https://doi.org/10.3389/fimmu.2018.00416.
[220] Y. Zheng, et al., Angiogenesis in liquid tumors: an in vitro assay for leukemic-cell-induced bone marrow angiogenesis, Adv. Healthcare Mater. 5 (9) (2016) 1014–1024.
[221] D. Kim, et al., Vascularized lung cancer model for evaluating the promoted transport of anticancer drugs and immune cells in an engineered tumor microenvironment, Adv. Healthcare Mater. 11 (12) (2022), e2102581.
[222] H. Mollica, et al., A 3D pancreatic tumor model to study T cell infiltration, Biomater. Sci. 9 (22) (2021) 7420–7431.
[223] J.M. Ayuso, et al., Microfluidic tumor-on-a-chip model to evaluate the role of tumor environmental stress on NK cell exhaustion, Sci. Adv. 7 (8) (2021), eabc2331.
[224] D.C. Wimalachandra, et al., Microfluidic-based Immunomodulation of immune cells using upconversion Nanoparticles in simulated blood vessel-tumor system, ACS Appl. Mater. Interfaces 11 (41) (2019) 37513–37523.
[225] E.A. Adjei-Sowah, et al., Investigating the interactions of glioma stem cells in the perivascular niche at single-cell resolution using a microfluidic tumor microenvironment model, Adv. Sci. 9 (21) (2022), e2201436.
[226] M.R. Haque, et al., Patient-derived pancreatic cancer-on-a-chip recapitulates the tumor microenvironment, Microsyst. Nanoeng. 8 (1) (2022) 36.
[227] Z. Hu, et al., Vascularized tumor spheroid-on-a-chip model verifies synergistic Vasoprotective and chemotherapeutic effects, ACS Biomater. Sci. Eng. 8 (3) (2022) 1215–1225.
[228] M. Geyer, et al., A microfluidic-based PDAC organoid system reveals the impact of hypoxia in response to treatment, Cell Death Discov. 9 (1) (2023) 20.
[229] N. Bargahi, et al., Recent advances for cancer detection and treatment by microfluidic technology, review and update, Biol. Proced. Online 24 (1) (2022) 5.
[230] S. Halldorsson, et al., Advantages and challenges of microfluidic cell culture in polydimethylsiloxane devices, Biosens. Bioelectron. 63 (2015) 218–231.
[231] K. Markstedt, et al., 3D bioprinting human Chondrocytes with nanocellulose–alginate Bioink for cartilage tissue engineering applications, Biomacromolecules 16 (5) (2015) 1489–1496.
[232] L.E. Bertassoni, et al., Direct-write bioprinting of cell-laden methacrylated gelatin hydrogels, Biofabrication 6 (2) (2014) 24105.
[233] N. Recek, et al., Cell adhesion on polycaprolactone modified by plasma treatment, Int. J. Polym. Sci. 2016 (2016) 7354396.
[234] S. Knowlton, et al., Photocrosslinking-based bioprinting: examining crosslinking schemes, Bioprinting 5 (2017) 10–18.
[235] I.T. Ozbolat, Scaffold-Based or scaffold-free bioprinting: Competing or complementing approaches? J. Nanotechnol. Eng. Med. 6 (2) (2015).
[236] H. Gudapati, M. Dey, I. Ozbolat, A comprehensive review on droplet-based bioprinting: past, present and future, Biomaterials 102 (2016) 20–42.
[237] Q. Liu, W. Zhai, Hierarchical porous ceramics with distinctive microstructures by emulsion-based direct ink writing, ACS Appl. Mater. Interfaces 14 (28) (2022) 32196–32205.
[238] A. Panwar, L.P. Tan, Current status of bioinks for micro-extrusion-based 3D bioprinting, Molecules 21 (6) (2016).
[239] Z. Wu, et al., Bioprinting three-dimensional cell-laden tissue constructs with controllable degradation, Sci. Rep. 6 (1) (2016) 24474.
[240] R. Yin, et al., Material design and photo-regulated hydrolytic degradation behavior of tissue engineering scaffolds fabricated via 3D fiber deposition, J. Mater. Chem. B 5 (2) (2017) 329–340.
[241] I.T. Ozbolat, M. Hospodiuk, Current advances and future perspectives in extrusion-based bioprinting, Biomaterials 76 (2016) 321–343.
[242] R.R. Langley, I.J. Fidler, Tumor cell-organ microenvironment interactions in the pathogenesis of cancer metastasis, Endocr. Rev. 28 (3) (2007) 297–321.
[243] V.K. Lee, et al., Generation of 3-D glioblastoma-vascular niche using 3-D bioprinting, in: 2015 41st Annual Northeast Biomedical Engineering Conference (NEBEC), 2015, pp. 1–2.
[244] H.G. Yi, et al., A bioprinted human-glioblastoma-on-a-chip for the identification of patient-specific responses to chemoradiotherapy, Nat. Biomed. Eng. 3 (7) (2019) 509–519.
[245] S. Chaji, J. Al-Saleh, C.T. Gomillion, Bioprinted three-dimensional cell-laden Hydrogels to evaluate adipocyte-breast cancer cell interactions, Gels 6 (1) (2020) 10.
[246] M. Tang, et al., Rapid 3D Bioprinting of glioblastoma model mimicking native biophysical heterogeneity, Small 17 (15) (2021), e2006050.
[247] H. Chen, et al., Modeling cancer metastasis using acoustically bio-printed patient-derived 3D tumor microtissues, J. Mater. Chem. B 10 (11) (2022) 1843–1852.
[248] H. Cui, et al., Engineering a novel 3D printed vascularized tissue model for investigating breast cancer metastasis to bone, Adv. Healthcare Mater. 9 (15) (2020), e1900924.
[249] M.A. Heinrich, et al., 3D-Bioprinted mini-brain: a glioblastoma Model to study cellular Interactions and therapeutics, Adv. Mater. 31 (14) (2019), e1806590.
[250] A. Künkele, et al., Preclinical assessment of CD171-directed CAR T-cell adoptive therapy for childhood neuroblastoma: CE7 epitope target safety and product manufacturing feasibility, Clin. Cancer Res. 23 (2) (2017) 466–477.
[251] L. Grunewald, et al., A reproducible bioprinted 3D tumor model Serves as a preselection Tool for CAR T cell therapy optimization, Front. Immunol. 12 (2021) 689697.
[252] C.D. Morley, et al., Spatiotemporal T cell dynamics in a 3D bioprinted immunotherapy model, Bioprinting 28 (2022), e00231.
[253] M. Dey, et al., Chemotherapeutics and CAR-T cell-based immunotherapeutics Screening on a 3D bioprinted vascularized breast tumor model, Adv. Funct. Mater. 32 (52) (2022) 2203966.
[254] L. Neufeld, et al., Microengineered perfusable 3D-bioprinted glioblastoma model for in vivo mimicry of tumor microenvironment, Sci. Adv. 7 (34) (2021).
[255] M.A. Hermida, et al., Three dimensional in vitro models of cancer: bioprinting multilineage glioblastoma models, Adv. Biol. Regul. 75 (2020) 100658.
[256] R. Li, et al., Three-dimensional Printing for cancer applications: research Landscape and technologies, Pharmaceuticals 14 (8) (2021).
[257] M. Zanoni, et al., Modeling neoplastic disease with spheroids and organoids, J. Hematol. Oncol. 13 (1) (2020) 97.
[258] K. Yuki, et al., Organoid models of tumor immunology, Trends Immunol. 41 (8) (2020) 652–664.
[259] D. Qin, Y. Xia, G.M. Whitesides, Soft lithography for micro- and nanoscale patterning, Nat. Protoc. 5 (3) (2010) 491–502.